

**ALMA MATER STUDIORUM - UNIVERSITÀ DI BOLOGNA**

---

**SCUOLA DI INGEGNERIA E ARCHITETTURA**

*DIPARTIMENTO DI INGEGNERIA CIVILE, AMBIENTALE E DEI  
MATERIALI*

*CORSO DI LAUREA MAGISTRALE IN CIVIL ENGINEERING*

**TESI DI LAUREA**

in  
Advanced Design of Structures

**SEMI-ENGINEERED EARTHQUAKE-RESISTANT  
STRUCTURES: ONE STORY BUILDING BUILT-UP WITH  
GABION-BOX WALLS**

CANDIDATO  
Julio Alfredo Samayoa Avalos

RELATORE:  
Chiar.mo Prof. Ing. Stefano Silvestri

CORRELATORI  
Dott. Ing. Luca Pieraccini  
Dott. Ing. Simonetta Baraccani

Anno Accademico 2015/2016

Sessione I

## ACKNOWLEDGEMENTS

I thank God for giving me this opportunity to realize my studies out of my country, it's a good wholesome for being with me and guided through my career, for being my strength in the hardest time and for giving me a life full of learning experiences and above all a life full of happiness.

To my supervisor Prof. Ing. Stefano Silvestri, to Arch. Martijn Schildkamp, to Dott. Ing. Luca Pieraccini and Dott. Ing. Simonetta Baraccani; I thank them the trust, support and time dedicated, used to share their knowledge and above all for being patient and encouraging me to move forward in all the difficult times that this process had me faced.

I would like to thank my parents Julio and Ana Gloria for supporting me unconditionally and all time for knowing that I was going to be far away but still close all the time cheering me up for the values that they have brought me up with that were the base and guidance throughout these two years for giving me an excellent education throughout my life about all for their love and being an excellent example of life to follow.

To my family and my future wife Kathy for encouraging me to always move forward and Pursuit my dreams supporting me despite the distance to my friends for all the moments we spent together and all the times we work together.

To the organization AMIDILA Erasmus Mundus, for putting their trust in me and allow me to study my master's degree in Italy with this scholarship.

## SOMMARIO

Questa tesi studia il comportamento statico e sismico di strutture semplici realizzate con un sistema costruttivo costituito da pareti portanti a gabbioni. Le analisi sono condotte con riferimento ad un edificio ad un piano, di dimensioni standard (pianta 6m x 5m) e con tetto leggero in legno. Questa tecnologia costruttiva, di carattere semi-ingegneristico, è già ampiamente utilizzata in alcune regioni del Nepal, ma è anche indirizzata alle popolazioni di nazioni in via di sviluppo poiché offre un vantaggio sia di tipo economico che di tipo tecnico rispetto ai materiali convenzionali (muratura in mattoni e cemento). Le informazioni ad oggi disponibili su questo genere di strutture sono molto limitate a causa della scarsa e poco approfondita ricerca eseguita sul tema.

L'obiettivo principale di questa ricerca è di definire gli aspetti principali del comportamento sismico di un edificio ad un piano composto da pareti a gabbioni, con scopo di prevenire crolli causati da azioni sismiche e quindi ridurre il rischio sismico in quelle regioni del mondo dove questi disastri hanno intensità significative. Non esistono attualmente in letteratura ricerche specifiche su pareti costruite con gabbioni poiché generalmente l'uso tipico di questa tecnologia è rivolta a sistemi di contenimento e di sostegno, campi in cui si possono trovare informazioni più dettagliate e specifiche.

Per quanto riguarda le pareti a gabbioni, sono stati effettuati calcoli e analisi allo scopo di capire il comportamento statico e sismico. L'analisi statica, è stata condotta una verifica a sforzo normale calcolando lo sforzo normale agente alla base del muro di gabbioni e la corrispondente capacità resistente.

Per quanto riguarda l'analisi sismica del muro in gabbioni, si è studiato sia il comportamento nel piano sia quello fuori dal piano. L'aspetto più delicato si è rivelato essere il comportamento fuori dal piano, per il quale sono stati sviluppati sia modelli manuali del tipo "rigido a tensioni nulle" per strutture in muratura con i quali si sono determinati diversi valori di moltiplicatori cinematicamente ammissibili che provocano meccanismi di rottura della struttura, che modelli FEM e DEM con i quali si sono determinati lo spostamento massimo in sommità del muro, le tensioni di trazione massime necessarie per il calcolo dei ganci in acciaio per il collegamento delle reti dei gabbioni adiacenti e le dimensioni (lunghezza dei muri e distanza tra muri ortogonali o contrafforti) di una configurazione geometrica del modulo standard dell'edificio tale da garantire adeguati margini di sicurezza per terremoti di PGA pari a circa 0.4 – 0.5 g.

Grazie ai risultati ottenuti è stato possibile stilare un insieme di regole basi che devono essere soddisfatte per assicurare un buon comportamento strutturale sotto l'azione sismica. Queste regole sono riportate in modo tale da essere recepite e comprese da chiunque e quindi da costituire istruzioni semplici per la corretta costruzione di pareti in gabbioni in ambito sismico anche da parte di personale né tecnico, né qualificato.

## ABSTRACT

This thesis studies the static and seismic behavior of simple structures made with gabion box walls. The analysis was performed considering a one-story building with standard dimensions in plan (6m x 5m) and a lightweight timber roof. This kind of semi-engineering technique has been used in some regions of Morocco and Nepal, but could be useful in developing countries because they offer an economical and technical advantage over the conventional materials (masonry blocks and concrete). There is a lack of information until now regarding the seismic behavior of such structures.

The main focus of the present investigation is to find the principal aspects of the seismic behavior of a one-story building made with gabion box walls, in order to prevent a failure due to seismic actions and in this way help to reduce the seismic risk of developing countries where this natural disaster has a significant intensity. Moreover, there is not any investigation regarding a gabion wall because the normal use for this kind of material is for retaining walls where it can be found more detailed and specific information.

Regarding the gabion box wall, it has been performed some calculations and analysis in order to understand the static and dynamic behavior. From the static point of view, it has been performed a verification of the normal stress computing the normal stress that arrives at the base of the gabion wall and the corresponding capacity of the ground.

Moreover, regarding the seismic analysis of the gabion walls, it has been studied the in-plane and out-of-plane behavior. The most critical aspect was discovered to be the out-of-plane behavior, for which have been developed models considering the “rigid- no tension model” for masonry, finding a kinematically admissible multiplier that will create a collapse mechanism for the structure.

Furthermore, it has been performed a FEM and DEM models to find the maximum displacement at the center of the wall, maximum tension stresses needed for calculating the steel connectors for joining consecutive gabions and the dimensions (length of the wall and distance between orthogonal walls or buttresses) of a geometrical configuration for the standard modulus of the structure, in order to ensure an adequate safety margin for earthquakes with a PGA around 0.4-0.5g.

Using the results obtained before, it has been created some rules of thumb, that have to be satisfied in order to ensure a good behavior of the structure under a seismic action, these rules are very simple and understandable for everybody, thus, to formulate simple instructions for the correct construction of the gabion walls in a seismic area for non-technical or qualified personnel.

## INDEX

ACKNOWLEDGEMENTS .....	i
SOMMARIO.....	ii
ABSTRACT.....	iii
INDEX .....	iv
LIST OF FIGURES .....	vi
LIST OF TABLES .....	x
SIMBOLOGY .....	xii
CHAPTER 1      INTRODUCTION .....	1
1.1      Global context .....	1
1.2      Justification of the document and objectives .....	1
1.2.1.      General objectives.....	2
1.2.2.      Specific objectives .....	2
1.3      Framework and limitations of the present study.....	2
1.4      Organization of the thesis.....	3
CHAPTER 2      GABION BOXES.....	4
2.1      General.....	4
2.2      Laboratory tests performed on gabion boxes .....	5
2.3.1 Compression test .....	5
2.3.2 Shear test.....	7
CHAPTER 3      STATIC BEHAVIOR OF ONE STORY BUILDING STRUCTURES BUILT UP WITH GABION BOXES AS STRUCTURAL COMPONENT.....	10
3.1      Gabion construction system .....	10
3.2      Simple component of a gabion wall.....	10
3.3      Single wall of the gabion box structure.....	12
3.4      Gabion box structure.....	14
3.4.1.      Roof system.....	15
3.4.2.      Openings .....	15
3.4.3.      Corners .....	18
3.4.4.      Steel wire connectors .....	19
CHAPTER 4      IN-PLANE SEISMIC BEHAVIOR OF ONE STORY BUILDING STRUCTURES BUILT UP WITH GABION BOXES AND FLEXIBLE DIAPHRAGM.....	20
4.1      General.....	20
4.2      Shear resistance of a gabion wall.....	20
4.2.1.      Shear resistance of a gabion wall with a force applied at the top .....	20

4.2.2.	Shear resistance of a gabion wall with lateral distribution of forces on height..	22
4.3	Sliding resistance of a gabion wall.....	25
4.3.1.	Sliding resistance of a gabion wall with force applied at the top.....	25
4.3.2.	Sliding resistance of a gabion wall with lateral distribution on height. ....	27
4.4	In-plane behavior of a gabion walls considering openings. ....	29
CHAPTER 5    OUT-OF-PLANE SEISMIC BEHAVIOR OF ONE STORY BUILDING		
STRUCTURES BUILT UP WITH GABION BOXES AND FLEXIBLE DIAPHRAGM.....		
5.1	General .....	34
5.2	Out-of-plane behavior of a rigid vertical strip .....	35
5.2.1.	Rigid body over rigid soil – hand calculations.....	35
5.2.2.	Rigid body over elastic soil – hand calculations. ....	43
5.2.3.	Elastic body over rigid soil – FEM model. ....	57
5.2.4.	Elastic body over elastic soil – FEM model.....	61
5.3	Out-of-plane behavior of a rigid horizontal strip. ....	66
5.3.1.	Rigid beam between rigid orthogonal walls - hand calculation. ....	67
5.3.2.	Rigid beam between elastic orthogonal walls - hand calculation. ....	69
5.3.3.	Elastic beam with fixed ends – FEM model. ....	72
5.4	Out-of-plane behavior of complete gabion boxes wall – FEM model .....	77
5.4.1.	Complete gabion wall over rigid soil – FEM model.....	77
5.4.2.	Complete gabion wall over elastic soil – FEM model. ....	79
5.5	Wall of 6m length over elastic soil – FEM model .....	80
5.6	Wall of 5m length over elastic soil – FEM model .....	83
5.7	Out-of-plane behavior of complete gabion boxes wall – DEM model.....	86
CHAPTER 6    PRACTICAL RULES OF THUMB FOR CONSTRUCTION OF GABION		
BOXES STRUCTURES .....		
6.1	Rules of thumb .....	89
CHAPTER 7    CONCLUSIONS AND RECOMMENDATIONS .....		
7.1	Conclusions .....	91
BIBLIOGRAPHY .....		
		92

## LIST OF FIGURES

Fig. 2. 1- Results of compression test on gabions with restricted and unrestricted lateral expansion (Agostini et al.,1987) .....	5
Fig. 2. 2 - Finite element numerical model and deformed mesh of uniaxial compression test on single gabion unit with (a) restricted (b) unrestricted lateral expansion (Lin et al., 2010).....	6
Fig. 2. 3 -The stress-strain curves of restricted and unrestricted lateral expansion uniaxial compression test on single gabion unit (Lin et al., 2010) .....	6
Fig. 2. 4 - Simple shear test in progress (Agostini et al.,1987).....	7
Fig. 2. 5 - Arrangement of gabions for the simple shear test (Agostini et al.,1987) .....	8
Fig. 2. 6 - Results of the simple shear test on gabion boxes (Agostini et al.,1987).....	8
Fig. 2. 7 - - Relation curves of shear stress vs normal stress (Jiang and Wang,2011)....	9
Fig. 2. 8 - Variation of shear strength with normal stress (Jiang and Wang,2011) .....	9
Fig. 3. 1 - simple component of a gabion wall.....	10
Fig. 3. 2 - gabion box dimensions .....	11
Fig. 3. 3 - Gabion wall dimensions, frontal view.....	12
Fig. 3. 4 - Gabion wall dimensions, lateral view .....	12
Fig. 3. 5 - Normal stresses acting on each layer of the wall .....	13
Fig. 3. 6 - Plan view of the gabion wall structure .....	14
Fig. 3. 7 - gabion box house with timber roof, picture given by A&D (Architecture and Developpement) .....	15
Fig. 3. 8 - Detail of “lintel” beam for openings .....	15
Fig. 3. 9 - Bending test with a span of 3.0m (Agostini et al., 1987).....	16
Fig. 3. 10 - Lintel timber beam .....	16
Fig. 3. 11 - Lintel timber beam considering the arch effect .....	17
Fig. 3. 12 - "Lego" connection of perpendicular gabion walls. ....	18
Fig. 3. 13 - Forces acting on the steel wire connectors .....	19
Fig. 4. 1 – Shear stress with force applied at the top of the wall. ....	21
Fig. 4. 2 – Uniform lateral distribution over the height of the wall. ....	22
Fig. 4. 3 – Results of the distribution of forces over the height of the wall. ....	24
Fig. 4. 4 – Friction force with a force applied at the top of the wall.....	25
Fig. 4. 5 – Friction force with lateral distribution over the height. ....	27
Fig. 4. 6 – Gabion wall with opening, with A lower than C.....	30
Fig. 4. 7 – Location of hinges when A is lower than C.....	30
Fig. 4. 8 – Gabion wall with opening, with A equal to C.....	32
Fig. 4. 9 – Location of hinges when A is equal to C.....	33

Fig. 5. 1 - Cases of study for the out-of-plane behavior.....	34
Fig. 5. 2 - Vertical strip of the gabion wall.....	35
Fig. 5. 3 – Rigid body over rigid soil with a force applied at the top. ....	35
Fig. 5. 4 - Hinge at the base with a force applied at the top of the wall.....	36
Fig. 5. 5 - Hinge at at general position with a force applied at the top of the wall.....	37
Fig. 5. 6 - Rigid body over rigid soil, considering the cohesion and a force applied at the top.....	38
Fig. 5. 7 - Rigid body over rigid soil with 2 forces applied on the wall.....	39
Fig. 5. 8 - Hinge at at general position with 2 forces applied in the wall.....	40
Fig. 5. 9 - Rigid body over rigid soil, considering the cohesion and 2 forces applied on the wall. ....	41
Fig. 5. 10 - Rigid body over elastic soil with 2 forces applied on the wall. ....	43
Fig. 5. 11 - Rigid body over elastic soil, considering the cohesion and 2 forces applied on the wall.....	44
Fig. 5. 12 – Point of equilibrium of moments when the first spring enters in tension...	45
Fig. 5. 13 – Point of equilibrium of moments when the second spring enters in tension. ....	47
Fig. 5. 14 – Point of equilibrium of moments when the third spring enters in tension..	48
Fig. 5. 15 – Point of equilibrium of moments when the fourth spring enters in tension.	50
Fig. 5. 16 – Rigid body over elastic soil with a force applied at the top.....	52
Fig. 5. 17 – Rigid body over elastic, considering the cohesion and a force applied at the top. ....	52
Fig. 5. 18 – System of forces acting on the vertical strip.....	57
Fig. 5. 19 - Deformed shapes of vertical strip considering $\alpha=0.144$ .....	58
Fig. 5. 20 - Map of displacement of the vertical strip considering $\alpha= 0.144$ .....	58
Fig. 5. 21 - Map of stresses of the vertical strip considering $\alpha= 0.144$ .....	59
Fig. 5. 22 – System of forces acting on the vertical strip considering the cohesion.....	59
Fig. 5. 23 - Deformed shapes of vertical strip considering cohesion and $\alpha=0.414$ .....	60
Fig. 5. 24 - Map of displacement of the vertical strip considering cohesion and $\alpha=0.414$ .....	60
Fig. 5. 25 - Map of stresses of the vertical strip considering cohesion and $\alpha=0.414$ .....	61
Fig. 5. 26 – Deformed shapes of 1 <sup>st</sup> and 2 <sup>nd</sup> spring entering in tension for a vertical strip .....	62
Fig. 5. 27 – Deformed shapes of 3 <sup>rd</sup> and 4 <sup>th</sup> spring entering in tension for a vertical strip.....	62
Fig. 5. 28 – Stress maps of 1 <sup>st</sup> and 2 <sup>nd</sup> spring entering in tension for a vertical strip.....	63
Fig. 5. 29 – Stress maps of 3 <sup>rd</sup> and 4 <sup>th</sup> spring entering in tension for a vertical strip.....	63
Fig. 5. 30 – Deformed shapes of 1 <sup>st</sup> and 2 <sup>nd</sup> spring entering in tension for a vertical strip with cohesion .....	64
Fig. 5. 31 – Deformed shapes of 3 <sup>rd</sup> and 4 <sup>th</sup> spring entering in tension for a vertical strip with cohesion .....	64



Fig. 5. 32 – Stress maps of 1 <sup>st</sup> and 2 <sup>nd</sup> spring entering in tension for a vertical strip with cohesion .....	65
Fig. 5. 33 – Stress maps of 3 <sup>rd</sup> and 4 <sup>th</sup> spring entering in tension for a vertical strip with cohesion .....	65
Fig. 5. 34 - Horizontal strip of the gabion wall .....	66
Fig. 5. 35 - Rigid beam between rigid orthogonal walls .....	67
Fig. 5. 36 – Collapse mechanism for the rigid beam between rigid orthogonal walls....	67
Fig. 5. 37 – Idealization of the rigid beam between rigid orthogonal walls.....	67
Fig. 5. 38 - Rigid beam between elastic orthogonal walls.....	69
Fig. 5. 39 – Collapse mechanism for the rigid beam between rigid orthogonal walls....	69
Fig. 5. 40 – Idealization of the rigid beam between elastic orthogonal walls .....	70
Fig. 5. 41 - Horizontal strip of gabion wall considering fixed ends .....	72
Fig. 5. 42 – Deformed shapes of the top horizontal vertical strip with $\alpha=0.108$ and $\alpha=0.12$ respectively considering fixed ends.....	73
Fig. 5. 43 – Stress maps of the top horizontal vertical strip with $\alpha=0.108$ and fixed ends .....	74
Fig. 5. 44 – Stress maps of the top horizontal vertical strip with $\alpha=0.12$ and fixed ends .....	74
Fig. 5. 45- Horizontal strip of gabion wall considering rotational springs.....	75
Fig. 5. 46 – Deformed shapes of the top horizontal vertical strip with $\alpha=0.108$ and $\alpha=0.114$ respectively considering rotational springs.....	75
Fig. 5. 47 – Stress maps of the top horizontal vertical strip with $\alpha=0.108$ and rotational springs.....	76
Fig. 5. 48 – Stress maps of the top horizontal vertical strip with $\alpha=0.114$ and rotational springs.....	76
Fig. 5. 49 - Map of displacement of the complete wall considering $\alpha= 0.5$ and a rigid soil .....	78
Fig. 5. 50 - Map of stresses of the complete wall considering $\alpha=0.5$ and a rigid soil....	78
Fig. 5. 51 – Springs working in compression of the complete gabion wall with $\alpha= 0.5$ .	79
Fig. 5. 52 - Map of displacement of the complete wall considering $\alpha= 0.5$ and an elastic soil. ....	79
Fig. 5. 53 - Map of stresses of the complete wall considering $\alpha=0.5$ and an elastic soil	79
Fig. 5. 54- Map of stresses of the complete wall considering $\alpha=0.25$ and an elastic soil .....	81
Fig. 5. 55 - Map of stresses of the complete wall considering $\alpha=0.35$ and an elastic soil .....	82
Fig. 5. 56 - Map of stresses of the complete wall of 5m, considering $\alpha=0.30$ and an elastic soil. ....	84
Fig. 5. 57 - Map of stresses of the complete wall of 5m, considering $\alpha=0.50$ and an elastic soil.....	85
Fig. 5. 58 - DEM model of the gabion wall.....	87
Fig. 5. 59 - Collapse of a gabion wall of 5m with a PGA around 0.4g.....	88

Fig. 6. 1 - Distribution of wires for a length of 6m and PGA=0.35 .....89  
Fig. 6. 2 - Distribution of wires for a length of 6m and PGA=0.50 g. ....90

## LIST OF TABLES

Table 4. 1 - Friction coefficient needed to sustain a certain value of $\alpha$ considering the force applied at the top .....	27
Table 4. 2 - Friction coefficient needed to sustain a certain value of $\alpha$ considering a force distribution on height.....	29
Table 5. 1 - Maximum load multiplier considering a hinge in a general position.....	41
Table 5. 2 – Values of $\alpha$ for considering a rigid body with rigid soil.....	42
Table 5. 3 – Values of $\alpha$ for considering a rigid body with elastic soil.....	56
Table 5. 4 - Maximum displacement of a vertical strip considering $\alpha=0.144$ .....	58
Table 5. 5 – Wire reinforcement for a vertical strip considering $\alpha=0.144$ .....	59
Table 5. 6 - Maximum displacement of a vertical strip considering cohesion and $\alpha=0.414$ .....	60
Table 5. 7 – Wire reinforcement for a vertical strip considering cohesion and $\alpha=0.414$	61
Table 5. 8 - Maximum displacement of a vertical strip considering an elastic soil.....	62
Table 5. 9 – Wire reinforcement for a vertical strip considering an elastic soil.....	63
Table 5. 10 - Maximum displacement of a vertical strip considering an elastic soil with cohesion.....	64
Table 5. 11 – Wire reinforcement for a vertical strip considering an elastic soil with cohesion.....	65
Table 5. 12 - values of $\alpha$ and their respective lateral displacement for top layer .....	71
Table 5. 13 - values of $\alpha$ and their respective lateral displacement for top layer .....	72
Table 5. 14 - Values of $\alpha$ and their respective lateral displacement for top layer with fixed ends.....	73
Table 5. 15 – Wire reinforcement the top horizontal strip with fixed ends, considering $\alpha=0.12$ .....	74
Table 5. 16 - Values of $\alpha$ and their respective lateral displacement for top layer with rotational springs.....	75
Table 5. 17 – Wire reinforcement the top horizontal strip with rotational springs, considering $\alpha=0.114$ .....	76
Table 5. 18 - Reaction values at supports of the wall, considering $\alpha=0.5$ and a rigid soil .....	78
Table 5. 19 - Reaction values at supports of the wall, considering $\alpha=0.5$ and an elastic soil .....	80
Table 5. 20 - Reaction values at supports of the wall, considering $\alpha=0.25$ and an elastic soil .....	80
Table 5. 21 - Maximum displacement of the wall considering $\alpha=0.25$ and an elastic soil .....	81
Table 5. 22- Reaction values at supports of the wall, considering $\alpha=0.35$ and an elastic soil .....	81

Table 5. 23 - Maximum displacement of the wall considering $\alpha=0.35$ and an elastic soil .....	82
Table 5. 24 – Wire reinforcement at corner of a gabion wall with a length of 6m.....	82
Table 5. 25 – Wire reinforcement at the center of a gabion wall with a length of 6m....	83
Table 5. 26 - Reaction values at supports of the 5m wall, considering $\alpha=0.30$ and an elastic soil .....	83
Table 5. 27 - Maximum displacement of the 5m wall, considering $\alpha=0.30$ and an elastic soil .....	83
Table 5. 28 - Reaction values at supports of the 5m wall, considering $\alpha=0.5$ and an elastic soil .....	84
Table 5. 29 - Maximum displacement of the 5m wall, considering $\alpha=0.5$ and an elastic soil .....	84
Table 5. 30 – Wire reinforcement at corner of a gabion wall with a length of 5m.....	85
Table 5. 31 – Wire reinforcement at the center of a gabion wall with a length of 5m....	85

## SIMBOLOGY

$\alpha$ = Load multiplier

$\Delta$ = proportional multiplier between 0 and 1

$\gamma$ : Specific weight

$\lambda$ : Slenderness

$\sigma_N$ : Normal stress

$\tau$ = shear stress

$\mu$ = friction coefficient

$A_s$ = Surface area

$B$ = Base of the wall

$c$ = cohesion

$F_f$ = Friction force

$F_j$ = distribute seismic force

$f_{\max}$ = maximum triangular distributed force

$F_s$ = seismic force

$H$ = Height of the wall

$k$ = Stiffness of the wall

$k_i$ =Stiffness of the soil

$L$ = Length of the wall

$M_{\text{ext}}$ : External moment

$M_{\text{sp}}$ : moment due to the sprigs

$q$ = Uniform distributed load

$t$ : Thickness

$V$ : Volume of the gabion box

$W_{\text{roof}}$ : Weight of the roof

$W_t$ : Weight of the wall

## **CHAPTER 1      INTRODUCTION**

### **1.1    Global context**

Gabions are cellular structures boxes made with steel wire mesh and filled with stones with appropriated size, normally stacked up one into another to form a retaining wall. In the recent years the gabion structures have been more used in the engineering field, this interest is due to the fact that gabions are environmental friendly and also by the versatility and the advantages that a gabion box structure can have, as Agostini et al., 1987 indicated, a gabion structure is characterized by a continuous construction process, flexibility, permeability, durability, noise proofing, and beneficial environmental impact.

Gabion boxes structures are very versatile, proof of this is that they have been used in many construction fields and types of structure such as revetments, channel linings, weirs, bridge abutments, offshore breakwaters and beach protection, and retaining walls and also they can be used as a new alternative building technique for houses.

Thus, this research was performed to ensure that this alternative building technique can be built in a seismic region knowing that it will be a safe structure and that can be used for a post-disaster reconstruction in developing countries.

### **1.2    Justification of the document and objectives**

The use of gabion boxes is an emerging technique in the construction field and it is widely used all over the world due to some factors such as durability of the structure, low environmental impact, cost-effective ratio.

Considering the advantages that this system carries, it can be an alternative building technique and post-disaster reconstruction for houses in developing countries where it can be used for individual housing or for community facilities. Thereby, this technique can be built in remote areas, locations difficult to reach and poorly supplied areas with the advantage that gabion boxes are easily installed and that deployment can be performed without special equipment and there is no need of highly trained personnel.

On the other hand, from a seismic point of view, there will be “weight issues” because the gabions are heavy due to the rocks (it’s known that the seismic forces acting on the structure are proportional to the weight). Thus, the need of research has been identified in order to understand the static and seismic behavior of this kind of structures focusing on the limitations of the system and the structural safety under a certain seismic action.

### **1.2.1. General objectives**

Based on the justification of this document, this dissertation aims at understand the behavior in-plane and out-of-plane under seismic actions of a wall built-up with gabion boxes and to give practical suggestions and simple formulas for the dimensioning of the structure, satisfying structural safety conditions.

### **1.2.2. Specific objectives**

- To comprehend the compression behavior and strength of a single gabion box Wall under vertical loads.
- To verify the structural safety under seismic actions in-plane and out-of-plane of a wall build-up with gabion boxes.
- Conduct analytical and numerical considerations to examine the effect of lateral forces on the behavior of a gabion box wall.
- Propose constructions details and limitations to acquire a good seismic behavior of the structure
- To develop rules of thumb for a proper dimensioning and construction of this kind of structures in order to be a seismic resistant structure.

### **1.3 Framework and limitations of the present study**

In the present study it has been considered a fix dimension for a gabion box unit of 0.5m x 0.5m x 1.0m (width—height—length); the infill material has to be deposited inside the cage by placing the stones in a randomly way. The gabion wall is constructed by stacking gabion boxes one over the other until the specified height of the wall is reached and connecting each unit in vertical and horizontal direction with the adjacent ones.

It has not been considered any connection between the gabion box wall and the soil below or with the roof system, this kind of interaction is out of the scope of this investigation.

The study of the seismic behavior of a gabion box house has been limited to a one story building with a flexible diaphragm, this could be a light-weight timber roof.

The maximum peak ground acceleration (PGA) that has been considered in the present study is the maximum that can occur in some countries such as Nepal, where the values can reach 0.5g.

## 1.4 Organization of the thesis

Chapter 1 gives an introductory outline of the purpose of a gabion box house, the objectives and limitations of the present study are also mentioned in this part. Chapter 2 deals with an overview of the gabion boxes such as materials, test that have been performed on a single unit, advantages and the common uses of this kind of system on the engineering field.

Chapter 3 contains a geometric and parametric description of the gabion construction system, starting from the simple component of a gabion wall where some parameters of the materials are presented, thus, to arrive to the single wall in order to describe the dimensions of analysis in the present document and the static behavior of it, and to close the chapter, the description of the general gabion wall structure where it is also mentioned the openings on the wall and the type of roof system that has been considered.

Chapter 4 briefs out the seismic in-plane behavior of a gabion wall performing hand calculations, here it has been developed the shear and sliding resistant  $a$  of the solid wall and also it has been taken into consideration the openings of doors; furthermore, in chapter 5, it has been analyzed the out-of-plane behavior with different approaches which brings into account the stiffness of the soil below the gabion wall, also it has been performed some calculation to find the flexural behavior of the horizontal strip of the wall, from all of these computations it has been obtained an maximum load multiplier that the wall can sustain for each approach which gives us the maximum for that can be applied to the system before the collapse.

Additionally, chapter 5 gives the outcomes of the DEM and FEM models performed in order to verify the results that were done by hand, moreover this models helped to find the maximum length of a wall without perpendicular walls or buttresses in order to avoid the out-of-plane failure with a certain PGA, as well as to understand where the stresses in tension on the wall are maximum.

Using the results obtained before, in Chapter 6, it has been created some rules of thumb, that have to be satisfy in order to ensure a good behavior of the structure under a seismic action, this rules are very simple, thus everybody can understand and replicate the way that the gabion box walls should be built up. Finally, Chapter 7 summarizes the results of the research, highlighting the conclusions drawn from analytical and numerical outcomes, following a list of references quoted in this investigation are listed at the end of the document.



## CHAPTER 2      GABION BOXES

### 2.1 General

Following the description given by Agostini et al., 1987, a gabion is a rectangular cage made with steel wire mesh and filled with stones; where the wire used has to meet the international standards.

For the infill material of the gabion, it can be used any kind of stone or other material as long as they satisfy the required characteristics from the functional and structural point of view, such as compression strength of the material.

The use of gabions for engineering purposes brings some technical advantages such as:

- **Deformability:** the flexibility of a gabion structure allows it to deform rather than break, this fact helps in improving the structural efficiency. As Agostini et al., 1987, mentioned that the deformability does not reduce the strength of the structure, but it is increased by bringing into action all the resisting elements.
- **Strength:** considering that the gabion boxes are bound together, they can be considered as a monolithic structure, capable of resisting tension and shear stresses. The wire mesh is strong under tension, hence, has not only the function of containing the infill material, but works as a reinforcement of the entire structure.

Moreover, the gabion boxes lead us to functional advantages such as durability of the structure, beneficial environmental impact, cost-effective ratio. From the economical point of view, gabions are less expensive comparing to the most used construction materials like concrete, this is due to the fact that stones fill are usually locally available.

Gabions structures are characterized by a continuous construction process, with the need of unskilled laborer and without any mechanical equipment, which leads to a reduced construction cost.

Gabion boxes structures are very versatile, proof of this is that they have been used in many construction fields, the most common use in the engineering field is to stabilize shorelines or slopes against erosion; gabions can be used for revetments, channel linings, weirs, bridge abutments, offshore breakwaters and beach protection, and retaining walls and also they can be used as a new alternative building technique for houses.

## 2.2 Laboratory tests performed on gabion boxes

It has been performed a literature review in order to identify some basic properties of the gabion boxes such as maximum compression stress, shear properties and equivalent elastic modulus, which are the principal parameter of interest in order to study the behavior of a gabion box wall for a one-story building.

Agostini et al., (1987), performed a compression and shear test on full size gabions for determining the strength and deformation parameters of the gabion box.

Lin et al., (2010), realized a numerical simulations regarding uniaxial compression test of a single gabion based on the results obtained by Agostini et al., (1987) in the structural science laboratory of the University of Bologna.

Jiang and Wang (2011), performed a compression and direct shear test for multi-group gabions. They obtained the mechanical properties and stress-strain behavior of gabions.

### 2.3.1 Compression test

The full size gabion test performed by Agostini et al., (1987) has the objective of understand the events that accompany the progressive deformation induced by loading and to determine the final failure of the structure involving the fracture of the stones and rupture of the wire mesh, the results of the test are shown in the picture below:

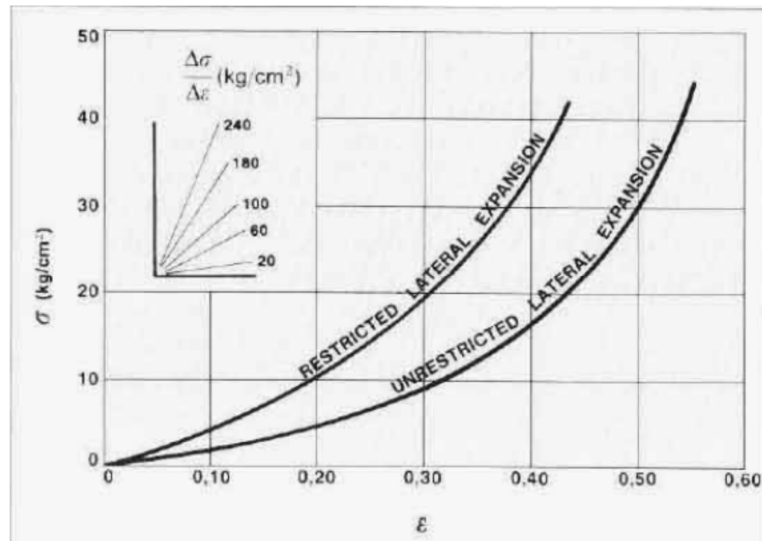


Fig. 2. 1- Results of compression test on gabions with restricted and unrestricted lateral expansion (Agostini et al.,1987)

Moreover, the numerical solution performed by Lin et al., (2010) were compared with the measurements given by Agostini et al., (1987), where the results of the simulations are very similar to the experimental test although a small variation occurs in the case of unrestricted lateral expansion. The results of the test are presented below:

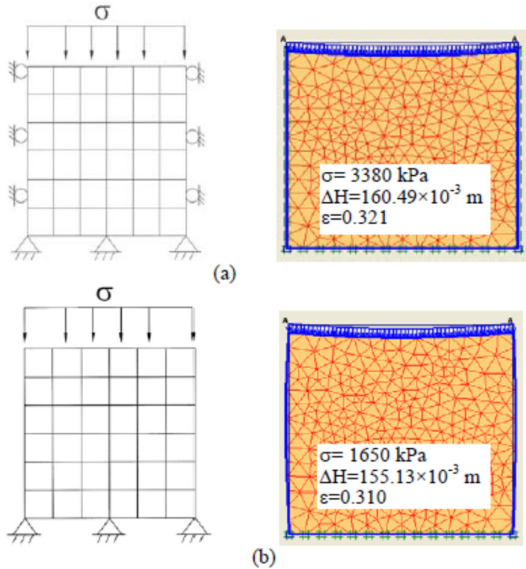


Fig. 2. 2 - Finite element numerical model and deformed mesh of uniaxial compression test on single gabion unit with (a) restricted (b) unrestricted lateral expansion (Lin et al., 2010)

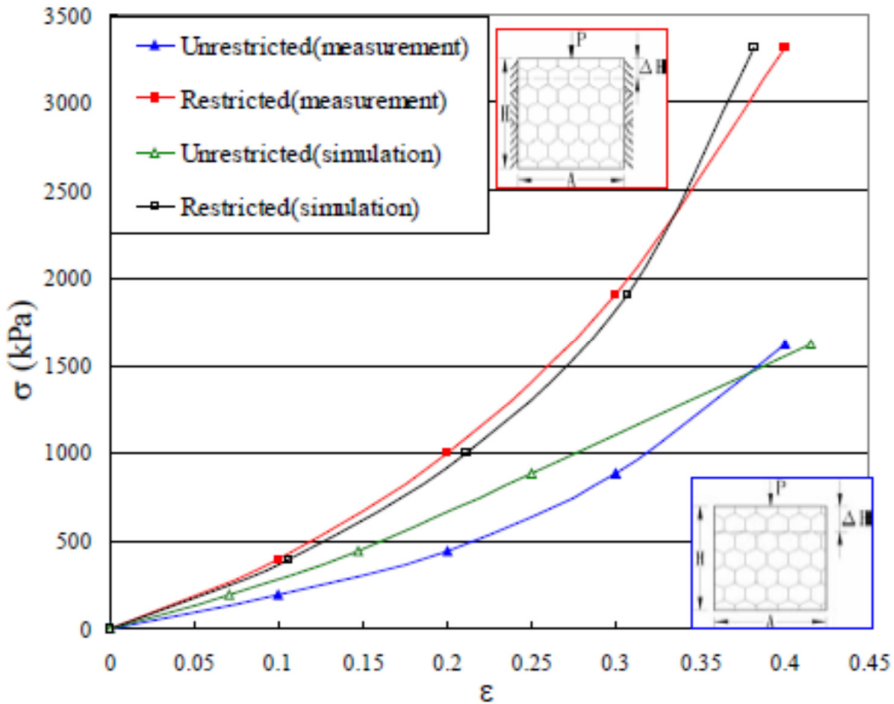


Fig. 2. 3 -The stress-strain curves of restricted and unrestricted lateral expansion uniaxial compression test on single gabion unit (Lin et al., 2010)

In order to select a value of the elastic for gabion boxes, it has been calculated following the experimental stress-strain curve of single gabion unit mentioned before.

The value of the elastic modulus change depending on the compression stress level. For the purpose of this investigation, it has been computed the elastic modulus  $E$  ( $\Delta\sigma/\Delta\varepsilon$ ) from the Figure 2, considering a compression strain  $\varepsilon=5\%$ , a mean value between the restricted and unrestricted configuration has been computed.

$$E_{restrain} = \frac{\Delta\sigma}{\Delta\varepsilon} = \frac{2 \text{ kg/cm}^2}{0.05} = 40 \text{ kg/cm}^2$$

$$E_{unrestrain} = \frac{\Delta\sigma}{\Delta\varepsilon} = \frac{1 \text{ kg/cm}^2}{0.05} = 20 \text{ kg/cm}^2$$

$$E_{mean} = 30 \text{ kg/cm}^2$$

### 2.3.2 Shear test

Simple shear tests were performed by Agostini et al., (1987), in the results can be seen a considerable shear resistance in the gabions accompanied by a significant deformation (Fig.2.6). From the analysis of the results, it has been observed that the behavior of a gabion box should be considered to be elastic just when the values of stresses are low.

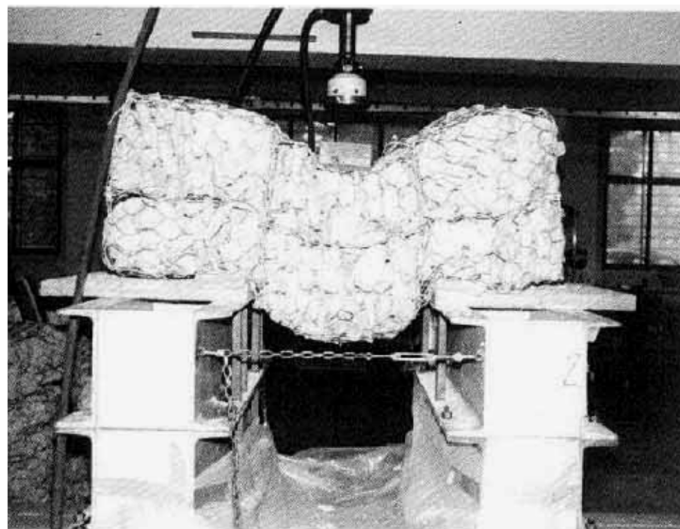


Fig. 2. 4 - Simple shear test in progress (Agostini et al.,1987)

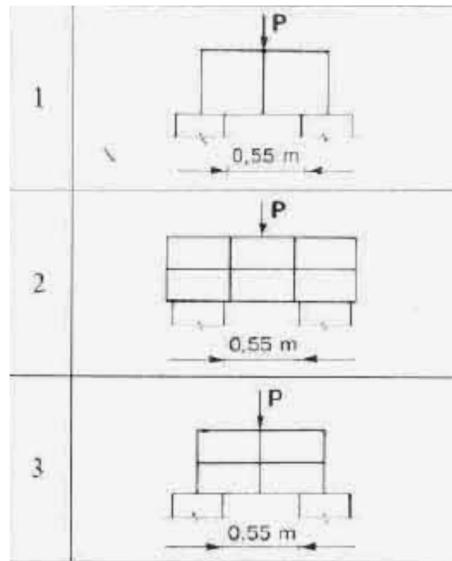


Fig. 2. 5 - Arrangement of gabions for the simple shear test (Agostini et al.,1987)

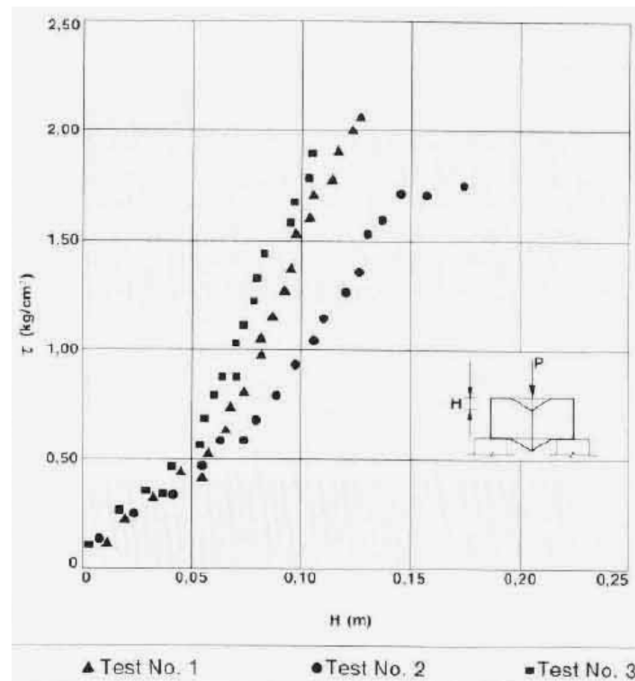


Fig. 2. 6 - Results of the simple shear test on gabion boxes (Agostini et al.,1987)

Furthermore, Jiang and Wang (2011), performed a direct shear test with different values for the normal stress in order to construct a relation curve of shear stress and normal stress (Fig. 2.7). They realize a linear regression of the results obtained from the tests and those shows that exist a good correlation for the data.

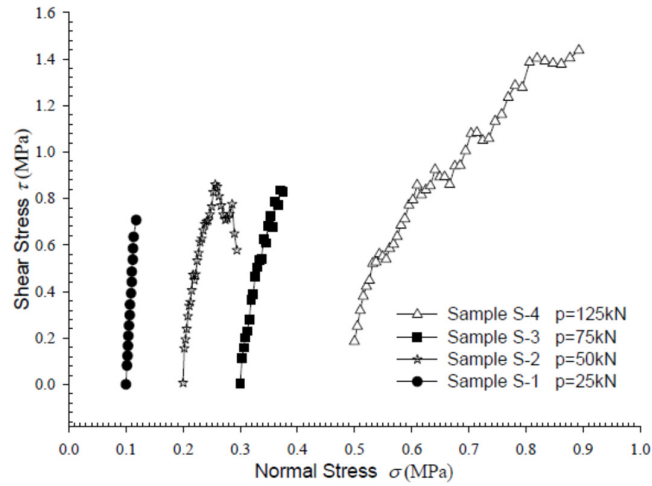


Fig. 2. 7 - - Relation curves of shear stress vs normal stress (Jiang and Wang,2011)

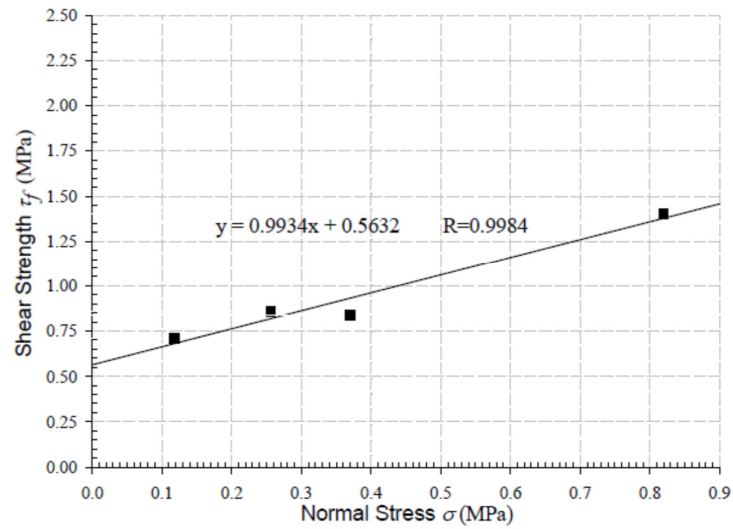


Fig. 2. 8 - Variation of shear strength with normal stress (Jiang and Wang,2011)

As an output from the figure above, the Mohr-Coulomb shear strength line for gabion boxes and the strength index of gabion, namely that  $c = 0.5632$  MPa,  $\phi = 44.8^\circ$ , were obtained.

## CHAPTER 3      **STATIC BEHAVIOR OF ONE STORY BUILDING STRUCTURES BUILT UP WITH GABION BOXES AS STRUCTURAL COMPONENT**

### **3.1 Gabion construction system**

A gabion box wall is formed by stacking vertically each single element and then joining them with steel wires in order to have a monolithic “cellular behavior”. In order to have an effectively behavior of the wall, the gabions must be wired in the vertical and horizontal direction.

A gabion box wall structure must be formed at least by 4 walls in order to have a good response of the structure against lateral forces. Some other features are mentioned later in this chapter.

In order to obtain useful information for the entire system, it has been studied the problem starting from the principal component of the wall until we arrive to the full structure, moreover it has been selected the dimensions and properties that have been taken into consideration in this document.

### **3.2 Simple component of a gabion wall**

The gabion boxes are rectangular cages made with steel wire mesh and filled with stones as shown in the next figure.

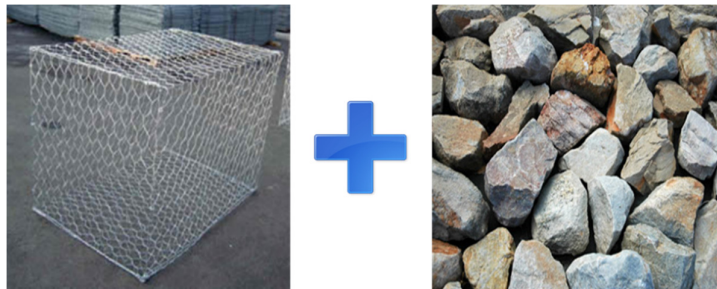


Fig. 3. 1 - simple component of a gabion wall

For the infill material of the gabion, it can be used any kind of stone or other material as long as they satisfy the required characteristics from the functional and structural point of view, such as compression strength of the material; where for the steel wire must satisfy the international standards.

In the present study it has been considered some parameters for the simple component, they are mentioned below:

Specific weight of the rocks:

$$\gamma_{stone} = 25.3 \text{ kN/m}^3$$

The size of the rocks should be selected according to the dimension of the mesh, thus, the infill material will be large enough to avoid the flow of the rocks outside the cage, thereby, the most appropriate size of the stones varies from 1.5 to 2 times the dimension of the mesh.

Following what Agostini et al., (1987) mentioned, the void ratio of the infill materials varies from 0.3 to 0.4, hence it has been selected the following value:

$$\text{Void ratio} = \eta = 0.3$$

Thus, the volumetric weight of the single gabion can be computed as follows:

$$\gamma_g = \gamma_{stone} * (1 - \eta)$$

$$\gamma_g = 25.5 * (1 - 0.3)$$

$$\gamma_g = 17.9 \text{ kN/m}^3$$

The dimensions that have been considered for the simple component in this document are the followings:

1 m (Length) x 0.5 m (height) x 0.5 m (width)

$$V = 0.25 \text{ m}^3$$

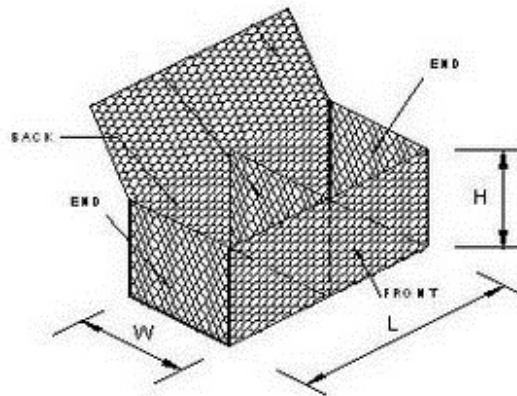


Fig. 3. 2 - gabion box dimensions

Hence:

$$W_g = \gamma_g * V = 17.9 * 0.25 = 4.475 \text{ kN}$$

$$W_g = 447.5 \text{ Kg} \approx 450 \text{ Kg}$$



### 3.3 Single wall of the gabion box structure

The Typical dimensions of a single wall that have been considered are shown in the figure below:

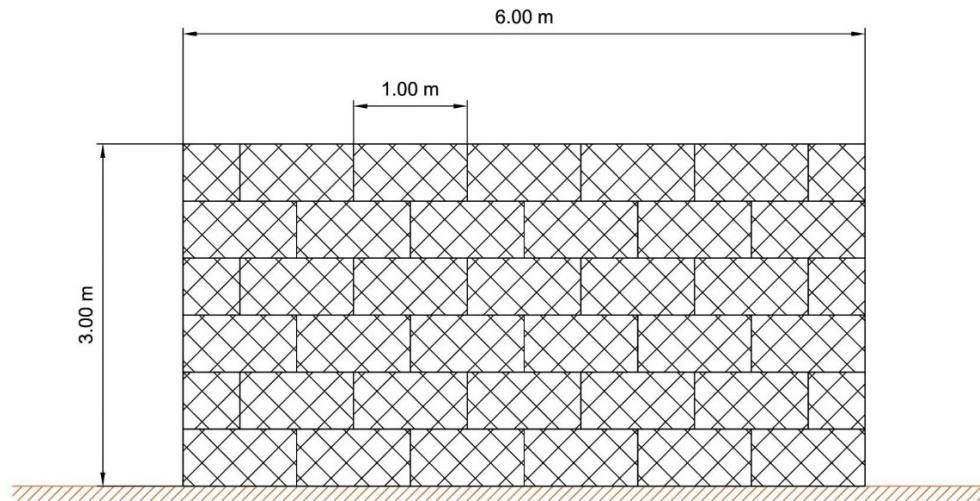


Fig. 3.3 - Gabion wall dimensions, frontal view

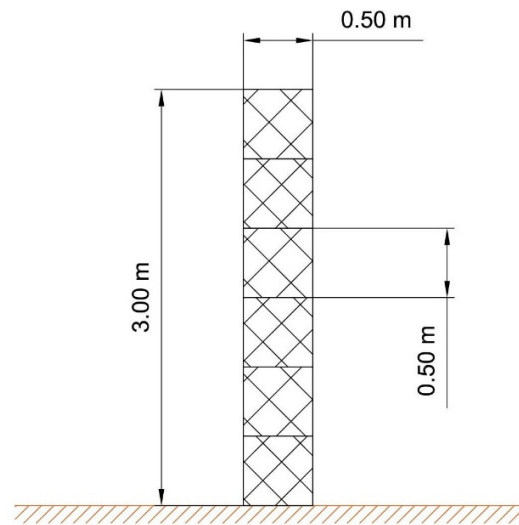


Fig. 3.4 - Gabion wall dimensions, lateral view

The total number of gabion boxes that are going to be used for constructing one wall is 36, with this quantity it's possible to compute the total weight of a single wall.

$$W_T = 450 \text{ Kg} * 36$$

$$W_T = 16,200 \text{ Kg} = 16.2 \text{ Ton}$$

The slenderness of the wall has been verified using the Italian code, and the computation has been done below.

$$\lambda = \frac{h_0}{t} = \frac{3 \text{ m}}{0.5 \text{ m}} = 6$$

$$\lambda < \lambda_{crit}$$

$$6 < 20 \therefore \text{satisfy}$$

It's important to know the stress that will arrive to the ground in order to know if the soil under the walls is able to sustain the loads, thus it has been compute the stresses on each layer of the gabion wall that has the load of the roof and the results are presented below:

$$\sigma_{Ni} = \frac{\sum_{N=1}^i W_i}{A_s}$$

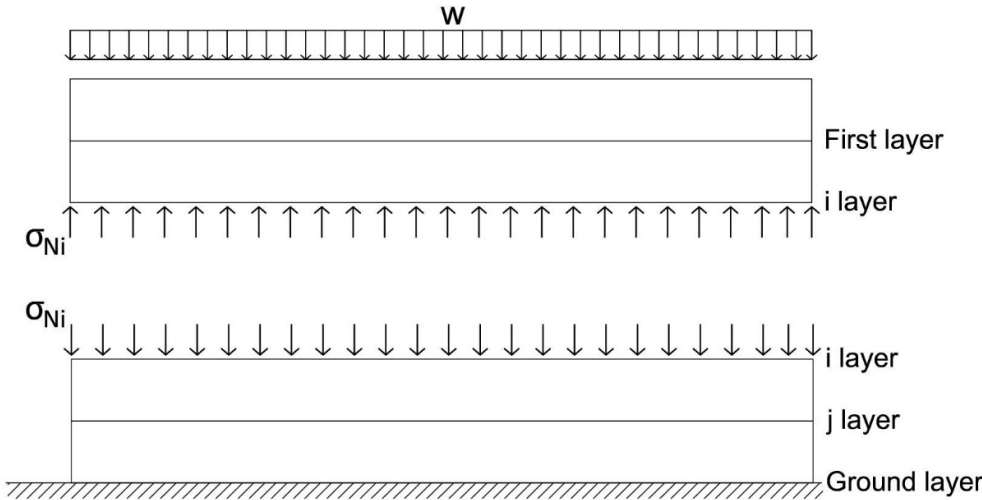


Fig. 3.5 - Normal stresses acting on each layer of the wall

Where:

$A_s$ = Surface area of each layer in  $m^2$

$W_i$ = weight above the layer of interest in Kg

$\sigma_i$ = Normal stress on the layer of interest

$$W_{roof} = \frac{200 \text{ Kg/m}^2 * 30 \text{ m}^2}{2} = 3000 \text{ Kg}$$

$$A_s = 6 \text{ m} * 0.5 \text{ m} = 3 \text{ m}^2$$

$$\sigma_{N1} = \frac{W_{roof} + W_{g1}}{A_s} = \frac{3000 + 2700}{3} = 1900 \text{ Kg/m}^2 = 0.19 \text{ Kg/cm}^2$$

$$\sigma_{N2} = \sigma_{N1} + \frac{W_{g2}}{A_s} = 1900 + \frac{2700}{3} = 2800 \text{ Kg/m}^2 = 0.28 \text{ Kg/cm}^2$$

$$\sigma_{N3} = \sigma_{N2} + \frac{W_{g3}}{A_s} = 2800 + \frac{2700}{3} = 3700 \text{ Kg/m}^2 = 0.37 \text{ Kg/cm}^2$$

$$\sigma_{N4} = \sigma_{N3} + \frac{W_{g4}}{A_s} = 3700 + \frac{2700}{3} = 4600 \text{ Kg/m}^2 = 0.46 \text{ Kg/cm}^2$$

$$\sigma_{N5} = \sigma_{N4} + \frac{W_{g5}}{A_s} = 4600 + \frac{2700}{3} = 5500 \text{ Kg/m}^2 = 0.55 \text{ Kg/cm}^2$$

$$\sigma_{ground} = \sigma_{N5} + \frac{W_{g6}}{A_s} = 5500 + \frac{2700}{3} = 6400 \text{ Kg/m}^2 = 0.64 \text{ Kg/cm}^2$$

### 3.4 Gabion box structure

The analysis that has been performed in the present study takes into account one-story buildings composed of gabion structural walls and a flexible diaphragm, where each of the principal elements (gabion walls) are mainly self-supporting.

The dimensions in plan of the structure that have been taken in consideration are shown in the figure below:

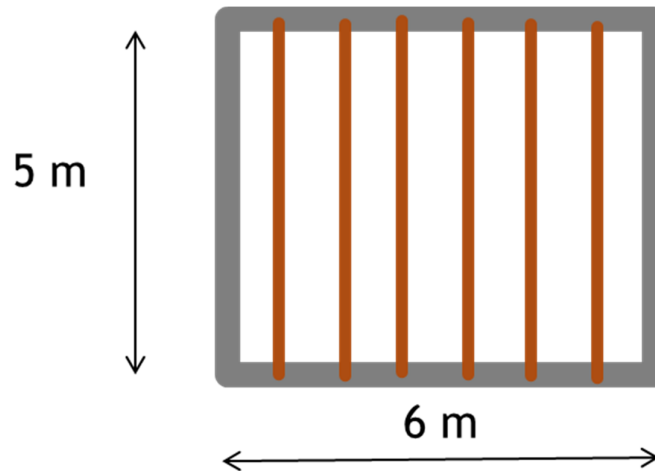


Fig. 3. 6 - Plan view of the gabion wall structure

It can be notice from the figure above that the load of the roof will be applied to the longest wall; hence, the wall that will be analyzed in the present investigation has a length of 6m.

### 3.4.1. Roof system

A flexible diaphragm has been considered for the analysis of the seismic behavior of the gabion wall. This assumption can be achieved using a light-weight timber roof structure as shown in the figure 3.7.

The roof load that has been considered is  $200 \text{ Kg/m}^2$ , this value takes into account a possible usage for storing goods.



Fig. 3. 7 - gabion box house with timber roof, picture given by A&D (Architecture and Developpement)

### 3.4.2. Openings

It has been considered the width of openings not higher than 1.0m, and the maximum high of the doors was considered 2.0m.

It has been detailed the way that the span of the opening should be constructed, this can be seen in the pictures below.

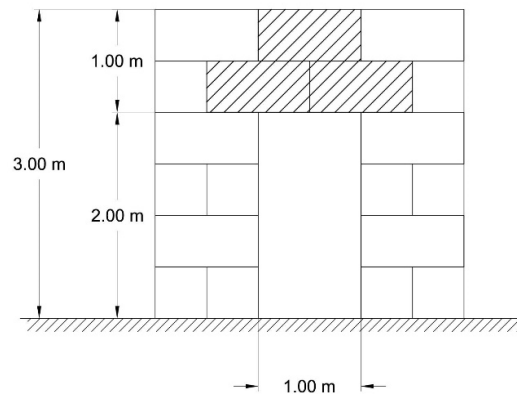


Fig. 3. 8 - Detail of “lintel” beam for openings

It can be noticed from the figure 3.8, that the gabions above the door are working as a cantilever beam if they have at least the half of the length inside the wall and with some weight over it in order to avoid uplifting of that part.

The detailing of the “lintel beam” was proven by Agostini et al., (1987), performing a bending test with a span of 3m and a maximum load of 20Ton.

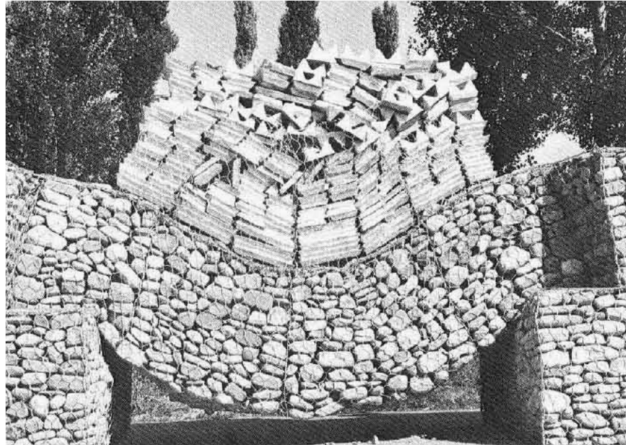


Fig. 3. 9 - Bending test with a span of 3.0m (Agostini et al., 1987)

Hence the gabions above the opening can be easily build without any other material to take forces, but it is recommended to introduce a timber beam in order to avoid large deformations of the gabion box if this timber it’s not considered.

It has been calculated the resistance of the timber over the door, considering twice the span of the door (Fig. 3.10), that is a distance where we can be sure that the timber beam will behave as a fix end support, and it’s in the safe side; the results are shown below.

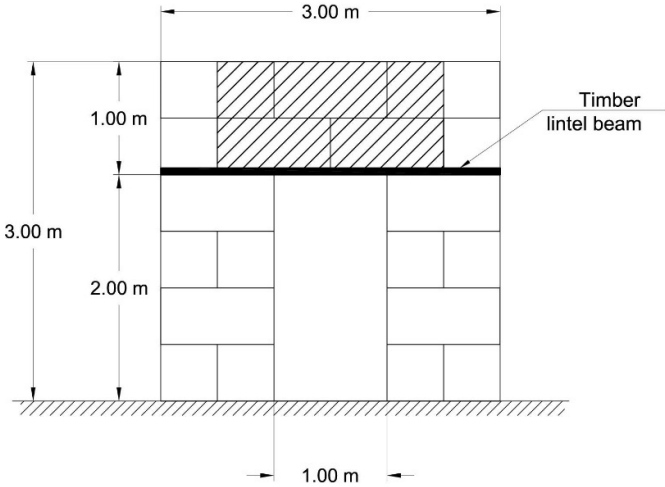


Fig. 3. 10 - Lintel timber beam

The uniform load that will be acting on the timber is:

$$q = \frac{4 \text{ blocks} * 450 \frac{Kg}{\text{block}}}{2 \text{ m}}$$

$$q = 900 \text{ kg/m}$$

The maximum moment acting on the beam is:

$$M = \frac{q * l^2}{12}$$

$$M = \frac{900 * 2^2}{12} = 300 \text{ kg * m} = 30000 \text{ kg * cm}$$

The dimensions considered for the timber beam are 24cm x 6 cm x 3m (B x thickness x length). It is going to be needed 2 timber beams, one next to the other in order to cover the thickness of the gabion wall.

Thus,

$$W = 2 * \frac{B * h^2}{6}$$

$$W = 2 * \frac{24 * 6^2}{6} = 288 \text{ cm}^3$$

$$\sigma = \frac{M}{W} = \frac{30000}{288} = 104 \text{ Kg/cm}^2$$

Additionally, it has been performed the same calculations considering the arch effect over the opening (Fig. 3.11), so this change the load that will arrive to the timber beam and also the span was reduced to 1.75m, and the results are shown below.

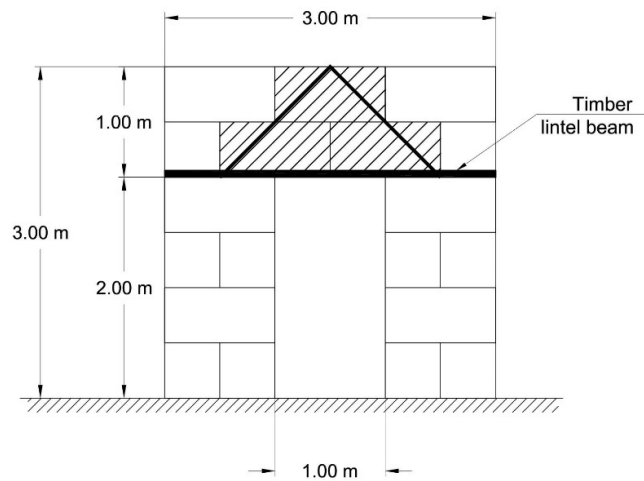


Fig. 3. 11 - Lintel timber beam considering the arch effect

The uniform load that will be acting on the timber is:

$$q = \frac{3 \text{ blocks} * 450 \frac{Kg}{\text{block}}}{1.75 \text{ m}}$$

$$q = 771 \text{ kg/m}$$

The maximum moment acting on the beam is:

$$M = \frac{q * l^2}{12}$$

$$M = \frac{771 * 1.75^2}{12} = 197 \text{ kg} * \text{m} = 19700 \text{ kg} * \text{cm}$$

Thus,

$$\sigma = \frac{M}{W} = \frac{19700}{288} = 68.44 \text{ Kg/cm}^2$$

Thereby, from the results obtained before, the selected section of timber is satisfactory.

### 3.4.3. Corners

The connection in a gabion structure between perpendicular wall is essential in the seismic behavior of the building; in order to have a properly response, the two orthogonal walls should be interlocked, simulating a “Lego” connection (Fig.3.10).

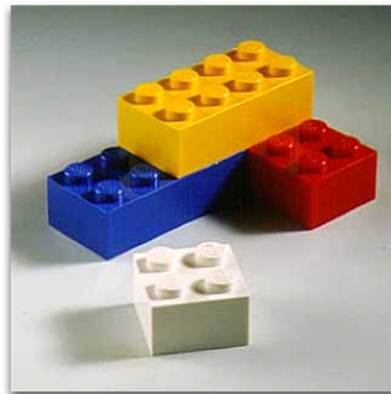


Fig. 3. 12 - "Lego" connection of perpendicular gabion walls.

### 3.4.4. Steel wire connectors

In order to be able to sustain lateral loads, it is necessary to include some reinforcements where the tension stresses appear, thereby is possible to achieve values at the connection with the perpendicular wall that are higher than the value that will cause sliding of the blocks. The tension stresses that will be acting on the gabion wall as well the amount of reinforcement needed for sustaining those stresses are computed in chapter 5 of this document.

It can be notice from the picture that the wire is working in pure shear only at the bended part, elsewhere the wire is working in tension.

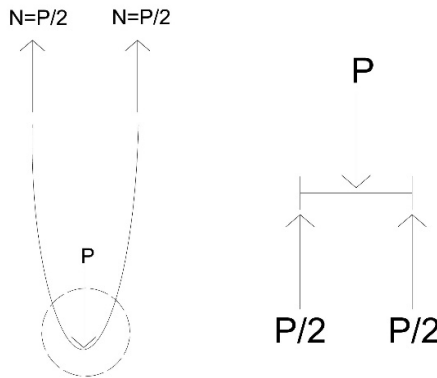


Fig. 3. 13 - Forces acting on the steel wire connectors

“The magnitude of the shear yield stress in pure shear is ( $\sqrt{3}$ ) times lower than the tensile yield stress in the case of simple tension” [4]. Thus, we have:

$$\tau \leq \frac{f_y}{\sqrt{3}}$$

The general shear stress for the forces acting on the wire is:

$$\tau \leq \frac{P}{2A}$$

Thus,

$$\frac{P}{2A} \leq \frac{f_y}{\sqrt{3}}$$

It has been assumed the yield stress of the steel as  $f_y=3000\text{kg/cm}^2$  and the diameter of the wire as  $\Phi=3\text{mm}$

$$A_{\Phi 3} = \frac{\pi * (0.3)^2}{4} = 0.0707 \text{ cm}^2$$



## **CHAPTER 4      IN-PLANE SEISMIC BEHAVIOR OF ONE STORY BUILDING STRUCTURES BUILT UP WITH GABION BOXES AND FLEXIBLE DIAPHRAGM**

### **4.1    General**

The seismic in-plane behavior of gabion boxes structures is the principal subject of this chapter, in order to start studying this kind of structures, it has been realized different verifications such as the shear resistance of the wall, the sliding between 2 consecutive layers of gabion boxes, these 2 verifications have been performed on each layer and considering different force distributions scenarios such as the total force applied at the top of the wall and also a uniform lateral distribution over the height of the wall, furthermore, it has been analyzed the effect of openings applying the kinematic theorem for masonry structures finding the loads that are necessary and sufficient to the existence of the masonry equilibrium.

For all the analysis that have been performed in this chapter, it has been assumed that the gabion wall behavior is influenced by a very low strength in tension comparing it with the high compression strength. It has been idealized the wall as rigid in compression and no tension as the Heyman masonry model does, considering the constitutive assumptions for this model that were formulated by Heyman (1966), such as; masonry is incapable of withstanding tension, masonry has infinite compressive strength and elastic strains are negligible.

### **4.2    Shear resistance of a gabion wall**

It has been computed the maximum shear force that will cause failure on the structure; this calculation has been performed considering failure upon each layer and taking into account that all the seismic force is applied on the top of the wall (Fig.4.1) and also considering a distribution on height of the lateral force (Fig.4.2), these calculations were carried out using the formula obtained from the shear test described in 2.3.2.

#### **4.2.1.    Shear resistance of a gabion wall with a force applied at the top**

The following equations are derived considering the force applied as shown on the figure below.

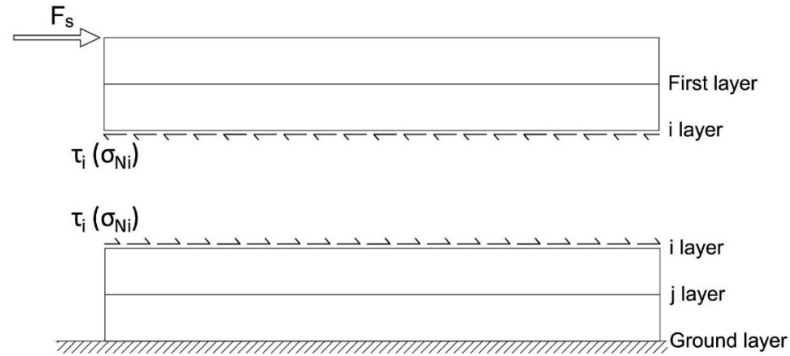


Fig. 4. 1 – Shear stress with force applied at the top of the wall.

$$F_s \leq \tau_i(\sigma_n) * A_s$$

Where:

$F_s$  = seismic force =  $\alpha (W_t + W_{roof})$

$\tau_i(\sigma_n)$  = shear stress upon each layer

$A_s$  = Surface area of each layer in  $cm^2$

$$\tau_i(\sigma_n) = 5.63 + 0.993 * \sigma_n [Kg/cm^2]$$

After substituting on the first equation, it has been obtained:

$$\alpha * (W_T + W_{roof}) \leq (5.63 + 0.993 * \sigma_n) * A_s$$

$$\alpha \leq \frac{(5.63 + 0.993 * \sigma_n) * A_s}{W_T + W_{roof}}$$

Using the equation above in order to obtain the factor  $\alpha$  with the respective values of the typical gabion wall, the results are presented below.

$W_t = 16200$  Kg

$W_{roof} = 3000$  Kg

$A_s = 600 \times 50 = 30000$   $cm^2$

First layer

$$\alpha \leq \frac{(5.63 + 0.993 * 0.19) * 30000}{19200} \leq 9.09$$

Second layer

$$\alpha \leq \frac{(5.63 + 0.993 * 0.28) * 30000}{19200} \leq 9.23$$

Third layer

$$\alpha \leq \frac{(5.63 + 0.993 * 0.37) * 30000}{19200} \leq 9.37$$

Fourth layer

$$\alpha \leq \frac{(5.63 + 0.993 * 0.46) * 30000}{19200} \leq 9.51$$

Fifth layer

$$\alpha \leq \frac{(5.63 + 0.993 * 0.55) * 30000}{19200} \leq 9.65$$

Sixth layer

$$\alpha \leq \frac{(5.63 + 0.993 * 0.64) * 30000}{19200} \leq 9.79$$

Looking the results, the factor  $\alpha$  that will cause shear failure considering the applied load on the top is  $\alpha=9.09$ , and will happen on the first layer of the single gabion wall.

#### 4.2.2. Shear resistance of a gabion wall with lateral distribution of forces on height.

In the following procedure for analyzing the shear resistance of a gabion wall, it has been performed a lateral distribution of the seismic force using the formula below:

$$F_j = F_s * \frac{W_j * h_j}{\sum_{i=1}^N W_i * h_i + W_{roof} * H}$$

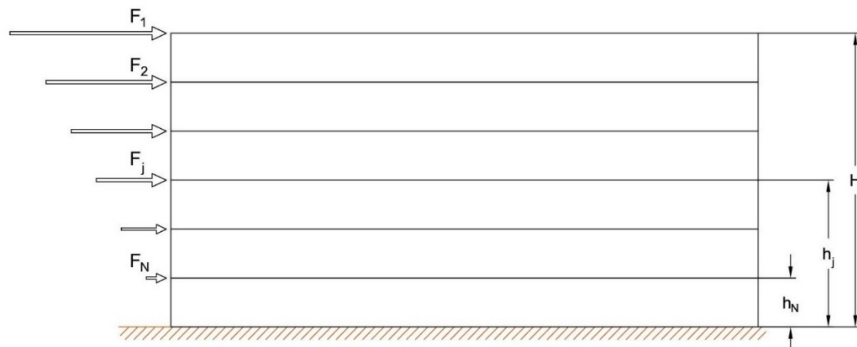


Fig. 4. 2 – Uniform lateral distribution over the height of the wall.

The evaluation of the shear resistance of the wall remain as:

$$\sum_{i=1}^j F_j \leq \tau_i(\sigma_n) * A_s$$

Where:

$F_j$ = distribute seismic force on each layer in Kg

$\tau_i(\sigma_n)$  = shear force upon each layer

$A_s$ = Surface area of each layer in  $cm^2$

$$\tau_i(\sigma_n) = 5.63 + 0.993 * \sigma_n \text{ [Kg/cm}^2\text{]}$$

After substituting on the first equation, it has been obtained:

$$\alpha * (W_T + W_{roof}) * \sum_{i=i}^j \frac{W_j * h_j}{\sum_{i=1}^N W_i * h_i + W_{roof} * H} \leq (5.63 + 0.993 * \sigma_n) * A_s$$

$$\alpha \leq \frac{(5.63 + 0.993 * \sigma_n) * A_s}{(W_T + W_{roof}) * \sum_{i=i}^j \frac{W_j * h_j}{\sum_{i=1}^N W_i * h_i + W_{roof} * H}}$$

Using the equation above in order to obtain the factor  $\alpha$  with the respective values of the typical gabion wall, the results are presented below.

$$W_t = 16200 \text{ Kg}$$

$$W_{roof} = 3000 \text{ Kg}$$

$$A_s = 600 \times 50 = 30000 \text{ cm}^2$$

It has been performed the distribution of the lateral forces and the results are shown below.

$$\sum_{i=1}^N W_i * h_i + W_{roof} * H = 2700 * (0.5 + 1 + 1.5 + 2 + 2.5 + 3) + 3000 * 3$$

$$\sum_{i=1}^N W_i * h_i + W_{roof} * H = 37350$$

$$F_1 = F_s * \frac{(2700 + 3000) * 3}{37350} = 0.458 * F_s$$

$$F_2 = F_s * \frac{2700 * 2.5}{37350} = 0.181 * F_s$$

$$F_3 = F_s * \frac{2700 * 2}{37350} = 0.145 * F_s$$

$$F_4 = F_s * \frac{2700 * 1.5}{37350} = 0.108 * F_s$$

$$F_5 = F_s * \frac{2700 * 1}{37350} = 0.072 * F_s$$

$$F_6 = F_s * \frac{2700 * 0.5}{37350} = 0.036 * F_s$$



Fig. 4. 3 – Results of the distribution of forces over the height of the wall.

First layer

$$\alpha \leq \frac{(5.63 + 0.993 * 0.19) * 30000}{19200 * 0.458} \leq 19.85$$

Second layer

$$\alpha \leq \frac{(5.63 + 0.993 * 0.28) * 30000}{19200 * (0.458 + 0.181)} \leq 14.45$$

Third layer

$$\alpha \leq \frac{(5.63 + 0.993 * 0.37) * 30000}{19200 * (0.639 + 0.145)} \leq 11.95$$

Fourth layer

$$\alpha \leq \frac{(5.63 + 0.993 * 0.46) * 30000}{19200 * (0.784 + 0.108)} \leq 10.66$$

Fifth layer

$$\alpha \leq \frac{(5.63 + 0.993 * 0.55) * 30000}{19200 * (0.892 + 0.072)} \leq 9.85$$

Sixth layer

$$\alpha \leq \frac{(5.63 + 0.993 * 0.64) * 30000}{19200 * (0.964 + 0.036)} \leq 9.79$$

Looking the results, the factor  $\alpha$  that will cause shear failure considering the lateral distribution of load is  $\alpha=9.79$ , and will happen on the bottom layer of the single gabion wall.

**4.3 Sliding resistance of a gabion wall.**

The mechanism against the sliding of two consecutive layers of the gabion wall is the friction force that will develop on an earthquake, this friction should be able to oppose the force coming from the seismic action  $F_s$  in order to prevent a relative movement of layers; in order to evaluate this, it has been considered the seismic force at the top and a lateral distribution of forces on height such as it has been done with the evaluation of the shear resistance.

The Mohr-Coulomb friction hypothesis has been used to determine the friction coefficient that is needed in order to sustain a certain load multiplier. Thus, the relation of the friction force is expressed as:

$$F_f = c * A_s + \mu * N$$

Where:

$\mu$ =friction coefficient

$c$ = cohesion of the material

**4.3.1. Sliding resistance of a gabion wall with force applied at the top**

In the following procedure for analyzing the sliding resistance of a gabion wall, it has been considered that all the force is applied at the top of the wall, in order to obtain the minimum friction coefficient to avoid failure due to the seismic force.

The following equation is derived considering the force applied at the top of the wall as shown on the figure 4.4.

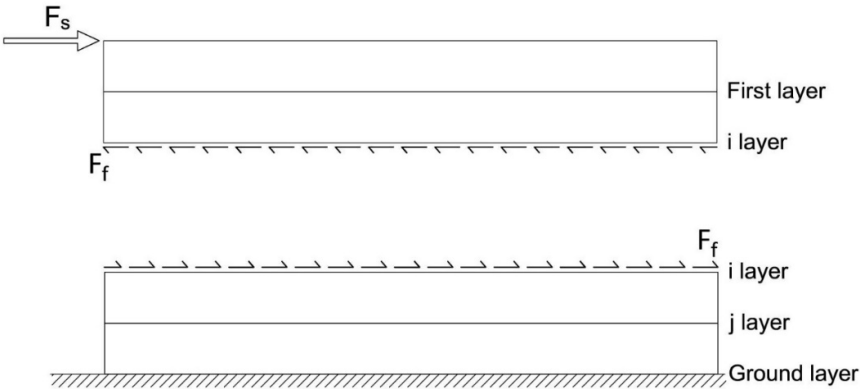


Fig. 4. 4 – Friction force with a force applied at the top of the wall.

$$F_s \leq F_f$$

$$F_f = c * A_s + \mu * N = c * A_s + \mu * \sigma_N * A_s$$

Where:

$F_s$ = seismic force=  $\alpha (W_t + W_{roof})$

$F_f$ = Friction force

$A_s$ = Surface area of each layer in  $cm^2$

After substituting on the first equation, it has been obtained:

$$\alpha * (W_T + W_{roof}) \leq c * A_s + \mu * \sigma_n * A_s$$

$$\frac{\alpha * (W_T + W_{roof}) - c * A_s}{\sigma_n * A_s} \leq \mu$$

Using the equation above in order to obtain the friction coefficient  $\mu$  with the respective values of the typical gabion wall; the results are presented below.

$W_t=16200$  Kg

$W_{roof}=3000$ Kg

$A_s= 600 \times 50= 30000$   $cm^2$

$c=0.2$  kg/ $cm^2$

First layer

$$\mu \geq \frac{19200 * \alpha - 0.2 * 30000}{0.19 * 600 * 50} \geq 3.36 * \alpha - 1.05$$

Second layer

$$\mu \geq \frac{19200 * \alpha - 0.2 * 30000}{0.28 * 600 * 50} \geq 2.28 * \alpha - 0.71$$

Third layer

$$\mu \geq \frac{19200 * \alpha - 0.2 * 30000}{0.37 * 600 * 50} \geq 1.73 * \alpha - 0.54$$

Fourth layer

$$\mu \geq \frac{19200 * \alpha - 0.2 * 30000}{0.46 * 600 * 50} \geq 1.39 * \alpha - 0.43$$

Fifth layer

$$\mu \geq \frac{19200 * \alpha - 0.2 * 30000}{0.55 * 600 * 50} \geq 1.16 * \alpha - 0.36$$

Sixth layer

$$\mu \geq \frac{19200 * \alpha - 0.2 * 30000}{0.64 * 600 * 50} \geq 1.00 * \alpha - 0.31$$

Looking the results, the minimum friction coefficient that it's needed for avoiding sliding considering the applied load on the top is  $3.36 * \alpha - 1.05$ , and failure will happen first on the top layer of the single gabion wall.

In the following table it has been obtained the minimum friction coefficient that is needed to sustain a specific ground acceleration.

		$\alpha=0.1g$	$\alpha=0.2g$	$\alpha=0.3g$	$\alpha=0.4g$	$\alpha=0.5g$
Friction coefficient on each layer considering an applied force at the top of the wall	$\mu_1$	-0.716	-0.379	-0.042	0.295	0.632
	$\mu_2$	-0.486	-0.257	-0.029	0.200	0.429
	$\mu_3$	-0.368	-0.195	-0.022	0.151	0.324
	$\mu_4$	-0.296	-0.157	-0.017	0.122	0.261
	$\mu_5$	-0.247	-0.131	-0.015	0.102	0.218
	$\mu_6$	-0.213	-0.113	-0.013	0.088	0.188

Table 4. 1 - Friction coefficient needed to sustain a certain value of  $\alpha$  considering the force applied at the top

It can be notice that for low values of ground accelerations, the friction coefficient needed to avoid sliding has negative values, which means that it is enough with the cohesion of the material to resist the sliding of 2 consecutive gabion boxes.

In the other hand, for high values of ground acceleration the friction coefficient needed is increasing, being the most unfavorable layer the one at the top of the wall; this results are conservative because we are considering that all the force is applied at the top of the gabion wall and neglecting the cohesion of the material.

**4.3.2. Sliding resistance of a gabion wall with lateral distribution on height.**

In the following procedure for analyzing the sliding resistance of a gabion wall, it has been performed the lateral distribution of the seismic force on height as it was done before, in order to obtain the minimum friction coefficient to avoid failure due to the seismic force.

The following equation is derived considering a distribution of the force over the height of the wall as shown on the figure 4.5.

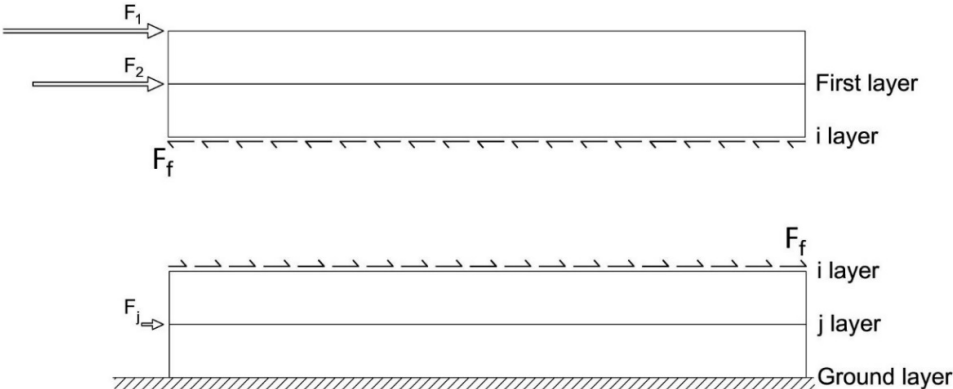


Fig. 4. 5 – Friction force with lateral distribution over the height.



$$\sum_{i=1}^j F_j \leq F_f$$

$$\sum_{i=1}^j F_j = F_s * \sum_{i=i}^j \frac{W_j * h_j}{\sum_{i=1}^N W_i * h_i + W_{roof} * H}$$

$$F_f = c * A_s + \mu * N = c * A_s + \mu * \sigma_N * A_s$$

Where:

$F_s$ = seismic force=  $\alpha (W_t + W_{roof})$

$F_f$ = Friction force

$F_j$ =distribute seismic force on each layer

$A_s$ = Surface area of each layer in  $cm^2$

$c=0.2 \text{ kg/cm}^2$

After substituting on the first equation, it has been obtained:

$$\alpha * (W_T + W_{roof}) * \sum_{i=i}^j \frac{W_j * h_j}{\sum_{i=1}^N W_i * h_i + W_{roof} * H} \leq c * A_s + \mu * \sigma_N * A_s$$

$$\frac{\alpha * (W_T + W_{roof}) * \sum_{i=i}^j \frac{W_j * h_j}{\sum_{i=1}^N W_i * h_i + W_{roof} * H} - c * A_s}{\sigma_n * A_s} \leq \mu$$

It has been used the equation above in order to obtain the required friction coefficient  $\mu$  in order to prevent sliding, with the respective values of the typical gabion wall, the results are presented below.

First layer

$$\mu \geq \frac{19200 * \alpha * 0.458 - 0.2 * 30000}{0.19 * 600 * 50} \geq 1.543 * \alpha - 1.05$$

Second layer

$$\mu \geq \frac{19200 * \alpha * (0.458 + 0.181) - 0.2 * 30000}{0.28 * 600 * 50} \geq 1.461 * \alpha - 0.71$$

Third layer

$$\mu \geq \frac{19200 * \alpha * (0.639 + 0.145) - 0.2 * 30000}{0.37 * 600 * 50} \geq 1.356 * \alpha - 0.54$$

Fourth layer

$$\mu \geq \frac{19200 * \alpha * (0.784 + 0.108) - 0.2 * 30000}{0.46 * 600 * 50} \geq 1.241 * \alpha - 0.43$$

Fifth layer

$$\mu \geq \frac{19200 * \alpha * (0.892 + 0.072) - 0.2 * 30000}{0.55 * 600 * 50} \geq 1.122 * \alpha - 0.36$$

Sixth layer

$$\mu \geq \frac{19200 * \alpha * (0.964 + 0.036) - 0.2 * 30000}{0.64 * 600 * 50} \geq 1.00 * \alpha - 0.31$$

In the table below it has been obtained the required friction coefficient that is needed in order to sustain a specific ground acceleration.

		$\alpha=0.1g$	$\alpha=0.2g$	$\alpha=0.3g$	$\alpha=0.4g$	$\alpha=0.5g$
Friction coefficient on each layer considering a distribution of the force on the height of the wall	$\mu_1$	-0.898	-0.744	-0.590	-0.436	-0.281
	$\mu_2$	-0.568	-0.422	-0.276	-0.130	0.016
	$\mu_3$	-0.405	-0.269	-0.134	0.002	0.138
	$\mu_4$	-0.311	-0.187	-0.062	0.062	0.186
	$\mu_5$	-0.251	-0.139	-0.027	0.085	0.197
	$\mu_6$	-0.213	-0.113	-0.013	0.088	0.188

Table 4. 2 - Friction coefficient needed to sustain a certain value of  $\alpha$  considering a force distribution on height.

It can be observed from the results of the table above, that for most of the cases when a negative value was obtained, it is enough with the cohesion of the material to resist the sliding of consecutive layers; for higher values of the load multiplier, it has been obtained very low friction coefficients in order to have failure on bottom part of the gabion wall, which means that a gabion walls are not prone to sliding considering this configuration of forces.

#### 4.4 In-plane behavior of a gabion walls considering openings.

It has been performed the analysis for a single wall applying the kinematic theorem for masonry considering the rigid-no tension model. Using this theorem, it's not going to be found the collapse multiplier, which would imply that it has to be determine the minimum of all the set of kinematically admissible multipliers, hence it has been computed 2 different admissible multipliers and the result are presented below.

First of all, it has been considered the gabion wall shown below in order to calculate the first mechanism that is going to be performed in this analysis. It can be notice that A is lower than C.

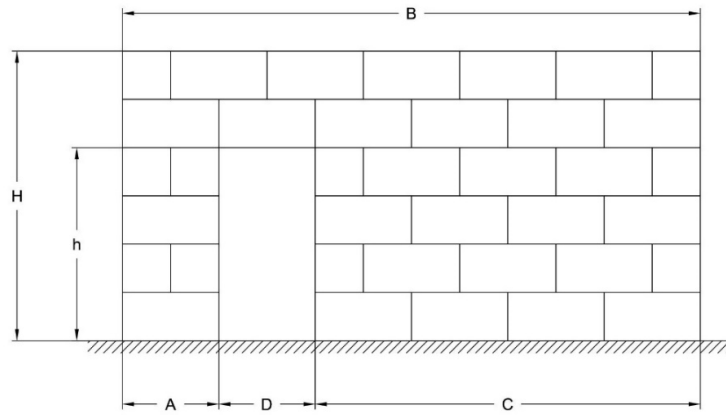


Fig. 4. 6 – Gabion wall with opening, with A lower than C.

Considering the following location of the hinges

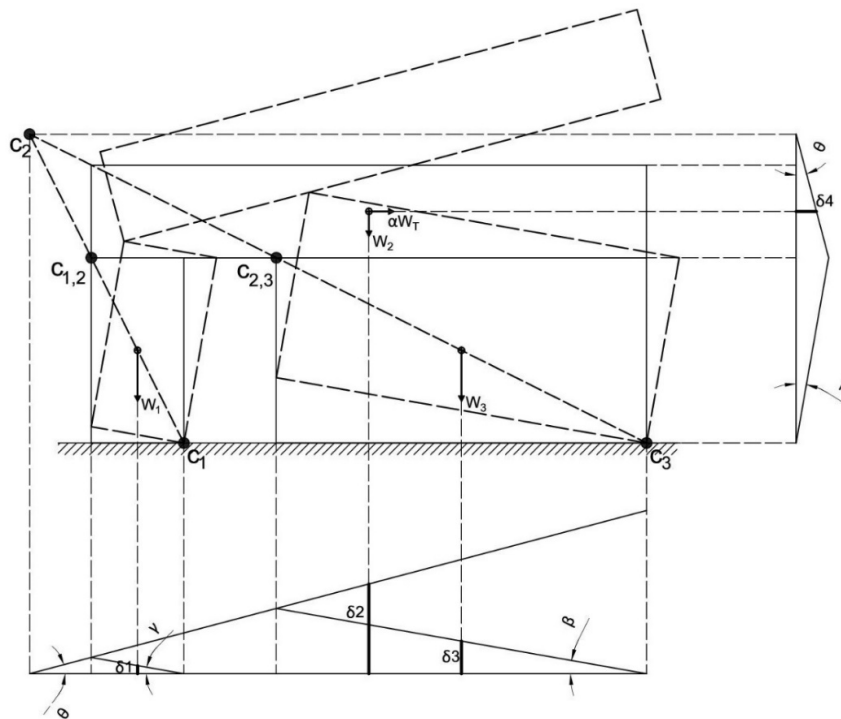


Fig. 4. 7 – Location of hinges when A is lower than C.

It has been assigned the location of four hinges in order to have a mechanism, thus, the center of rotations  $C_1$  and  $C_3$  are known, in addition the relative centers of rotation  $C_{1,2}$  and  $C_{2,3}$  are known. The rule of the centers of rotation allows to determine the location of the center  $C_2$  that is the one for the top block of the wall.

The location of  $C_2$  can be determined using the equations of the lines of each center of rotation with the respective relative center of rotation, considering the origin on the left bottom corner of the wall, then finding the intersection between them.

The corresponding equation for each line are presented below:

$$\text{For line } C_3 - C_{2,3} \text{ the equation is } y = -\frac{h}{C} * x + \frac{B}{C} * h$$

$$\text{For line } C_1 - C_{1,2} \text{ the equation is } y = -\frac{h}{A} * x + h$$

After performing the intersection between the 2 lines, it has been obtained the coordinates of the center of rotation  $C_2$ .

$$x = \frac{A * (B - C)}{A - C} \quad \text{and} \quad y = \frac{h * (C - B)}{A - C} + h$$

Knowing that  $A < C$  and  $C < B$ , the results can be rewritten as:

$$x = -\frac{A * (B - C)}{C - A} \quad \text{and} \quad y = \frac{h * (B - C)}{C - A} + h$$

The principal of virtual works (PVW) yields:

$$\begin{aligned} -W_1 * \delta 1 - W_2 * \delta 2 - W_3 * \delta 3 + \alpha * W_{tot} * \delta 4 = 0 \\ -W_1 * \gamma * \frac{A}{2} - W_2 * \theta * \left( \frac{A * (B - C)}{C - A} + \frac{B}{2} \right) - W_3 * \beta * \frac{C}{2} + \alpha * W_{tot} * \theta \\ * \left[ \left( \frac{h * (B - C)}{C - A} + h \right) - \left( \frac{H + h}{2} \right) \right] = 0 \end{aligned}$$

Where:

$$t = \text{thickness of the wall} = 0.5m$$

$$W_1 = \gamma_g * t * A * h = 0.5 * \gamma_g * A * h$$

$$W_2 = \gamma_g * t * B * (H - h) = 0.5 * \gamma_g * B * (H - h)$$

$$W_3 = \gamma_g * t * C * h = 0.5 * \gamma_g * C * h$$

$$W_{tot} = \gamma_g * t * (A * h + B * h - B * h + C * h) = 0.5 * \gamma_g * (A * h + B * H - B * h + C * h)$$

$$\alpha = \beta, \text{ this has been obtained from the graphic of rotation (Fig. xxx)}$$

The relation between  $\theta$  and  $\beta$  has been performed with relationship of triangles, as follows:

$$\theta * \left[ \left( \frac{h * (B - C)}{C - A} + h \right) - h \right] = \beta * h$$

$$\theta = \frac{(C - A) * \beta * h}{h * (B - C)} = \frac{(C - A)}{(B - C)} * \beta$$

Substituting all the parameters, the PVW is written as:

$$\begin{aligned} -0.5 * \gamma_g * A * H * \frac{A}{2} * \beta - 0.5 * \gamma_g * B * (H - h) * \frac{(C - A)}{(B - C)} * \left( \frac{A * (B - C)}{C - A} + \frac{B}{2} \right) * \beta \\ - 0.5 * \gamma_g * C * H * \frac{C}{2} * \beta + \alpha * 0.5 * \gamma_g * (A * h + B * h - B * h + C * h) \\ * \frac{(C - A)}{(B - C)} * \left[ \left( \frac{h * (B - C)}{C - A} + h \right) - \left( \frac{H + h}{2} \right) \right] * \beta = 0 \end{aligned}$$

The foregoing equation can be simplified and the kinematically admissible multiplier  $\alpha$  can be determined.

$$\alpha = \frac{[A * (B - 2C) + BC] * (B * H) + [A^2 * (B - C) - A * B * (B - 2C) - (B^2 - BC + C^2) * C] * h}{[B * H + (A - B + C) * h] * [(A - C) * H - (A - 2B + C) * H]}$$

Using the following dimensions of the wall and substituting on the previous equation, it has been obtained:

$$H=3\text{m}, B=6\text{m}, h=2\text{m}, D=1\text{m}$$

$$A = B - D - C = 6 - 1 - C$$

$$A = 5 - C, \quad \text{where } A < C$$

$$\alpha = \frac{2C^3 - 28C^2 + 115C - 240}{8 * (6C - 29)}$$

It has been considered different values for “A” and “C” in order to understand how “ $\alpha$ ” varies when changing those parameters.

	A (m)	C (m)	$\alpha$ (g)
Configuration 1	1.00	4.00	2.50
Configuration 2	1.50	3.50	1.48
Configuration 3	2.00	3.00	1.06

It can be notice how the kinematic multiplier  $\alpha$  is decreasing when “A” and “C” tends to be equal, in order to verify this, it has been considered the second possible mechanism with the gabion wall shown below, imposing that A=C.

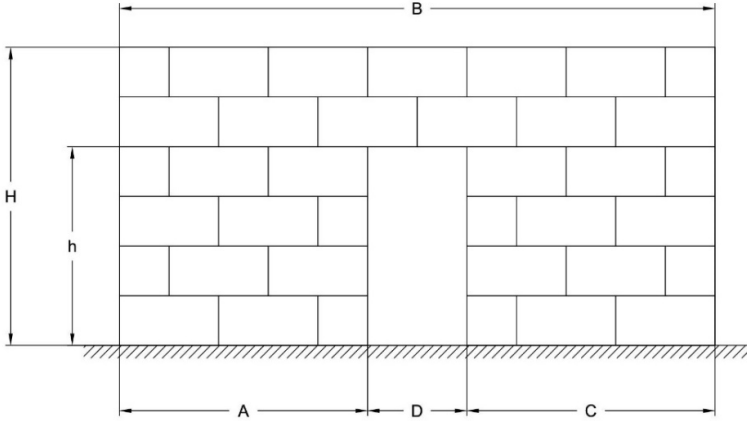


Fig. 4. 8 – Gabion wall with opening, with A equal to C.

Considering the following location of the hinges

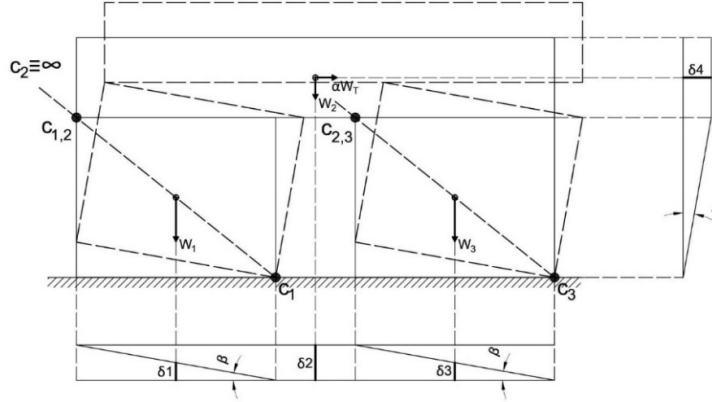


Fig. 4. 9 – Location of hinges when A is equal to C.

It has been assigned the location of the hinges in order to have a possible mechanism, the rule of the centers of rotation allows to determine the center of rotation  $C_2$ , that in this case is at infinite (there will never be an intersection between the two lines) and this means that the top block of the wall will translate but doesn't rotate.

The PVW yields:

$$\begin{aligned} -W_1 * \delta_1 - W_2 * \delta_2 - W_3 * \delta_3 + \alpha * W_{tot} * \delta_4 &= 0 \\ -W_1 * \frac{A}{2} * \beta - W_2 * A * \beta - W_3 * \frac{A}{2} * \beta + \alpha * W_{tot} * h * \beta &= 0 \end{aligned}$$

Where:

$t = \text{thickness of the wall} = 0.5\text{m}$

$W_1 = W_3 = \gamma_g * t * A * h = 0.5 * \gamma_g * A * h$

$W_2 = \gamma_g * t * B * (H - h) = 0.5 * \gamma_g * B * (H - h)$

$W_{tot} = \gamma_g * t * (2A * h + B * H - B * h) = 0.5 * \gamma_g * (2A * h + B * H - B * h)$

Substituting all the parameters, the PVW is written as:

$$-0.5 * \gamma_g * A * h * A - 0.5 * \gamma_g * B * (H - h) * A + \alpha * (2A * h + B * H - B * h) * h = 0$$

Which provides the kinematically admissible multiplier  $\alpha$  when "A=C"

$$\alpha = \frac{A^2 * h + AB * (H - h)}{(2Ah + BH - Bh) * h}$$

Considering the following dimension,  $H=3\text{m}$ ,  $B=6\text{m}$ ,  $h=2\text{m}$ ,  $D=1\text{m}$ , and substituting them on the previous equation in order to find the value of the load multiplier, that has been reported below.

$$\begin{aligned} A &= \frac{B - D}{2} = \frac{6 - 1}{2} = 2.5 \\ \alpha &= 0.859 \end{aligned}$$

It can be notice that this configuration gives the lowest multiplier, which means that is better to use a configuration where  $A \neq C$  in order to have better behavior against lateral forces.

**CHAPTER 5 OUT-OF-PLANE SEISMIC BEHAVIOR OF ONE STORY BUILDING STRUCTURES BUILT UP WITH GABION BOXES AND FLEXIBLE DIAPHRAGM**

**5.1 General**

The seismic out-of-plane behavior of gabion boxes structures is the principal subject of this chapter, the assumptions that have been made in this section are the same that were discussed at the in-plane behavior of the gabion walls.

In order to study the behavior of the gabion wall in the out-of-plane failure mechanism, it has been performed the analysis applying the kinematic theorem for masonry structures considering the soil below the structure as rigid and also performing an analysis taking into account the supports at the base of the wall as springs and performing equilibrium of moments, both approaches are considering the element of interest without perpendicular walls, this is a conservative assumption, afterwards, it has been taken into account the effect of the corners considering a constant cohesion force in height.

Furthermore, it has been performed an analysis of a horizontal strip at the top and bottom of the wall considering the friction force between 2 consecutive layers and a rigid body motion, these calculations have been done in order to find the flexural behavior in the out-of-plane of the wall. Additionally, in this chapter it has been performed a FEM and DEM model in order to verify the results done by hand and obtaining further information that helps to understand the seismic behavior of the gabion walls, such as maximum displacements and tension stresses due to a certain load multiplier and a specific length between perpendicular walls.

All the previous cases of study mentioned before are resumed in the following picture:

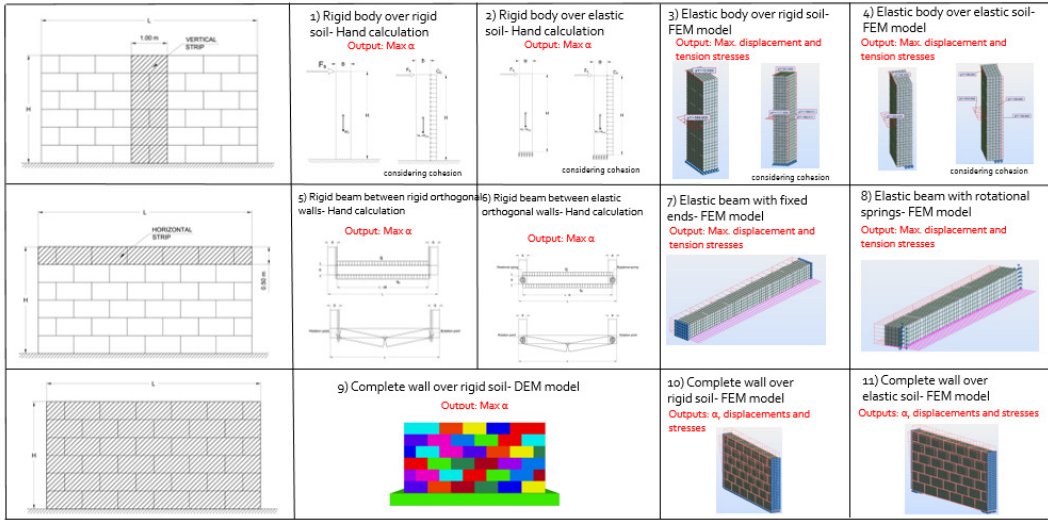


Fig. 5. 1 - Cases of study for the out-of-plane behavior

## 5.2 Out-of-plane behavior of a rigid vertical strip

In order to start the study of the behavior in the out-of-plane of a single gabion wall, it has been selected a vertical portion of the gabion wall (Fig. 5.2) and performing the analysis for different scenarios, in order to find the maximum load multiplier that a gabion wall can sustain under these considerations.

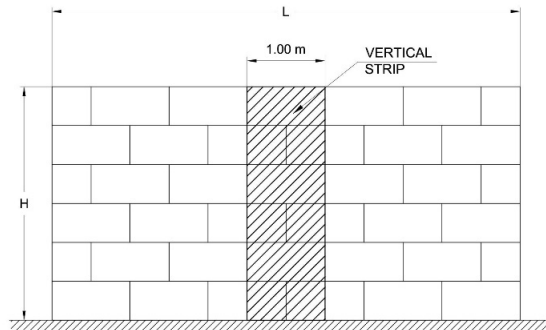


Fig. 5. 2 - Vertical strip of the gabion wall

### 5.2.1. Rigid body over rigid soil – hand calculations.

#### Rigid body over rigid soil, with a force applied at the top of the wall.

Considering a system of forces as shown in the figure 5.3, it has been calculated the load multiplier for the selected mechanism, that is considering the hinge on the right bottom corner of the wall (Fig. 5.4) and another location of the hinge in a general height of the external face of the wall (Fig. 5.5); the different locations of the hinges have been selected due to the fact that, it's not going to be found the collapse multiplier, which would imply that it has to be determine the minimum of all the set of kinematically admissible multipliers, hence it has been computed the 2 different admissible multipliers mentioned before and the result are presented below.

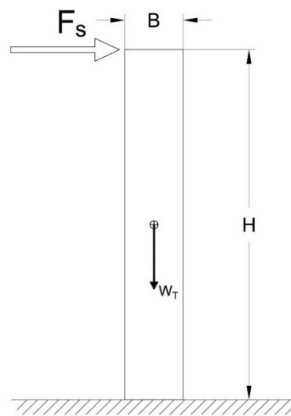


Fig. 5. 3 – Rigid body over rigid soil with a force applied at the top.



Considering the first location of the hinge, as show below.

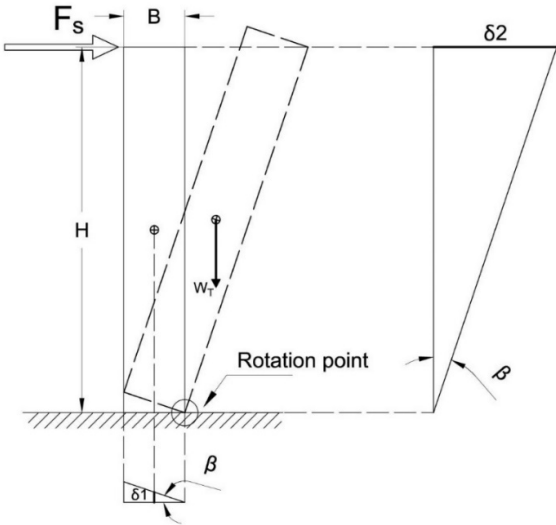


Fig. 5. 4 - Hinge at the base with a force applied at the top of the wall

The PVW for the actual mechanism yields:

$$F_s * \delta 2 - W_t * \delta 1 = 0$$

Where:

$$F_s = \text{seismic force} = \alpha * W_t$$

The PVW is written as:

$$\alpha * (W_t) * H * \beta - W_t * \frac{B}{2} * \beta = 0$$

$$\alpha = \frac{W_t * B}{W_t * 2 * H}$$

$$\alpha = \frac{B}{2 * H}$$

It can be notice that in the previous equation appears only geometrical parameters of the wall in the plane of analysis, therefore this equation governs disregarding the length and the weight of the wall.

Taking into account the dimensions of the wall considered in this document,  $H=3\text{m}$ ,  $B=0.5\text{m}$ , and substituting them on the previous equation, the load multiplier obtained is reported below.

$$\alpha = \frac{0.5}{2 * 3} = 0.083$$

Considering a general location of the hinge, as show below.

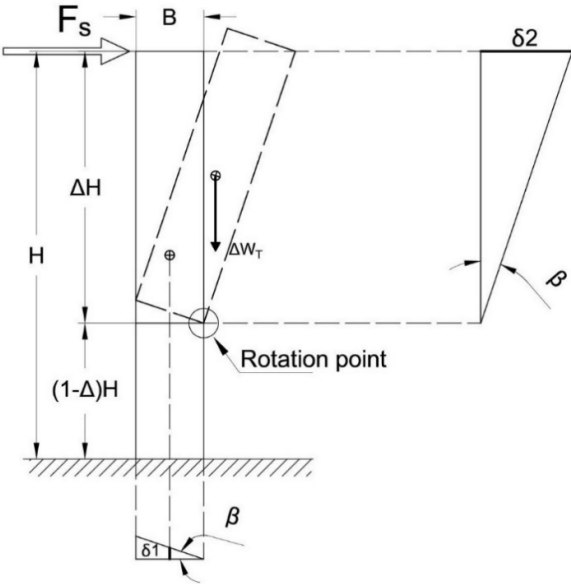


Fig. 5. 5 - Hinge at at general position with a force applied at the top of the wall

The PVW yields:

$$F_s * \delta 2 - \Delta W_t * \delta 1 = 0$$

Where:

$F_s = \text{seismic force} = \alpha * W_t$

$\Delta = \text{proportional multiplier between 0 and 1}$

The PVW is written as:

$$\alpha * (W_t) * \Delta * H * \beta - \Delta * W_t * \frac{B}{2} * \beta = 0$$

$$\alpha = \frac{\Delta * W_t * B}{\Delta * W_t * 2 * H}$$

$$\alpha = \frac{B}{2 * H}$$

As it can be notice it has been obtained the same general equation as before, which indicates that under this assumption, the failure mechanism can be developed on the external side of the wall at any position on height, with the same lateral force applied at the top.

**Rigid body over rigid soil, considering the cohesion and a force applied at the top of the wall.**

It has been considered the cohesion due to the perpendicular walls on this configuration, as shown on the following figure.

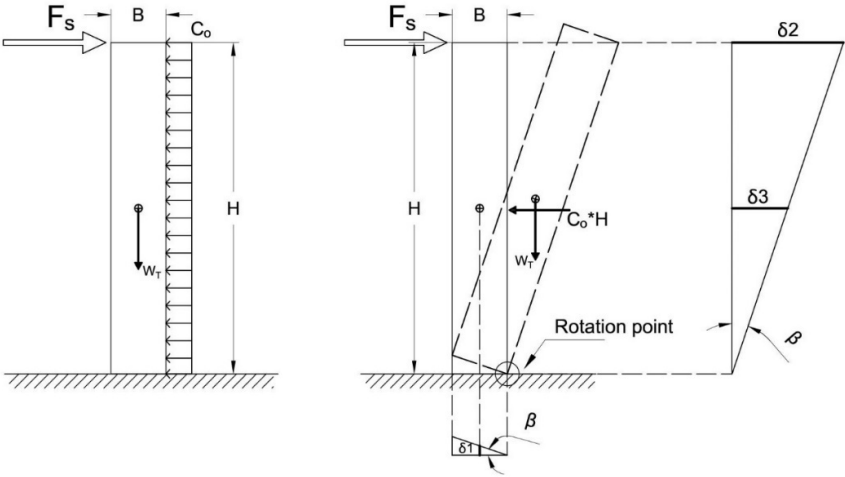


Fig. 5. 6 - Rigid body over rigid soil, considering the cohesion and a force applied at the top.

The PVW for the actual mechanism yields:

$$F_s * \delta 2 - W_t * \delta 1 - 2 * C_o * H * \delta 3 = 0$$

Where:

$F_s = \text{seismic force} = \alpha * W_t$

$C_o = C * B$ , where  $c$  is the cohesion value.

It has been considered twice the cohesion force due to both perpendicular walls.

The PVW is written as:

$$\alpha * (W_t) * H * \beta - W_t * \frac{B}{2} * \beta - 2 * C * B * H * \frac{H}{2} * \beta = 0$$

$$\alpha = \frac{W_t * B}{W_t * 2 * H} + \frac{C * B * H^2}{H * W_t}$$

$$\alpha = \frac{B}{2 * H} + \frac{C * B * H}{W_t}$$

It can be notice that in the previous equation, the effect of the cohesion is increasing the load multiplier that the wall can sustain which helps to improve the out-of-plane behavior of the gabion wall.

Substituting the parameters of the wall on the previous equation, it has been obtained the following load multiplier.

$$C=2000 \text{ kg/m}^2$$

$$\alpha = \frac{0.5}{2 * 3} + \frac{2000 * 0.5 * 3}{19200} = 0.239$$

**Rigid body over rigid soil, with two forces applied on the wall.**

It has been performed another computation of the load multiplier considering the first location of the hinge and considering the force due to the weight of the roof and the force due to the weight of the wall in different positions, this can be seen on the following picture.

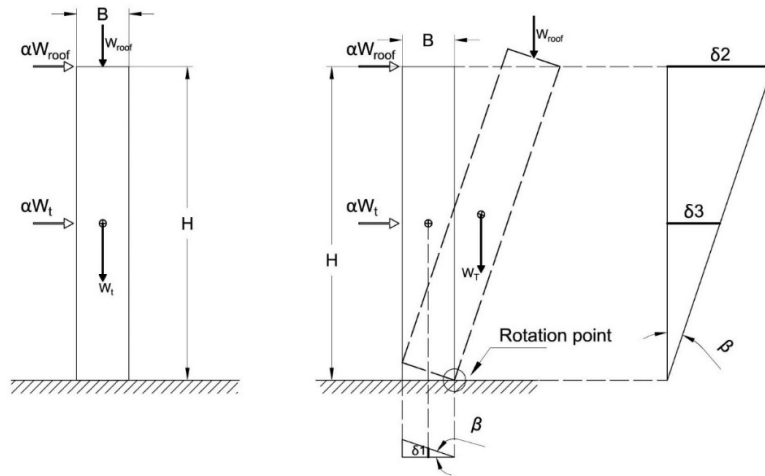


Fig. 5. 7 - Rigid body over rigid soil with 2 forces applied on the wall.

The PVW for the actual mechanism yields:

$$\alpha * W_{roof} * \delta 2 + \alpha * W_t * \delta 3 - (W_{roof} + W_t) * \delta 1 = 0$$

$$\alpha * W_{roof} * H * \beta + \alpha * W_t * \frac{H}{2} * \beta - (W_{roof} + W_t) * \frac{B}{2} * \beta = 0$$

$$\alpha * H * \left( W_{roof} + \frac{W_t}{2} \right) = \frac{(W_{roof} + W_t) * B}{2}$$

$$\alpha = \frac{B}{2 * H} * \frac{(W_{roof} + W_t)}{\left( W_{roof} + \frac{W_t}{2} \right)}$$

Taking into account the dimensions and weights of the wall considered in this document, H=3m, B=0.5m, and substituting them on the previous equation, the load multiplier obtained is reported below.

$$\alpha = \frac{0.5}{2 * 3} * \frac{(3000 + 16200)}{\left(3000 + \frac{16200}{2}\right)} = 0.144$$

As it can be seen, the value of the load multiplier  $\alpha$  is higher than the one computed before considering the total force applied at the top which makes the calculations conservative.

Considering a general location of the hinge, as show below.

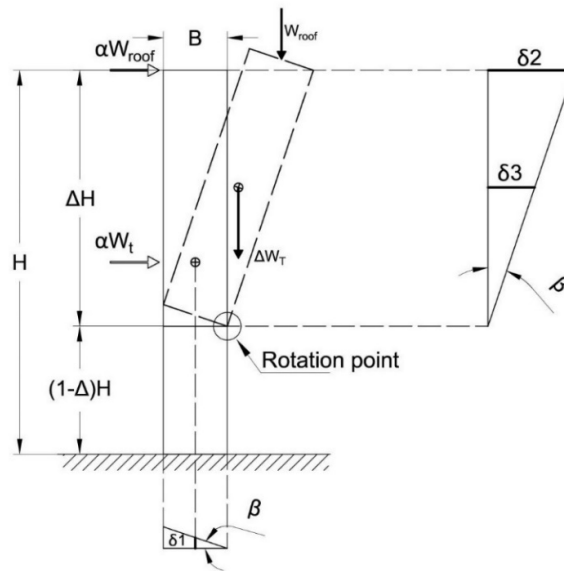


Fig. 5. 8 - Hinge at general position with 2 forces applied in the wall.

The PVW for  $\Delta > 0.5$  yields:

$$\alpha * W_{roof} * \delta 2 + \alpha * W_t * \delta 3 - (W_{roof} + \Delta W_t) * \delta 1 = 0$$

Where:

$\Delta$ = proportional multiplier between 0 and 1

The PVW is written as:

$$\alpha * W_{roof} * \Delta H * \beta + \alpha * W_t * \frac{\Delta H}{2} * \beta - (W_{roof} + \Delta W_t) * \frac{B}{2} * \beta = 0$$

$$\alpha * \Delta H * \left(W_{roof} + \frac{W_t}{2}\right) = \frac{(W_{roof} + \Delta W_t) * B}{2}$$

$$\alpha = \frac{B}{2 * H} * \frac{(W_{roof} + \Delta W_t)}{\Delta * \left(W_{roof} + \frac{W_t}{2}\right)}$$

The PVW for  $\Delta \leq 0.5$  yields:

$$\alpha * W_{roof} * \delta 2 - (W_{roof} + \Delta W_t) * \delta 1 = 0$$

The PVW is written as:

$$\alpha * W_{roof} * \Delta H * \beta - (W_{roof} + \Delta W_t) * \frac{B}{2} * \beta = 0$$

$$\alpha * \Delta H * (W_{roof}) = \frac{(W_{roof} + \Delta W_t) * B}{2}$$

$$\alpha = \frac{B}{2 * H} * \frac{(W_{roof} + \Delta W_t)}{\Delta * (W_{roof})}$$

It has been performed the computation of the load multiplier considering different values of  $\Delta$ , which corresponds to the hinge located at each layer of the wall, the results are presented below.

	$\Delta H$ (m)	$\Delta$	$\alpha$
Layer 1	0.5	0.167	0.950
Layer 2	1.0	0.333	0.700
Layer 3	1.5	0.500	0.617
Layer 4	2.0	0.667	0.155
Layer 5	2.5	0.833	0.149
Layer 6	3.0	1.000	0.144

Table 5. 1 - Maximum load multiplier considering a hinge in a general position.

As it can be notice with this configuration of forces, the load multiplier is lower at the bottom part of the wall which is the most prone to develop the failure mechanism, and the load multiplier increases as the height increase.

### Rigid body over rigid soil considering the cohesion and two forces applied on the wall.

Taking into account this configuration of forces, it has been performed the analysis considering the cohesion due to the perpendicular walls, as shown on the following figure.

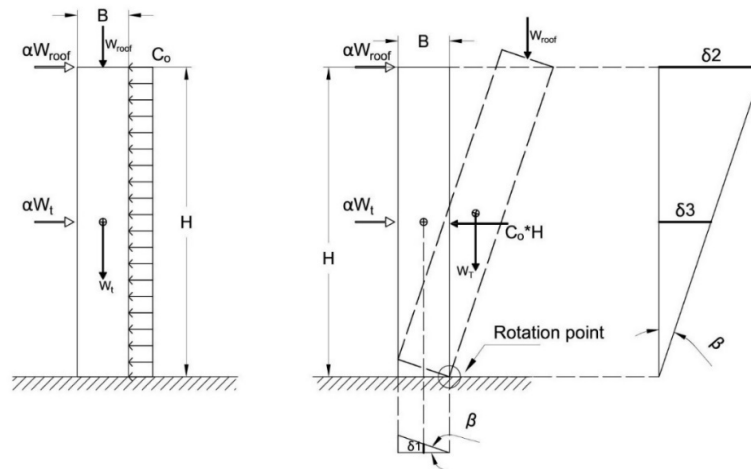


Fig. 5. 9 - Rigid body over rigid soil, considering the cohesion and 2 forces applied on the wall.

The PVW for the actual mechanism yields:

$$\alpha * W_{roof} * \delta 2 + \alpha * W_t * \delta 3 - (W_{roof} + W_t) * \delta 1 - 2 * C_o * H * \delta 3 = 0$$

Where:

$C_o = C * B$ , where  $c$  is the cohesion value.

It has been considered twice the cohesion force due to both perpendicular walls.

The PVW for the actual mechanism yields:

$$\alpha * W_{roof} * H * \beta + \alpha * W_t * \frac{H}{2} * \beta - (W_{roof} + W_t) * \frac{B}{2} * \beta - 2 * C * B * H * \frac{H}{2} * \beta = 0$$

$$\alpha * H * \left( W_{roof} + \frac{W_t}{2} \right) = \frac{(W_{roof} + W_t) * B}{2} + C * B * H^2$$

$$\alpha = \frac{B}{2 * H} * \frac{(W_{roof} + W_t)}{\left( W_{roof} + \frac{W_t}{2} \right)} + \frac{C * B * H}{\left( W_{roof} + \frac{W_t}{2} \right)}$$

It can be notice that the cohesion has a positive effect in the out-of-plane behavior of the gabion wall, due to an increment of the load multiplier.

Substituting the parameters of the wall on the previous equation, it has been obtained the following load multiplier.

$C = 2000 \text{ kg/m}^2$

$$\alpha = \frac{0.5}{2 * 3} * \frac{(3000 + 16200)}{\left( 3000 + \frac{16200}{2} \right)} + \frac{2000 * 0.5 * 3}{\left( 3000 + \frac{16200}{2} \right)} = 0.414$$

The values computed of the load multiplier have been reported in the following table.

Values of "α" for rigid body with rigid soil			
Total force at the top		Force due to the roof applied at the top and force due to the self-weight applied at the center of gravity	
with-out cohesion	with cohesion	with-out cohesion	with cohesion
0.083	0.239	0.144	0.414

Table 5. 2 – Values of  $\alpha$  for considering a rigid body with rigid soil.

As it can be seen from the results, considering the total force applied at the top is a conservative calculation, and taking into account the cohesion helps to improve the behavior of the out-of-plane considerably for both cases.

## 5.2.2. Rigid body over elastic soil – hand calculations.

### Rigid body over elastic soil, with two forces applied on the wall.

It has been performed the calculation of the load multiplier  $\alpha$  for the gabion wall shown in the figure 5.9, considering the stiffness of the soil below. In order to take into account this assumption, it has been considered springs with the stiffness of the soil, besides this, the springs can only work in compression, once they start working in tension the effect of the spring is neglected.

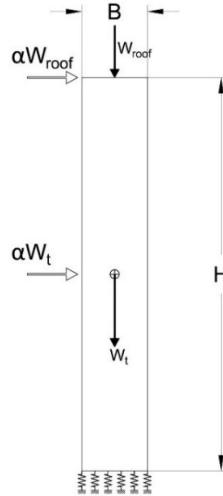


Fig. 5. 10 - Rigid body over elastic soil with 2 forces applied on the wall.

Where:

$$W_t = 16200 \text{ Kg}$$

$$W_{roof} = 3000 \text{ Kg}$$

The general equations of equilibrium for the wall have been computed as follows:

The compression force on each spring due to gravitational loads is:

$$N_{spring} = \frac{W_{roof} + W_t}{ns}$$

The external moment at the center of rotation in the base is given by:

$$M_{ext} = \alpha * W_{roof} * H + \alpha * W_t * \frac{H}{2} - (W_{roof} + W_t) * \left( \frac{B}{2} - r_{max} \right)$$

$$M_{ext} = \alpha * H * \left( W_{roof} + \frac{W_t}{2} \right) - (W_{roof} + W_t) * \left( \frac{B}{2} - r_{max} \right)$$

The internal force on each spring due to the external moment is computed as:

$$F_i = k_i * \delta_i$$

$$F_i = k_i * r_i * \theta$$



The moments due to the springs is computed as follows:

$$M_{sp} = \sum_{i=1}^{ns} F_i * r_i = \sum_{i=1}^{ns} k_i * \theta * r_i^2 = k * \theta * \sum_{i=1}^{ns} r_i^2$$

Therefore, the total force that each spring will be carrying is given by the next equation.

$$F_{i-tot} = N_{spring} - F_i$$

$$F_{i-tot} = N_{spring} - k_i * r_i * \theta$$

Where:

ns= number of springs receiving the vertical loads

r<sub>max</sub>= maximum distance between springs and the center of rotation.

k<sub>i</sub>=stiffness of the soil, where k<sub>i</sub>=k for all values of i

r<sub>i</sub>= distance between springs and the center of rotation.

Considering the cohesion for the system show below, the general equations of external moments for the wall remains as:

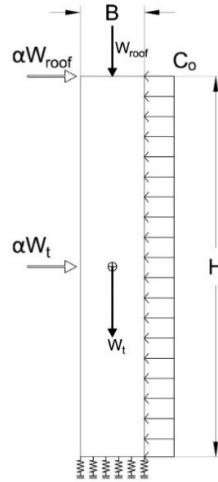


Fig. 5. 11 - Rigid body over elastic soil, considering the cohesion and 2 forces applied on the wall.

$$M_{ext} = \alpha * H * \left( W_{roof} + \frac{W_t}{2} \right) - (W_{roof} + W_t) * \left( \frac{B}{2} - r_{max} \right) - 2 * C_0 * B * \frac{H^2}{2}$$

Where:

C<sub>0</sub>= C\*B, where c is the cohesion value.

It has been considered twice the cohesion force due to both perpendicular walls.

$$M_{ext} = \alpha * H * \left( W_{roof} + \frac{W_t}{2} \right) - (W_{roof} + W_t) * \left( \frac{B}{2} - r_{max} \right) - C * B * H^2$$

Where the additional term due to the cohesion after substituting the parameters of the wall is the following one

$$\text{additional term} = -C * B * H^2 = -4.5 * C$$

With  $C=2000 \text{ kg/m}^2$

The rest of the equations remain the same for this configuration of forces acting on the gabion wall.

*First spring entering in tension*

At this steps all the springs are in compression, the objective of this calculation is to find the load multiplier  $\alpha$  that will cause tension on the first spring. In order to achieve this, it has been compute the equilibrium of moments at the point shown in figure 5.11, after finding the equilibrium it has been compute the force at the first spring of interest and check when will start the tension force, the calculations for this step are show below.

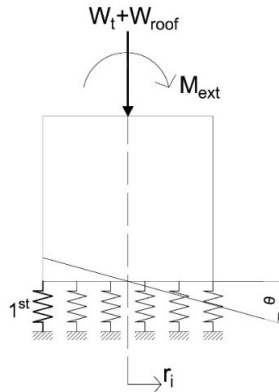


Fig. 5. 12 – Point of equilibrium of moments when the first spring enters in tension.

Calling the general equations mentioned before and substituting with the values of the specific problem, it has been obtained the following results.

$$N_{spring} = \frac{W_{roof} + W_t}{ns} = \frac{3000 + 16200}{6} = 3200 \text{ kg}$$

$$M_{ext} = \alpha * H * \left( W_{roof} + \frac{W_t}{2} \right) - (W_{roof} + W_t) * \left( \frac{B}{2} - r_{max} \right)$$

$$M_{ext} = \alpha * 3 * \left( 3000 + \frac{16200}{2} \right) - (3000 + 16200) * \left( \frac{0.5}{2} - 0.25 \right)$$

$$M_{ext} = 33300 * \alpha$$

$$M_{sp} = k * \theta * \sum_{i=1}^{ns} r_i^2 = k * \theta * [(0.05^2 * 2) + (0.15^2 * 2) + (0.25^2 * 2)]$$

$$M_{sp} = k * \theta * 0.175$$

The moments of the system have to be in equilibrium, hence:

$$M_{ext} = M_{sp}$$

$$33300 * \alpha = k * \theta * 0.175$$

$$\theta = \frac{33300 * \alpha}{0.175 * k}$$

Hence, the total force at the first spring is:

$$F_{1-tot} = N_{spring} - k * r_1 * \theta$$

$$F_{1-tot} = 3200 - k * 0.25 * \frac{33300 * \alpha}{0.175 * k}$$

In order to remain in compression, the force at the spring has to be positive, thus the maximum load multiplier can be computed.

$$3200 - 0.25 * \frac{33300 * \alpha}{0.175} > 0$$

$$\alpha < 0.067$$

Considering the cohesion and performing the same calculations, it has been obtained the following results:

$$M_{ext} = 33300 * \alpha - 4.5 * C$$

Thus,

$$\theta = \frac{33300 * \alpha - 4.5 * C}{0.175 * k}$$

$$F_{1-tot} = 3200 - k * 0.25 * \frac{33300 * \alpha - 4.5 * C}{0.175 * k}$$

$$3200 - 0.25 * \frac{33300 * \alpha - 4.5 * 2000}{0.175} > 0$$

$$\alpha < 0.336$$

*Second spring entering in tension*

At this steps it has been considered five springs in compression, it has been repeated the same procedure as before to compute the load multiplier  $\alpha$  that will cause tension on the second spring. In order to achieve this, it has been compute the equilibrium of moments at the point shown in figure below.

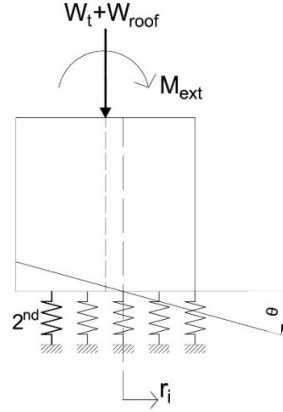


Fig. 5. 13 – Point of equilibrium of moments when the second spring enters in tension.

Calling the general equations mentioned before and substituting with the values of the specific problem, it has been obtained the following results.

$$N_{spring} = \frac{W_{roof} + W_t}{ns} = \frac{3000 + 16200}{5} = 3840 \text{ kg}$$

$$M_{ext} = \alpha * H * \left( W_{roof} + \frac{W_t}{2} \right) - (W_{roof} + W_t) * \left( \frac{B}{2} - r_{max} \right)$$

$$M_{ext} = \alpha * 3 * \left( 3000 + \frac{16200}{2} \right) - (3000 + 16200) * \left( \frac{0.5}{2} - 0.2 \right)$$

$$M_{ext} = 33300 * \alpha - 960$$

$$M_{sp} = k * \theta * \sum_{i=1}^{ns} r_i^2 = k * \theta * [(0.1^2 * 2) + (0.2^2 * 2) + (0^2)]$$

$$M_{sp} = k * \theta * 0.1$$

The moments of the system have to be in equilibrium, hence:

$$M_{ext} = M_{sp}$$

$$33300 * \alpha - 960 = k * \theta * 0.1$$

$$\theta = \frac{33300 * \alpha - 960}{0.1 * k}$$

Hence, the total force at the second spring is:

$$F_{2-tot} = N_{spring} - k * r_2 * \theta$$

$$F_{2-tot} = 3840 - k * 0.2 * \frac{33300 * \alpha - 960}{0.1 * k}$$

In order to remain in compression, the force at the spring has to be positive, thus the maximum load multiplier can be computed.

$$3840 - 0.2 * \frac{33300 * \alpha - 960}{0.1} > 0$$

$$\alpha < 0.086$$

Considering the cohesion and performing the same calculations, it has been obtained the following results:

$$M_{ext} = 33300 * \alpha - 960 - 4.5 * C$$

Thus

$$\theta = \frac{33300 * \alpha - 960 - 4.5 * C}{0.1 * k}$$

$$F_{2-tot} = 3840 - k * 0.2 * \frac{33300 * \alpha - 960 - 4.5 * C}{0.1 * k}$$

$$3840 - 0.2 * \frac{33300 * \alpha - 960 - 4.5 * 2000}{0.1} > 0$$

$$\alpha < 0.355$$

*Third spring entering in tension*

At this steps it has been considered four springs in compression, it has been repeated the same procedure as before to compute the load multiplier  $\alpha$  that will cause tension on the third spring. In order to achieve this, it has been compute the equilibrium of moments at the point shown in figure below.

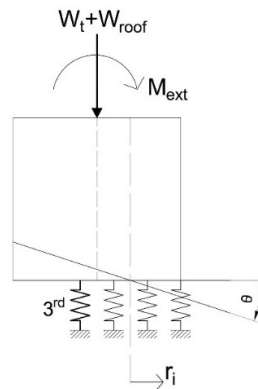


Fig. 5. 14 – Point of equilibrium of moments when the third spring enters in tension.

Calling the general equations mentioned before and substituting with the values of the specific problem, it has been obtained the following results.

$$N_{spring} = \frac{W_{roof} + W_t}{ns} = \frac{3000 + 16200}{4} = 4800 \text{ kg}$$

$$M_{ext} = \alpha * H * \left( W_{roof} + \frac{W_t}{2} \right) - (W_{roof} + W_t) * \left( \frac{B}{2} - r_{max} \right)$$

$$M_{ext} = \alpha * 3 * \left( 3000 + \frac{16200}{2} \right) - (3000 + 16200) * \left( \frac{0.5}{2} - 0.15 \right)$$

$$M_{ext} = 33300 * \alpha - 1920$$

$$M_{sp} = k * \theta * \sum_{i=1}^{ns} r_i^2 = k * \theta * [(0.05^2 * 2) + (0.15^2 * 2)]$$

$$M_{sp} = k * \theta * 0.05$$

The moments of the system have to be in equilibrium, hence:

$$M_{ext} = M_{sp}$$

$$33300 * \alpha - 1920 = k * \theta * 0.05$$

$$\theta = \frac{33300 * \alpha - 1920}{0.05 * k}$$

Hence, the total force at the third spring is:

$$F_{3-tot} = N_{spring} - k * r_3 * \theta$$

$$F_{3-tot} = 4800 - k * 0.15 * \frac{33300 * \alpha - 1920}{0.05 * k}$$

In order to remain in compression, the force at the spring has to be positive, thus the maximum load multiplier can be computed.

$$4800 - 0.15 * \frac{33300 * \alpha - 1920}{0.05} > 0$$

$$\alpha < 0.105$$

Considering the cohesion and performing the same calculations, it has been obtained the following results:

$$M_{ext} = 33300 * \alpha - 1920 - 4.5 * C$$

Thus

$$\theta = \frac{33300 * \alpha - 1920 - 4.5 * C}{0.05 * k}$$

$$F_{3-tot} = 4800 - k * 0.15 * \frac{33300 * \alpha - 1920 - 4.5 * C}{0.05 * k}$$

$$4800 - 0.15 * \frac{33300 * \alpha - 1920 - 4.5 * 2000}{0.05} > 0$$

$$\alpha < 0.375$$

*Fourth spring entering in tension*

At this steps it has been considered three springs in compression, it has been repeated the same procedure as before to compute the load multiplier  $\alpha$  that will cause tension on the fourth spring. In order to achieve this, it has been compute the equilibrium of moments at the point shown in figure below.

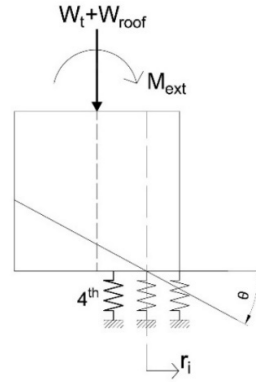


Fig. 5. 15 – Point of equilibrium of moments when the fourth spring enters in tension.

Calling the general equations mentioned before and substituting with the values of the specific problem, it has been obtained the following results.

$$N_{spring} = \frac{W_{roof} + W_t}{ns} = \frac{3000 + 16200}{3} = 6400 \text{ kg}$$

$$M_{ext} = \alpha * H * \left( W_{roof} + \frac{W_t}{2} \right) - (W_{roof} + W_t) * \left( \frac{B}{2} - r_{max} \right)$$

$$M_{ext} = \alpha * 3 * \left( 3000 + \frac{16200}{2} \right) - (3000 + 16200) * \left( \frac{0.5}{2} - 0.1 \right)$$

$$M_{ext} = 33300 * \alpha - 2880$$

$$M_{sp} = k * \theta * \sum_{i=1}^{ns} r_i^2 = k * \theta * [(0.1^2 * 2) + (0^2)]$$

$$M_{sp} = k * \theta * 0.02$$

The moments of the system have to be in equilibrium, hence:

$$M_{ext} = M_{sp}$$

$$33300 * \alpha - 2880 = k * \theta * 0.02$$

$$\theta = \frac{33300 * \alpha - 2880}{0.02 * k}$$

Hence, the total force at the fourth spring is:

$$F_{4-tot} = N_{spring} - k * r_4 * \theta$$

$$F_{4-tot} = 6400 - k * 0.1 * \frac{33300 * \alpha - 2880}{0.02 * k}$$

In order to remain in compression, the force at the spring has to be positive, thus the maximum load multiplier can be computed.

$$6400 - 0.1 * \frac{33300 * \alpha - 2880}{0.02} > 0$$

$$\alpha < 0.123$$

Considering the cohesion and performing the same calculations, it has been obtained the following results:

$$M_{ext} = 33300 * \alpha - 2880 - 4.5 * C$$

Thus,

$$\theta = \frac{33300 * \alpha - 2880 - 4.5 * C}{0.02 * k}$$

$$F_{4-tot} = 6400 - k * 0.1 * \frac{33300 * \alpha - 2880 - 4.5 * C}{0.02 * k}$$

$$6400 - 0.1 * \frac{33300 * \alpha - 2880 - 4.5 * 2000}{0.02} > 0$$

$$\alpha < 0.397$$

### **Rigid body over elastic soil, with a force applied at the top of the wall.**

It has been performed another calculation of the load multiplier  $\alpha$  for the gabion wall changing the configuration of the applied forces, that for this case it has been considered all the force applied at the top of the wall as shown in the picture below.



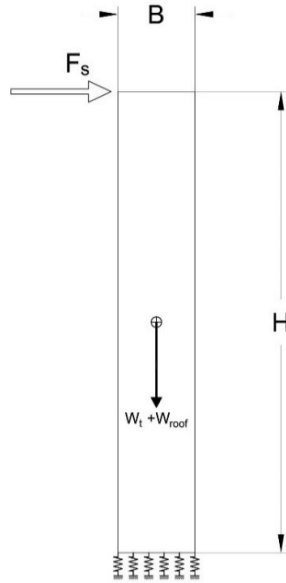


Fig. 5. 16 – Rigid body over elastic soil with a force applied at the top.

Where:

$$F_s = \text{seismic force} = \alpha * (W_t + W_{\text{roof}})$$

$$W_t = 16200 \text{ Kg}$$

$$W_{\text{roof}} = 3000 \text{ Kg}$$

The general equations of equilibrium for the wall are the same that have been used in the previous calculations with the exception of the external moment acting on the wall that is given by:

$$M_{\text{ext}} = \alpha * (W_{\text{roof}} + W_t) * H - (W_{\text{roof}} + W_t) * \left( \frac{B}{2} - r_{\text{max}} \right)$$

Considering the cohesion for the system show below, the general equations of external moments for the wall remains as:

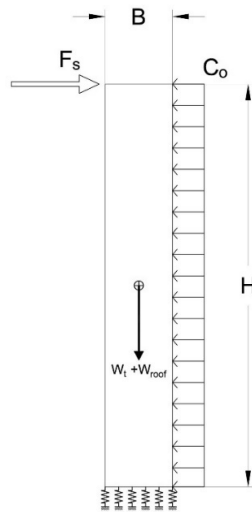


Fig. 5. 17 – Rigid body over elastic, considering the cohesion and a force applied at the top.

$$M_{ext} = \alpha * (W_{roof} + W_t) * H - (W_{roof} + W_t) * \left(\frac{B}{2} - r_{max}\right) - 2 * C_0 * B * \frac{H^2}{2}$$

Where:

$C_0 = C * B$ , where  $c$  is the cohesion value.

It has been considered twice the cohesion force due to both perpendicular walls.

$$M_{ext} = \alpha * (W_{roof} + W_t) * H - (W_{roof} + W_t) * \left(\frac{B}{2} - r_{max}\right) - C * B * H^2$$

Where the additional term due to the cohesion after substituting the parameters of the wall is the following one:

$$\text{additional term} = -C * B * H^2 = -4.5 * C$$

With  $C=2000 \text{ kg/m}^2$

The rest of the equations remain the same for this configuration of forces acting on the gabion wall.

*First spring entering in tension*

Calling the general equations mentioned before and substituting with the values of the specific problem, it has been obtained the following results.

$$M_{ext} = \alpha * (W_{roof} + W_t) * H - (W_{roof} + W_t) * \left(\frac{B}{2} - r_{max}\right)$$

$$M_{ext} = \alpha * 3 * (3000 + 16200) - (3000 + 16200) * \left(\frac{0.5}{2} - 0.25\right)$$

$$M_{ext} = 57600 * \alpha$$

Thus,

$$\theta = \frac{57600 * \alpha}{0.175 * k}$$

$$F_{1-tot} = 3200 - k * 0.25 * \frac{57600 * \alpha}{0.175 * k}$$

$$3200 - 0.25 * \frac{57600 * \alpha}{0.175} > 0$$

$$\alpha < 0.038$$

Considering the cohesion and performing the same calculations, it has been obtained the following results:

$$M_{ext} = 57600 * \alpha - 4.5 * C$$

Thus,

$$\theta = \frac{57600 * \alpha - 4.5 * C}{0.175 * k}$$

$$F_{1-tot} = 3200 - k * 0.25 * \frac{57600 * \alpha - 4.5 * C}{0.175 * k}$$

$$3200 - 0.25 * \frac{57600 * \alpha - 4.5 * 2000}{0.175} > 0$$

$$\alpha < 0.194$$

*Second spring entering in tension*

Calling the general equations mentioned before and substituting with the values of the specific problem, it has been obtained the following results.

$$M_{ext} = \alpha * (W_{roof} + W_t) * H - (W_{roof} + W_t) * \left(\frac{B}{2} - r_{max}\right)$$

$$M_{ext} = \alpha * 3 * (3000 + 16200) - (3000 + 16200) * \left(\frac{0.5}{2} - 0.2\right)$$

$$M_{ext} = 57600 * \alpha - 960$$

$$\theta = \frac{57600 * \alpha - 960}{0.1 * k}$$

$$F_{2-tot} = 3840 - k * 0.2 * \frac{57600 * \alpha - 960}{0.1 * k}$$

$$3840 - 0.2 * \frac{57600 * \alpha - 960}{0.1} > 0$$

$$\alpha < 0.048$$

Considering the cohesion and performing the same calculations, it has been obtained the following results:

$$M_{ext} = 57600 * \alpha - 960 - 4.5 * C$$

Thus,

$$\theta = \frac{57600 * \alpha - 960 - 4.5 * C}{0.1 * k}$$

$$F_{2-tot} = 3840 - k * 0.2 * \frac{57600 * \alpha - 960 - 4.5 * C}{0.1 * k}$$

$$3840 - 0.2 * \frac{57600 * \alpha - 960 - 4.5 * 2000}{0.1} > 0$$

$$\alpha < 0.205$$

*Third spring entering in tension*

Calling the general equations mentioned before and substituting with the values of the specific problem, it has been obtained the following results.

$$M_{ext} = \alpha * (W_{roof} + W_t) * H - (W_{roof} + W_t) * \left(\frac{B}{2} - r_{max}\right)$$

$$M_{ext} = \alpha * 3 * (3000 + 16200) - (3000 + 16200) * \left(\frac{0.5}{2} - 0.15\right)$$

$$M_{ext} = 57600 * \alpha - 1920$$

Thus,

$$\theta = \frac{57600 * \alpha - 1920}{0.05 * k}$$

$$F_{3-tot} = 4800 - k * 0.15 * \frac{57600 * \alpha - 1920}{0.05 * k}$$

$$4800 - 0.15 * \frac{57600 * \alpha - 1920}{0.05} > 0$$

$$\alpha < 0.061$$

Considering the cohesion and performing the same calculations, it has been obtained the following results:

$$M_{ext} = 57600 * \alpha - 1920 - 4.5 * C$$

Thus,

$$\theta = \frac{57600 * \alpha - 1920 - 4.5 * C}{0.05 * k}$$

$$F_{3-tot} = 4800 - k * 0.15 * \frac{57600 * \alpha - 1920 - 4.5 * C}{0.05 * k}$$

$$4800 - 0.15 * \frac{57600 * \alpha - 1920 - 4.5 * 2000}{0.05} > 0$$

$$\alpha < 0.216$$

*Fourth spring entering in tension*

Calling the general equations mentioned before and substituting with the values of the specific problem, it has been obtained the following results.

$$M_{ext} = \alpha * (W_{roof} + W_t) * H - (W_{roof} + W_t) * \left(\frac{B}{2} - r_{max}\right)$$

$$M_{ext} = \alpha * 3 * (3000 + 16200) - (3000 + 16200) * \left(\frac{0.5}{2} - 0.1\right)$$

$$M_{ext} = 57600 * \alpha - 2880$$

$$\theta = \frac{57600 * \alpha - 2880}{0.02 * k}$$

$$F_{4-tot} = 6400 - k * 0.1 * \frac{57600 * \alpha - 2880}{0.02 * k}$$

$$6400 - 0.1 * \frac{57600 * \alpha - 2880}{0.02} > 0$$

$$\alpha < 0.072$$

Considering the cohesion and performing the same calculations, it has been obtained the following results:

$$M_{ext} = 57600 * \alpha - 2880 - 4.5 * C$$

Thus,

$$\theta = \frac{57600 * \alpha - 2880 - 4.5 * C}{0.02 * k}$$

$$F_{4-tot} = 6400 - k * 0.1 * \frac{57600 * \alpha - 2880 - 4.5 * C}{0.02 * k}$$

$$6400 - 0.1 * \frac{57600 * \alpha - 2880 - 4.5 * 2000}{0.02} > 0$$

$$\alpha < 0.227$$

The values computed of the load multiplier have been reported in the following table.

Values of "α" for rigid body with elastic soil				
	Total force at the top		Force due to the roof applied at the top and force due to the self-weight applied at the center of gravity	
	with-out cohesion	with cohesion	with-out cohesion	with cohesion
1 <sup>st</sup> spring in tension	0.038	0.194	0.067	0.336
2 <sup>nd</sup> spring in tension	0.048	0.205	0.086	0.355
3 <sup>rd</sup> spring in tension	0.061	0.216	0.105	0.374
4 <sup>th</sup> spring in tension	0.072	0.227	0.123	0.393

Table 5. 3 – Values of α for considering a rigid body with elastic soil.

As it can be seen from the results, considering the total force applied at the top is a conservative calculation, and taking into account the cohesion helps to improve the behavior of the out-of-plane considerably. The results for the load multiplier are increasing until that the last spring is in tension that converges to the ones obtained considering a rigid soil.

### 5.2.3. Elastic body over rigid soil – FEM model.

It has been used a commercial program called “Autodesk Robot Structural Analysis Professional”, in order to carry out the FEM analysis of the gabion boxes wall; the parameters considered in program in order to model the wall, were described in chapter 2 of this document.

It has been performed a model of a vertical strip of gabion wall which has a length of 1m and considering two scenarios, the first one with free edges and the second one considering the cohesion due to the influence of the perpendicular walls.

Moreover, it has been considered in the model only when a force is applied at the top due to the weight of the roof and the second force applied at the center of gravity due to the weight of the gabion wall.

Once tension stresses appears in the gabion wall there is a need to carry-out the tension with additional elements, which are going to give enough tension resistance in order be able to resist the respective load multiplier and capable to have the maximum displacement derived from the analysis.

It has been considered steel wire connectors as reinforcement for the tension stresses, considering the properties of the steel wire mentioned in chapter 2, and the diameter of the wire as  $\Phi=3\text{mm}$ . A safety factor has been selected following the Italian code for a seismic actions action on masonry materials.

### Elastic body over rigid soil, with two forces applied on the wall.

It has been performed the FEM analysis using the load multiplier that has been obtained in the hand calculations and observing if the maximum displacement is not large enough that will have an imminent collapse of the vertical strip, additionally it has been obtained the tension stresses that will be acting on the vertical strip of the gabion wall in order to prescribe the connectors that will carry out those stresses.

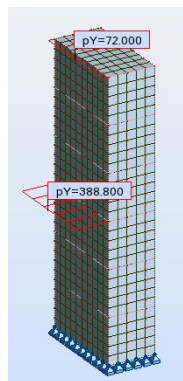


Fig. 5. 18 – System of forces acting on the vertical strip

The result of the maximum displacement is reported below.

Rigid Soil With-Out Cohesion	
Vertical Strip of 1m - simple support at base	
FEM model	
Load Multiplier $\alpha$	Maximum out-of-plane displacement (cm)
0.144	55.77

Table 5. 4 - Maximum displacement of a vertical strip considering  $\alpha=0.144$

The deformed shape of the vertical strip can be seen in the following figures, considering a load multiplier equal to 0.144.

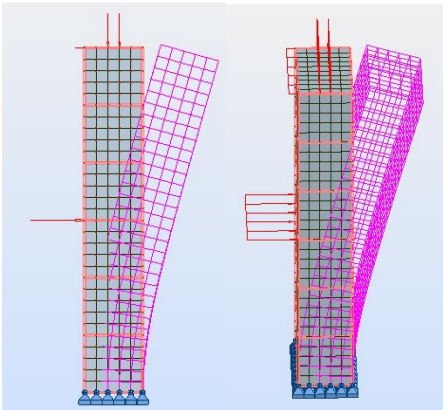


Fig. 5. 19 - Deformed shapes of vertical strip considering  $\alpha=0.144$

It can be seen in the following figures how the displacement develops on the vertical strip considering a load multiplier equal to 0.144.

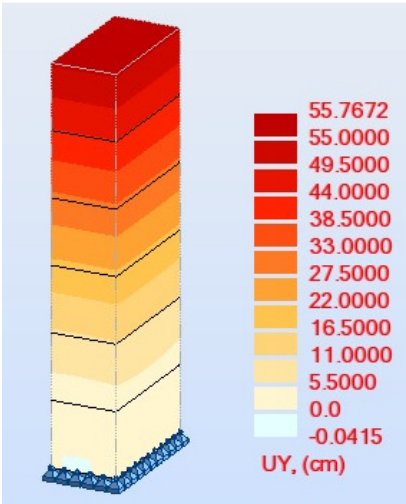


Fig. 5. 20 - Map of displacement of the vertical strip considering  $\alpha= 0.144$

The results of stresses acting on the body are shown in the following picture, where positive values mean tension stresses.

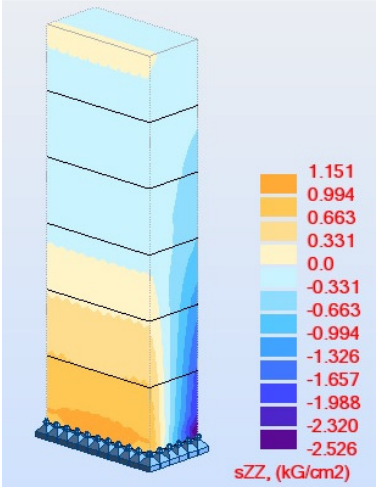


Fig. 5. 21 - Map of stresses of the vertical strip considering  $\alpha= 0.144$

It has been compute the number of wires needed in order to be able to resist the tension stress obtained from the FEM results, the calculations are shown below.

vertical strip of 1m width - rigid soil							
load multiplier $\alpha$ (g)	S (Kg/cm2)	L (cm)	$\phi$ (mm)	n	Spacing without SF (cm)	Safety factor (SF)	Spacing with SF (cm)
0.144	1.151	100	3	24	4.10	2	2.00
	0.663	100	3	14	7.10	2	3.50
	0.331	100	3	7	14.20	2	7.10

Table 5. 5 – Wire reinforcement for a vertical strip considering  $\alpha=0.144$

**Elastic body over rigid soil with cohesion and two forces applied on the wall.**

It has been performed the FEM analysis considering the same system of forces and additionally, taking into account the cohesion due to perpendicular walls. The load multiplier has been taken from the hand calculation regarding the rigid body and rigid soil with cohesion.

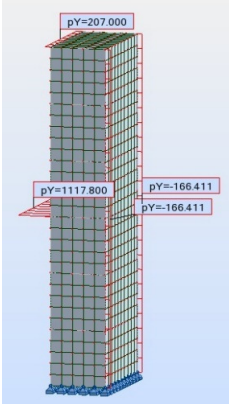


Fig. 5. 22 – System of forces acting on the vertical strip considering the cohesion



Hence, the result of the maximum displacement is reported below.

Rigid Soil With Cohesion	
Vertical Strip of 1m - simple support at base	
FEM model	
Load Multiplier $\alpha$	Maximum out-of-plane displacement (cm)
0.414	53.44

Table 5. 6 - Maximum displacement of a vertical strip considering cohesion and  $\alpha=0.414$

The deformed shape of the vertical strip can be seen in the following figures, considering a load multiplier equal to 0.414 and taking into account the cohesion at the edges of the strip.

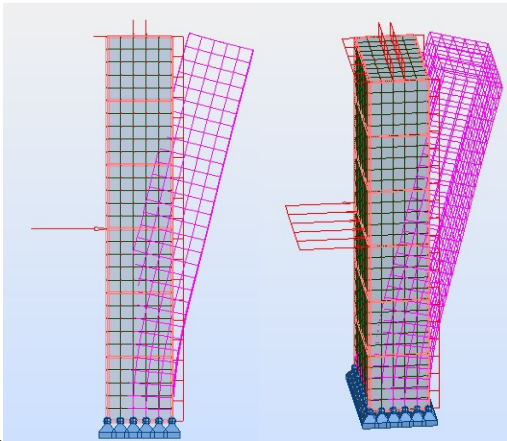


Fig. 5. 23 - Deformed shapes of vertical strip considering cohesion and  $\alpha=0.414$

It can be seen in the following figures how the displacement develops on the vertical strip considering a load multiplier equal to 0.414 and taking into account the cohesion at the edges of the strip.

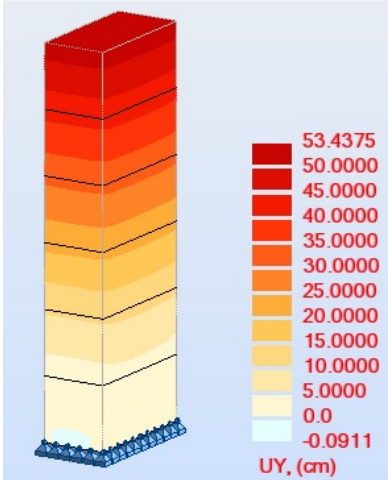


Fig. 5. 24 - Map of displacement of the vertical strip considering cohesion and  $\alpha=0.414$

The results of stresses acting on the body are shown in the following picture, where positive values mean tension stresses.

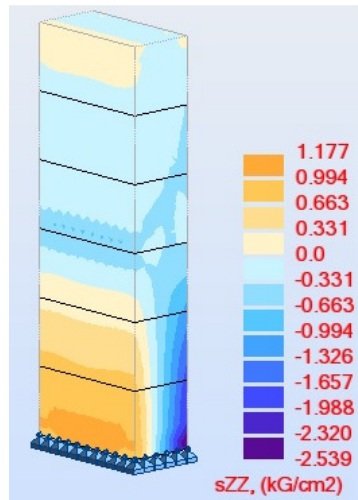


Fig. 5. 25 - Map of stresses of the vertical strip considering cohesion and  $\alpha=0.414$

It has been compute the number of wires needed in order to be able to resist the tension stress obtained from the FEM results, the calculations are shown below.

vertical strip of 1m width with cohesion - rigid soil							
load multiplier $\alpha$ (g)	S (Kg/cm <sup>2</sup> )	L (cm)	$\phi$ (mm)	n	Spacing without SF (cm)	Safety factor (SF)	Spacing with SF (cm)
0.414	1.177	100	3	25	4.00	2	2.00
	0.663	100	3	14	7.10	2	3.50
	0.331	100	3	7	14.20	2	7.10

Table 5. 7 – Wire reinforcement for a vertical strip considering cohesion and  $\alpha=0.414$

#### 5.2.4. Elastic body over elastic soil – FEM model.

It has been performed a model of a vertical strip of gabion wall which has a length of 1m and considering two scenarios, the first one with free edges and the second one considering the cohesion due to the influence of the perpendicular walls, in order to compare the results obtained by hand. Also it has been considered steel wire connectors in the same way that has been done before.

#### Elastic body over elastic soil, with two forces applied on the wall.

It has been performed the FEM analysis finding the load multiplier that will cause tension on the first row of springs and observing if the maximum displacement is not large enough that will have an imminent collapse of the vertical strip, additionally it has been obtained the tension stresses that will be acting on the body. It has been repeated this procedure for all the others springs.

The results of the maximum displacement when a spring enters in tension are reported below, it can be notice that the displacement increases very fast after the third spring enters in tension.

Elastic Soil With-out Cohesion			
Vertical Strip of 1m - springs at base			
Spring working in tension	Hand calculation	FEM model	
	Load Multiplier $\alpha$	Load Multiplier $\alpha$	Maximum out-of-plane displacement (cm)
First spring	0.067	0.061	29.26
Second spring	0.086	0.080	40.09
Third spring	0.105	0.099	58.84
Fourth spring	0.123	0.120	93.62

Table 5. 8 - Maximum displacement of a vertical strip considering an elastic soil

The deformed shapes of the vertical strip for each spring entering in tension can be seen in the following figures.

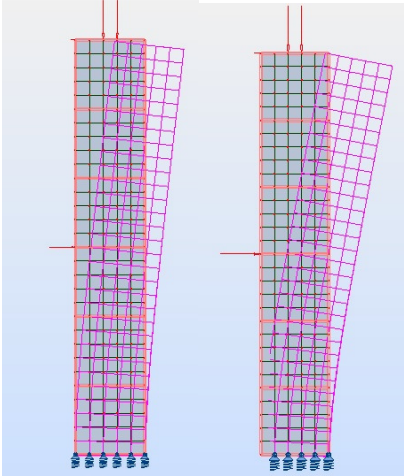


Fig. 5. 26 – Deformed shapes of 1<sup>st</sup> and 2<sup>nd</sup> spring entering in tension for a vertical strip

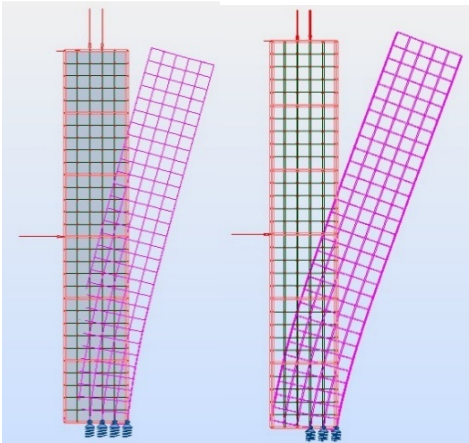


Fig. 5. 27 – Deformed shapes of 3<sup>rd</sup> and 4<sup>th</sup> spring entering in tension for a vertical strip

The results of stresses acting on the body for each spring entering in tension are shown in the following picture, where positive values mean tension stresses.

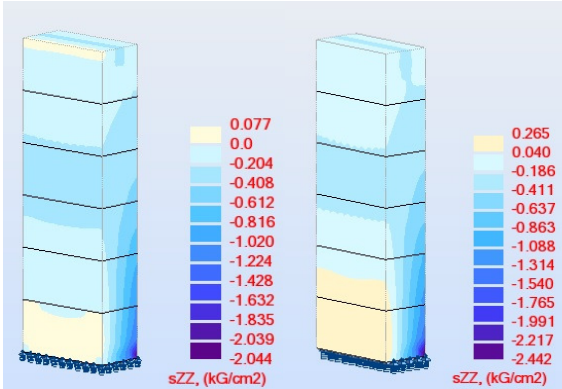


Fig. 5. 28 – Stress maps of 1<sup>st</sup> and 2<sup>nd</sup> spring entering in tension for a vertical strip

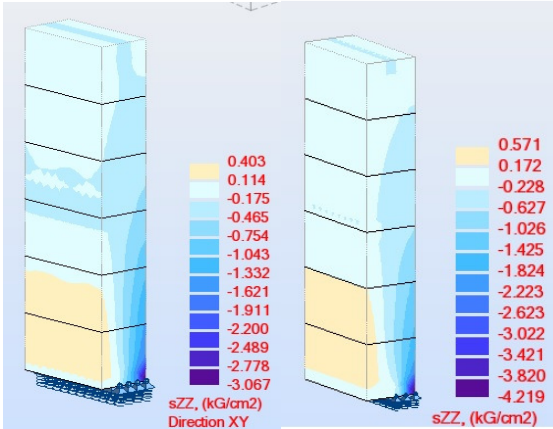


Fig. 5. 29 – Stress maps of 3<sup>rd</sup> and 4<sup>th</sup> spring entering in tension for a vertical strip

It has been calculated the reinforcement needed to carry-out the tension that will be acting on the vertical strip when the 4<sup>th</sup> spring is neglected; the results are presented below.

vertical strip of 1m width - elastic soil							
load multiplier $\alpha$ (g)	S (Kg/cm <sup>2</sup> )	L (cm)	$\phi$ (mm)	n	Spacing without SF (cm)	Safety factor (SF)	Spacing with SF (cm)
0.12	0.571	100	3	12	8.30	2	4.10
	0.172	100	3	4	25.00	2	12.50

Table 5. 9 – Wire reinforcement for a vertical strip considering an elastic soil

**Elastic body over elastic soil, considering the cohesion and two forces applied on the wall.**

It has been performed the FEM analysis, finding the load multiplier that will cause tension on the first row of springs. Moreover, it has been obtained the tension stresses that will be acting on the body. It has been repeated this procedure for all the others springs.

Hence, the result of the maximum displacement when a spring enter in tension are mentioned in the table below. It can be notice that the displacement grows faster after the third spring enters in tension.

Elastic Soil With Cohesion			
Vertical Strip of 1m - springs at base			
Spring working in tension	Hand calculation	FEM model	
	Load Multiplier $\alpha$	Load Multiplier $\alpha$	Maximum out-of-plane displacement (cm)
First spring	0.336	0.330	26.28
Second spring	0.355	0.349	36.99
Third spring	0.374	0.369	54.38
Fourth spring	0.393	0.390	91.36

Table 5. 10 - Maximum displacement of a vertical strip considering an elastic soil with cohesion

The deformed shapes of the vertical strip for each spring entering in tension can be seen in the following figures.

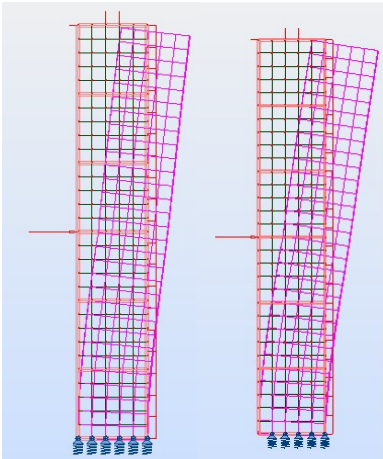


Fig. 5. 30 – Deformed shapes of 1<sup>st</sup> and 2<sup>nd</sup> spring entering in tension for a vertical strip with cohesion

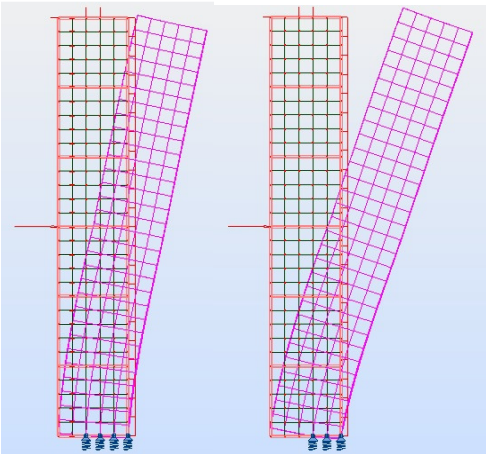


Fig. 5. 31 – Deformed shapes of 3<sup>rd</sup> and 4<sup>th</sup> spring entering in tension for a vertical strip with cohesion

The results of stresses acting on the body for each spring entering in tension are shown in the following picture, where positive values mean tension stresses.

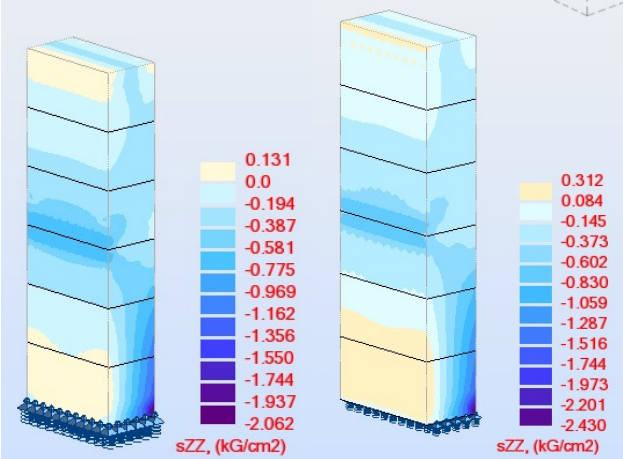


Fig. 5. 32 – Stress maps of 1<sup>st</sup> and 2<sup>nd</sup> spring entering in tension for a vertical strip with cohesion

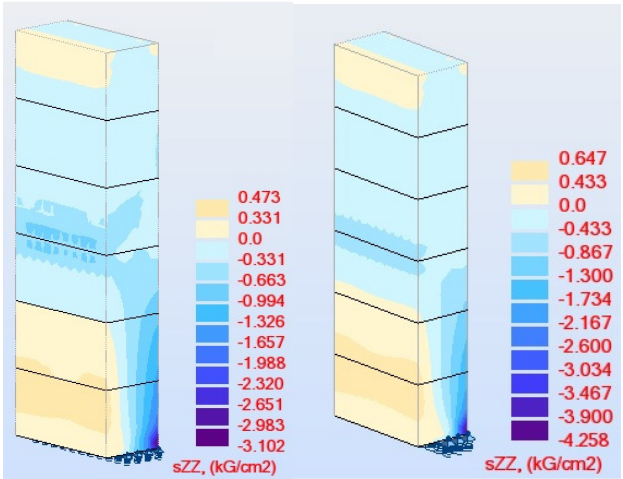


Fig. 5. 33 – Stress maps of 3<sup>rd</sup> and 4<sup>th</sup> spring entering in tension for a vertical strip with cohesion

It has been calculated the reinforcement needed to carry-out the tension that will be acting on the vertical strip when the 4<sup>th</sup> spring is neglected; the results are presented below.

vertical strip of 1m width considering the cohesion - elastic soil							
load multiplier $\alpha$ (g)	S (Kg/cm <sup>2</sup> )	L (cm)	$\phi$ (mm)	n	Spacing without SF (cm)	Safety factor (SF)	Spacing with SF (cm)
0.12	0.647	100	3	14	7.10	2	3.50
	0.433	100	3	9	11.10	2	5.50

Table 5. 11 – Wire reinforcement for a vertical strip considering an elastic soil with cohesion

### 5.3 Out-of-plane behavior of a rigid horizontal strip.

It has been performed the calculation of the load multiplier  $\alpha$  for the gabion wall considering the friction force between 2 consecutive layers and a rigid body motion in order to study the out-of-plane behavior from the flexural point of view, selecting a horizontal portion of the wall (Fig. 33), beside this, it has been considered two different models to achieve this purpose, which are mentioned below.

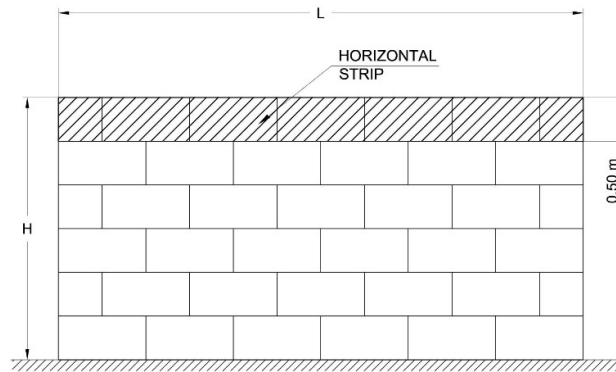


Fig. 5. 34 - Horizontal strip of the gabion wall

In order to compute the force that will be applied on the system, it has been considered a triangular uniform distributed load on height applied to the wall, the force has been computed as follows:

$$q_{max} = \frac{2 * \alpha * (W_T + W_{roof})}{H} \text{ (Kg/m)}$$

Using a relation of triangles to find the q that will be acting on different horizontal layers it has been obtained the following equation:

$$q = \frac{2 * \alpha * (W_T + W_{roof})}{H} * \frac{h_i}{H}$$

Where  $h_i$  is measured from the ground.

**5.3.1. Rigid beam between rigid orthogonal walls - hand calculation.**

The system that has been analyzed is show on the following figures.

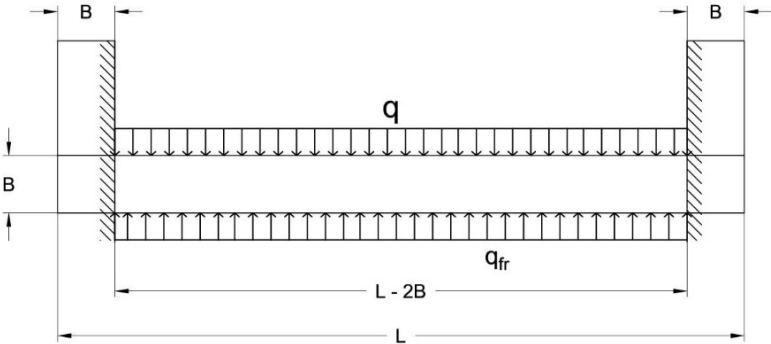


Fig. 5. 35 - Rigid beam between rigid orthogonal walls

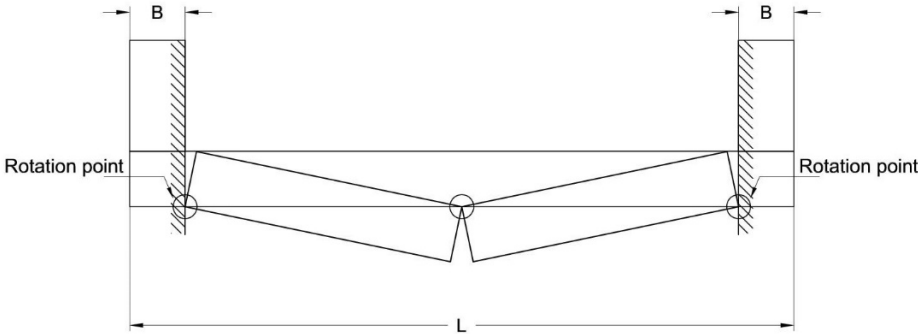


Fig. 5. 36 – Collapse mechanism for the rigid beam between rigid orthogonal walls

Where:

$$q_{fr} = \tau * B$$

$$\tau_i = C + \mu * \sigma_{ni}$$

$\mu$ =friction coefficient between 2 consecutive layers, has been considered 0.4

$C$ =cohesion

In order to find a solution for the problem, it has been considered the following scheme of a beam:

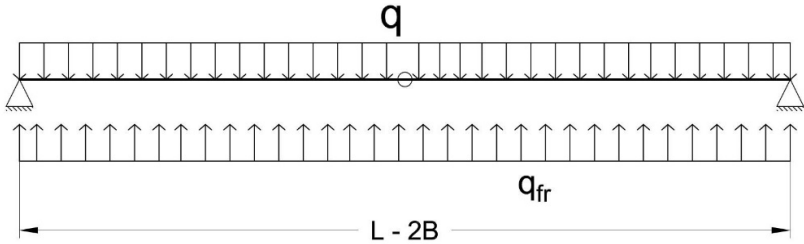


Fig. 5. 37 – Idealization of the rigid beam between rigid orthogonal walls



It can be notice that the equilibrium of the system is possible only if:

$$q_{fr} \geq q$$

$$q_{fr} \geq \frac{2 * \alpha * (W_T + W_{roof})}{H} * \frac{h_i}{H}$$

$$\alpha \geq \frac{q_{fr} * H^2}{2 * (W_T + W_{roof}) * h_i}$$

The results of this system are not taking into account the length of the wall, hence they are going to be valid for all the walls disregarding the length.

Performing the analysis on the top layer of the wall, it has been obtained the following load multiplier that will cause the collapse of the wall:

$$\tau_1 = C + \mu * \sigma_{n1}$$

$$\tau_1 = 0.2 + 0.4 * 0.19 = 0.276 \text{ kg/cm}^2$$

$$q_{fr1} = \tau_1 * B$$

$$q_{fr1} = 0.276 * 50 = 13.8 \text{ kg/cm}$$

$$\alpha \geq \frac{13.8 * 300^2}{2 * (16200 + 3000) * 300}$$

$$\alpha \geq 0.108$$

It has been performed also the analysis on the bottom layer of the wall, in order to obtain the load multiplier as it shown below:

$$\tau_6 = C + \mu * \sigma_{n6}$$

$$\tau_6 = 0.2 + 0.4 * 0.64 = 0.456 \text{ kg/cm}^2$$

$$q_{fr6} = \tau_6 * B$$

$$q_{fr6} = 0.456 * 50 = 22.8 \text{ kg/cm}$$

$$\alpha \geq \frac{22.8 * 300^2}{2 * (16200 + 3000) * 300}$$

$$\alpha \geq 1.068$$

Therefore, the lowest load multiplier  $\alpha$  will occur at the top layer of the wall while it is increasing until the bottom of it.

**5.3.2. Rigid beam between elastic orthogonal walls - hand calculation.**

It has been considered the following system to be analyzed.

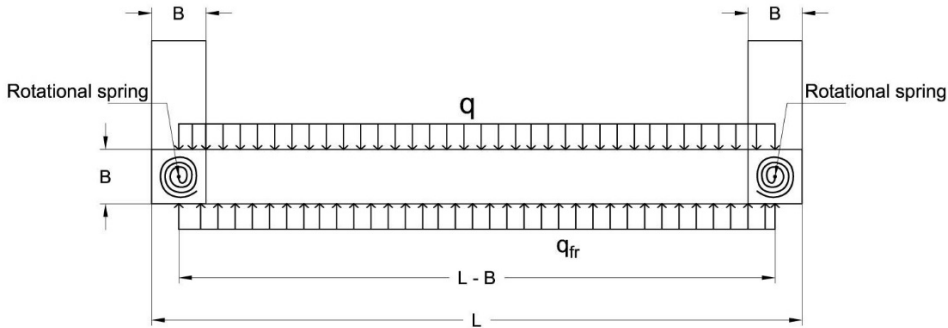


Fig. 5. 38 - Rigid beam between elastic orthogonal walls

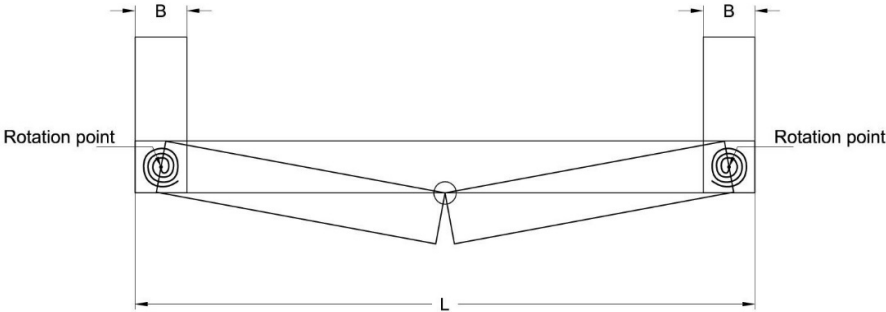


Fig. 5. 39 – Collapse mechanism for the rigid beam between rigid orthogonal walls

The rotational spring is giving a resisting moment equal to

$$M = k * \theta$$

Where:

$$q_{fr} = \tau * B$$

$$\tau_i = C + \mu * \sigma_{ni}$$

$\mu$ = friction coefficient between 2 consecutive layers, has been considered 0.4

C= cohesion

k= stiffness of the perpendicular wall

$\theta$ = rotation of the corner of the wall

$$k = \frac{6 * E * I}{L_{perpendicular}}$$

With:

$$E= 30 \text{ kg/cm}^2$$

$$I = \frac{h_{gabion} * B^3}{12} = \frac{50 * 50^3}{12} = 520833 \text{ cm}^4$$

Thus:

$$k = \frac{6 * 30 * 520833}{600} = 156250 \text{ kg} * \text{cm}$$

In order to find a solution for the problem, it has been considered the following scheme of a beam:

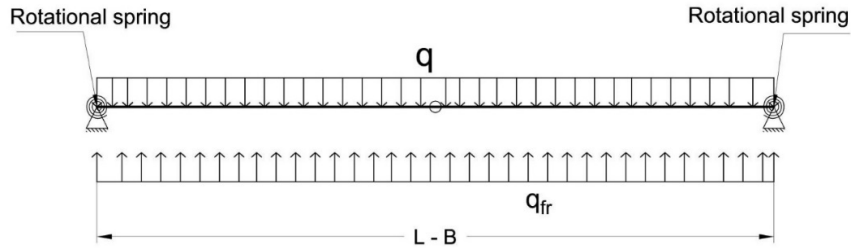
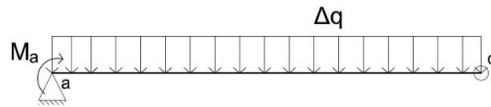


Fig. 5. 40 – Idealization of the rigid beam between elastic orthogonal walls

Considering the first part of the beam in order to solve the system:



$$\Sigma M d = 0$$

$$M_a + \Delta q * \frac{(L - B)}{2} * \frac{(L - B)}{4} - R_a * \frac{(L - B)}{2} = 0$$

Where:

$$\Delta q = q - q_{fr}$$

$$R_a = \frac{\Delta q * (L - B)}{2}, \text{ due to the symmetry of the problem}$$

The equation of moments can be written as:

$$M_a + \Delta q * \frac{(L - B)^2}{8} - \frac{\Delta q * (L - B)^2}{4} = 0$$

$$M_a = \Delta q * \frac{(L - B)^2}{8}$$

Knowing that

$$M_a = k * \theta a$$

It can be obtained the rotation of the connection between perpendicular walls with the following equation:

$$\theta = \frac{\Delta q * (L - B)^2}{8 * k}$$

Performing the analysis on the top layer of the wall, it has been obtained the following results:

$$q = \frac{2 * \alpha * (16200 + 3000)}{300} * \frac{300}{300}$$

$$q = 128 * \alpha$$

$$q_{fr1} = 13.8 \text{ kg/cm}$$

$$\Delta q = q - q_{fr} = 128 * \alpha - 13.8$$

$$\theta = \frac{(128 * \alpha - 13.8) * (600 - 50)^2}{8 * 156250}$$

$$\theta = 30.976 * (\alpha - 0.108)$$

The maximum displacement at the center of the beam is computed as:

$$\Delta = \frac{(L - B)}{2} * tg\theta$$

It has been computed different values of displacement at the center of the wall considering different values of the load multiplier knowing that  $\alpha > 0.108$ , the results are presented in the table below.

Top layer of the wall		
$\alpha$	$\theta$	$\Delta$ (cm)
0.110	0.062	17.059
0.112	0.124	34.249
0.114	0.186	51.707
0.116	0.248	69.577
0.118	0.310	88.017
0.120	0.372	107.204

Table 5. 12 - values of  $\alpha$  and their respective lateral displacement for top layer

It has been performed also the analysis on the bottom layer of the wall, in order to obtain the load multiplier as it shown below:

$$q = \frac{2 * \alpha * (16200 + 3000)}{300} * \frac{50}{300}$$

$$q = 21.33 * \alpha$$

$$q_{fr6} = 22.8 \text{ kg/cm}$$

$$\Delta q = q - q_{fr} = 21.33 * \alpha - 22.8$$

$$\theta = \frac{(21.33 * \alpha - 22.8) * (600 - 50)^2}{8 * 156250}$$

$$\theta = 5.162 * (\alpha - 1.068)$$

The maximum displacement at the center of the beam is computed as:

$$\Delta = \frac{(L - B)}{2} * tg\theta$$

It has been calculated different values of displacement at the center of the wall considering different values of the load multiplier knowing that  $\alpha > 1.068$ , the results are presented in the table below.

Bottom layer of the wall		
$\alpha$	$\theta$	$\Delta$ (cm)
1.070	0.010	2.839
1.080	0.062	17.056
1.090	0.114	31.365
1.100	0.165	45.843
1.110	0.217	60.573
1.120	0.268	75.642

Table 5. 13 - values of  $\alpha$  and their respective lateral displacement for top layer

It has not been performed more calculations changing the load multiplier  $\alpha$  because the displacement will be large enough that the gabion wall cannot sustain that deformation.

### 5.3.3. Elastic beam with fixed ends – FEM model.

It has been performed a model of the top horizontal strip of gabion wall which has a height of 0.5m and a length of 6m, and considering two scenarios, the first one with fixed ends and the second one considering a rotational spring due to the influence of the perpendicular walls. Moreover, it has been considered in the model only a distributed force applied at the lateral surface of the horizontal layer and the friction force acting against the lateral force.

#### Elastic beam with fixed ends – FEM model.

It has been performed the FEM modeling considering the scenario that the connection is infinite rigid, thus can be represented as a fix end, beside this, it has been taken into account the friction force between 2 consecutive layers as can be seen in the next figure.

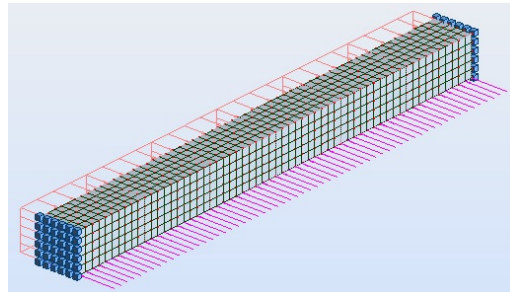


Fig. 5. 41 - Horizontal strip of gabion wall considering fixed ends

The distributed load considered in order to perform the FEM analysis, has been computed using the load multiplier that has been obtained in the hand calculations.

$$q = \frac{\left( \frac{2 * \alpha * (W_T + W_{roof})}{H} * \frac{h_i}{H} \right)}{0.5} \text{ (Kg/m}^2\text{)}$$

$$q = \frac{\left( \frac{2 * 0.108 * (16200 + 3000)}{3} * \frac{3}{3} \right)}{0.5} \text{ (Kg/m}^2\text{)}$$

$$q = 2764.8 \text{ Kg/m}^2$$

The friction force has been calculated considering the Mohr-coulomb friction as it has been performed in the previous chapters.

$$q_{fr1} = \tau_1 * B$$

$$\tau_1 = 0.2 + 0.4 * 0.19 = 0.276 \text{ kg/cm}^2$$

$$q_{fr1} = 0.276 * 50 = 13.8 \frac{\text{kg}}{\text{cm}} = 1380 \text{ Kg/m}$$

Additionally, it has been performed another analysis incrementing the load multiplier in order to obtain a maximum displacement around 50cm. Hence, the results of maximum displacement considering the different scenarios are reported below.

Horizontal strip of 0.5m - fix ends		
FEM model		
load multiplier $\alpha$ (g)	Maximum out-of-plane displacement (cm)	Average Stress at the connection with perpendicular walls (Kg/cm <sup>2</sup> )
0.108	6.44	-0.0001
0.120	41.66	-0.128

Table 5. 14 - Values of  $\alpha$  and their respective lateral displacement for top layer with fixed ends

The deformed shapes of the top horizontal strip for each value of  $\alpha$  can be seen in the following figures.

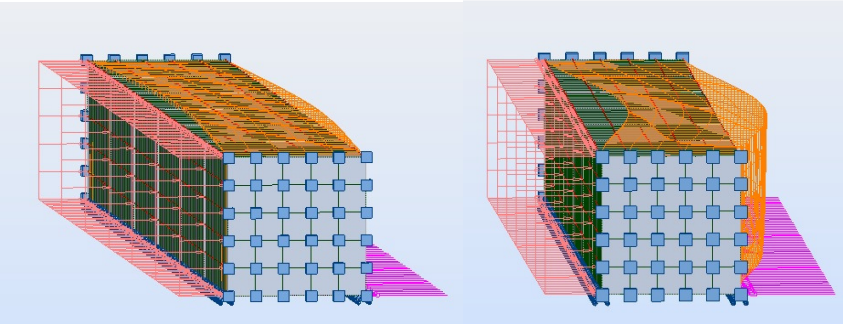


Fig. 5. 42 – Deformed shapes of the top horizontal vertical strip with  $\alpha=0.108$  and  $\alpha=0.12$  respectively considering fixed ends.

The results of stresses acting on the body for both load cases are shown in the following pictures, where positive values mean tension stresses.

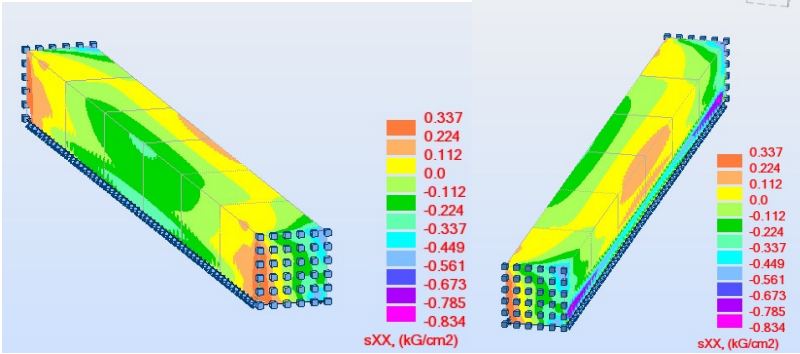


Fig. 5. 43 – Stress maps of the top horizontal vertical strip with  $\alpha=0.108$  and fixed ends

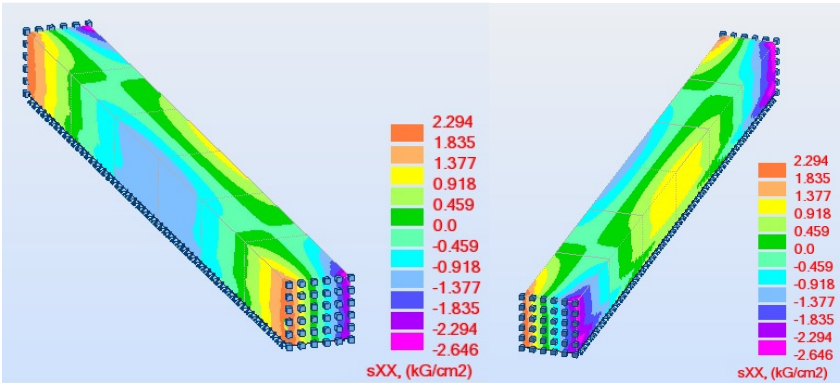


Fig. 5. 44 – Stress maps of the top horizontal vertical strip with  $\alpha=0.12$  and fixed ends

Furthermore, it has been calculated the reinforcement needed to carry-out the tension that will be acting on the top horizontal strip with the load multiplier equal to 0.12, the results are presented below.

Horizontal strip of 0.5m height- fix ends							
load multiplier $\alpha$ (g)	S (Kg/cm <sup>2</sup> )	L (cm)	$\phi$ (mm)	n	Spacing without SF (cm)	Safety factor (SF)	Spacing with SF (cm)
0.12	2.294	100	3	47	3.10	2	1.50
	0.918	100	3	19	7.80	2	3.90
	1.377	200	3	57	6.10	2	3.00

Table 5. 15 – Wire reinforcement the top horizontal strip with fixed ends, considering  $\alpha=0.12$

**Elastic beam with fixed ends – FEM model.**

It has been performed the FEM modeling considering the scenario that the connection has the stiffness of the perpendicular wall, that can be represented as a rotational spring, beside this, it has been taken into account the friction force between 2 consecutive layers as can be seen in the next figure.

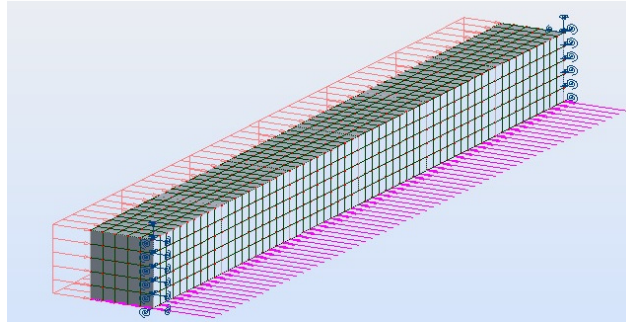


Fig. 5. 45- Horizontal strip of gabion wall considering rotational springs

The distributed loads and the friction forces considered in order to perform the FEM analysis have been calculated as was done previously in this chapter.

Thus, the results of maximum displacement considering the different scenarios are reported below.

Horizontal strip of 0.5m - rotational springs	
FEM model	
load multiplier $\alpha$ (g)	Maximum out-of-plane displacement (cm)
0.108	13.90
0.114	52.52

Table 5. 16 - Values of  $\alpha$  and their respective lateral displacement for top layer with rotational springs.

The deformed shapes of the top horizontal strip for each value of  $\alpha$  can be seen in the following figures.

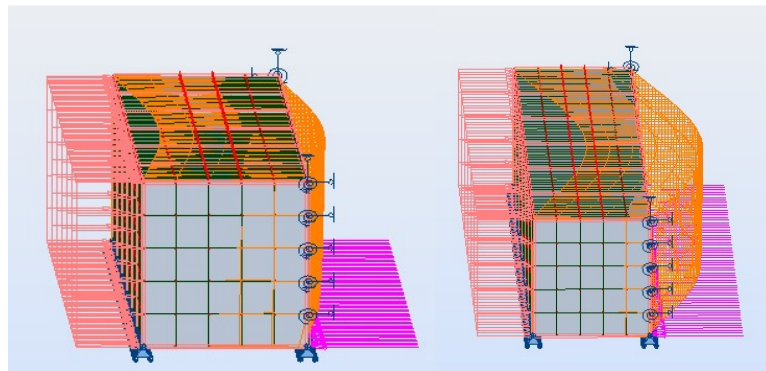


Fig. 5. 46 – Deformed shapes of the top horizontal vertical strip with  $\alpha=0.108$  and  $\alpha=0.114$  respectively considering rotational springs.



The results of stresses acting on the body for both load cases are shown in the following pictures, where positive values mean tension stresses.

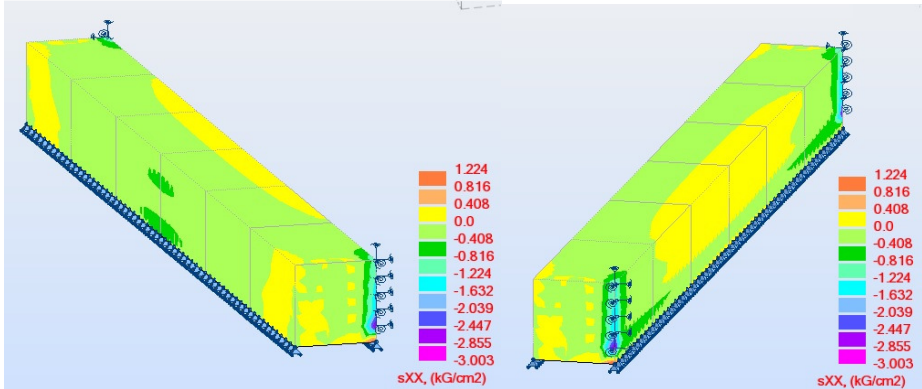


Fig. 5. 47 – Stress maps of the top horizontal vertical strip with  $\alpha=0.108$  and rotational springs

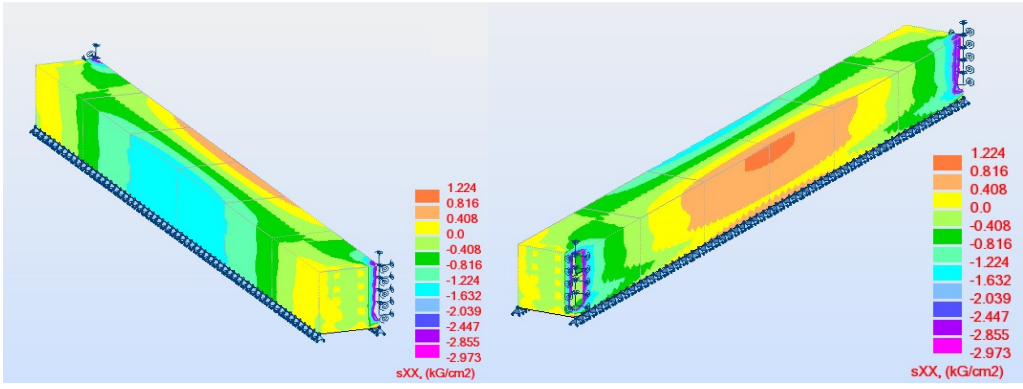


Fig. 5. 48 – Stress maps of the top horizontal vertical strip with  $\alpha=0.114$  and rotational springs

Furthermore, it has been calculated the reinforcement needed to carry-out the tension that will be acting on the top horizontal strip with the load multiplier equal to 0.114, the results are presented below.

Horizontal strip of 0.5m height- rotational springs							
load multiplier $\alpha$ (g)	S (Kg/cm <sup>2</sup> )	L (cm)	$\phi$ (mm)	n	Spacing without SF (cm)	Safety factor (SF)	Spacing with SF (cm)
0.114	0.408	100	3	9	16.60	2	8.30
	0.816	100	3	17	8.80	2	4.40
	1.224	200	3	50	7.00	2	3.50

Table 5. 17 – Wire reinforcement the top horizontal strip with rotational springs, considering  $\alpha=0.114$

## 5.4 Out-of-plane behavior of complete gabion boxes wall – FEM model

It has been performed a model of a complete gabion wall which has a length of 6m and height of 3m, considering two scenarios, the first one with rigid soil below the wall and the second one considering the stiffness of the soil under the structure.

Moreover, it has been considered in the model a triangular uniform distributed load on height applied to the wall; the distribution of the force has been computed as follows:

$$\frac{f_{max} * H * L}{2} = F_s$$
$$\frac{f_{max} * H * L}{2} = \alpha * (W_T + W_{roof})$$
$$f_{max} = \frac{2 * \alpha * (W_T + W_{roof})}{H * L}$$

Where:

$F_s$ = seismic force=  $\alpha (W_t + W_{roof})$

$f_{max}$ = maximum triangular distributed force (Kg/m<sup>2</sup>)

$W_t$ =16200 Kg

$W_{roof}$ =3000 Kg

It has been considered a load multiplier  $\alpha=0.5$  in order to verify if the gabion wall considered is able to sustain such PGA; thereby, it has been substituting the values into the previous equation in order to obtain the force that is going to be applied to the wall.

$$f_{max} = \frac{2 * 0.5 * (16200 + 3000)}{3 * 6} = 1066.7 \text{ Kg/m}^2$$

### 5.4.1. Complete gabion wall over rigid soil – FEM model.

It has been performed the FEM analysis considering the force computed before that represents a load multiplier  $\alpha=0.5$  and taking into account the soil below the structure as rigid; it has been observed if the maximum displacement is not large enough that will have an imminent collapse of the wall, additionally it has been obtained the tension stresses that will be acting on the gabion wall.

It can be seen in the following figure how the displacement develops on the complete wall considering a load multiplier equal to 0.5.

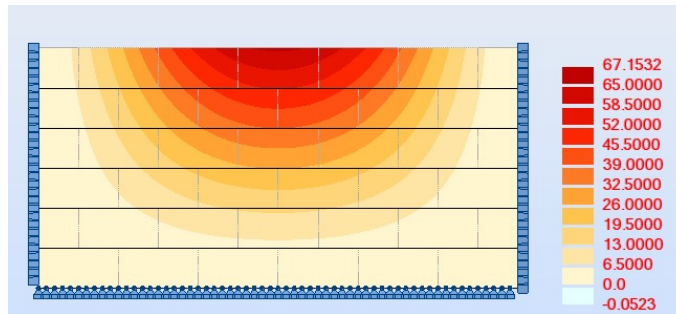


Fig. 5. 49 - Map of displacement of the complete wall considering  $\alpha=0.5$  and a rigid soil

The results of stresses acting on the body are shown in the following picture, where positive values mean tension stresses.

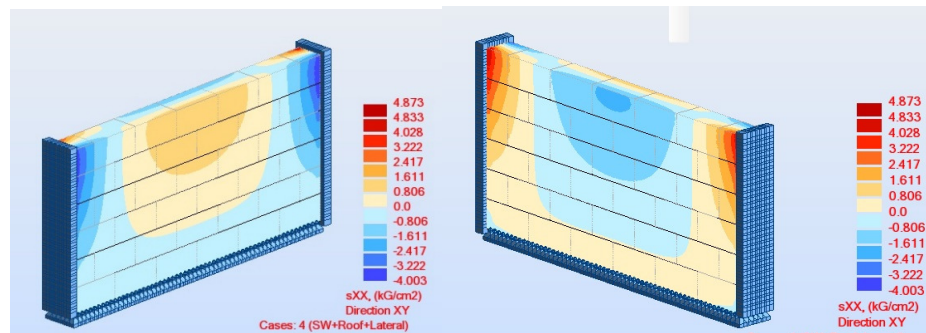


Fig. 5. 50 - Map of stresses of the complete wall considering  $\alpha=0.5$  and a rigid soil

It has also been reported the reactions of the supports, with the objective to compare the results with the cohesion of the material at the connection between two perpendicular walls; the forces on the supports should be lower than the maximum value of cohesion to ensure that the connection will be working at maximum capacity, if this condition is not satisfied for a certain load multiplier, the length of the wall should be reduced or ensure that the wire reinforcement is placed in a proper way.

height from 0 to 0.5		height from 0.5 to 1		height from 1 to 1.5	
Max	6.849	Max	6.699	Max	2.857
Min	-8.062	Min	-19.186	Min	-34.379
Mean (Kg)	1.709972	Mean (Kg)	-1.66475	Mean (Kg)	-10.0188
$T_{mean}$ (kg/cm2)	0.0171	$T_{mean}$ (kg/cm2)	-0.01665	$T_{mean}$ (kg/cm2)	-0.10019

height from 1.5 to 2		height from 2 to 2.5		height from 2.5 to 3	
Max	-2.487	Max	-8.936	Max	-9.16
Min	-51.523	Min	-74.774	Min	-86.334
Mean (Kg)	-20.2143	Mean (Kg)	-32.7989	Mean (Kg)	-41.1282
$T_{mean}$ (kg/cm2)	-0.20214	$T_{mean}$ (kg/cm2)	-0.32799	$T_{mean}$ (kg/cm2)	-0.41128

Table 5. 18 - Reaction values at supports of the wall, considering  $\alpha=0.5$  and a rigid soil

**5.4.2. Complete gabion wall over elastic soil – FEM model.**

It has been performed the FEM analysis considering the force computed before, that represents a load multiplier  $\alpha=0.5$  and taking into account the soil below the structure as elastic, neglecting the springs that are working in tension (Fig. 5.50); it has been observed if the maximum displacement is not large enough that will have an imminent collapse of the wall, additionally it has been obtained the tension stresses that will be acting on the gabion wall.

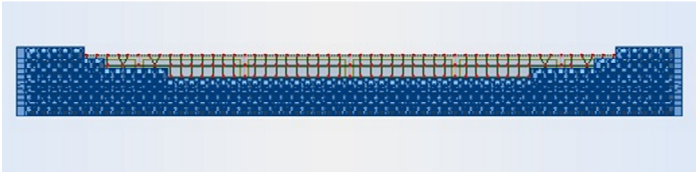


Fig. 5. 51 – Springs working in compression of the complete gabion wall with  $\alpha= 0.5$

It can be seen in the following figure how the displacement develops on the complete wall considering a load multiplier equal to 0.5.

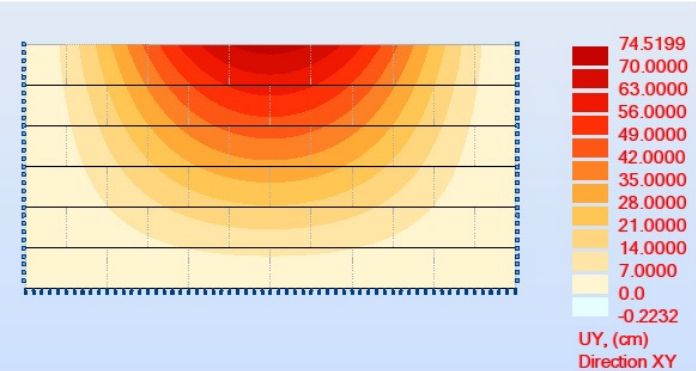


Fig. 5. 52 - Map of displacement of the complete wall considering  $\alpha= 0.5$  and an elastic soil.

The results of stresses acting on the body are shown in the following picture, where positive values mean tension stresses.

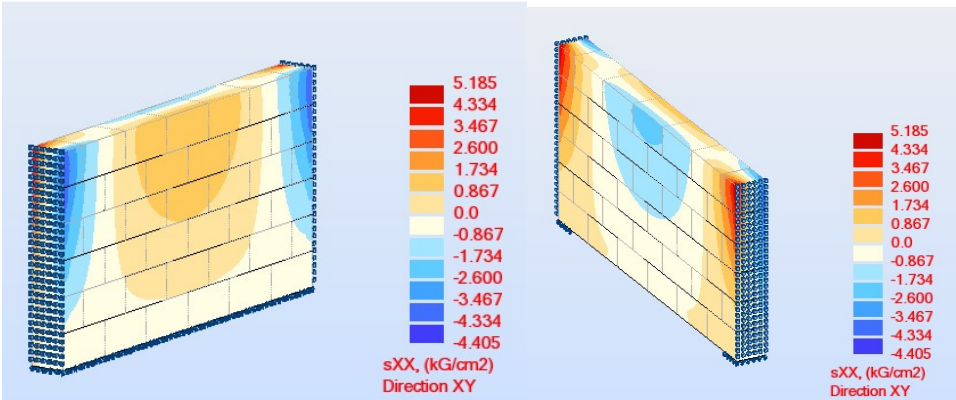


Fig. 5. 53 - Map of stresses of the complete wall considering  $\alpha=0.5$  and an elastic soil

The reaction at the supports are shown in the following table.

height from 0 to 0.5		height from 0.5 to 1		height from 1 to 1.5	
Max	5.866	Max	5.499	Max	1.387
Min	-11.075	Min	-25.128	Min	-41.438
Mean (Kg)	0.719	Mean (Kg)	-4.49158	Mean (Kg)	-13.3993
T <sub>mean</sub> (kg/cm <sup>2</sup> )	0.00719	T <sub>mean</sub> (kg/cm <sup>2</sup> )	-0.04492	T <sub>mean</sub> (kg/cm <sup>2</sup> )	-0.13399

height from 1.5 to 2		height from 2 to 2.5		height from 2.5 to 3	
Max	-3.35	Max	-9.236	Max	-7.272
Min	-58.778	Min	-81.012	Min	-90.588
Mean (Kg)	-23.4183	Mean (Kg)	-35.7333	Mean (Kg)	-42.8419
T <sub>mean</sub> (kg/cm <sup>2</sup> )	-0.23418	T <sub>mean</sub> (kg/cm <sup>2</sup> )	-0.35733	T <sub>mean</sub> (kg/cm <sup>2</sup> )	-0.42842

Table 5. 19 - Reaction values at supports of the wall, considering  $\alpha=0.5$  and an elastic soil

It can be notice that considering springs at the base gives less conservatives results than considering a rigid soil below the wall, thus it has been performed additional calculations considering only this scenario.

Considering a load multiplier of 0.5g for this length of the wall, gives results that are not stables for the structures, such as the maximum displacement and also, reaction values at the connection with perpendicular walls higher that the cohesion.

As it can be notice in all the previous results that have been performed, the displacement that occurs when it has been found the maximum load multipliers is around 50-60 cm, thereby, it has been considered the maximum displacement of a gabion wall equal to 50cm.

### 5.5 Wall of 6m length over elastic soil – FEM model

It has been performed the FEM analysis in order to find the load multiplier that will generate reaction forces equal or less than the cohesion values at the lateral supports; this condition was satisfied with a load multiplier  $\alpha=0.25$  and the results are show below.

The reaction at the supports are shown in the following table.

height from 1.5 to 2		height from 2 to 2.5		height from 2.5 to 3	
Max	-1.055	Max	-4.395	Max	-2.799
Min	-27.471	Min	-39.666	Min	-50.164
Mean (Kg)	-10.6068	Mean (Kg)	-16.8997	Mean (Kg)	-20.8822
T <sub>mean</sub> (kg/cm <sup>2</sup> )	-0.10607	T <sub>mean</sub> (kg/cm <sup>2</sup> )	-0.169	T <sub>mean</sub> (kg/cm <sup>2</sup> )	-0.20882

Table 5. 20 - Reaction values at supports of the wall, considering  $\alpha=0.25$  and an elastic soil

The maximum displacement of the wall has been reported below:

L=6m and alpha=0.25g		
Springs at base (only compression) - fix edges		
Maximum in-plane displacement (cm)	Maximum out-of-plane displacement (cm)	Maximum Vertical displacement (cm)
4.42	35.21	-7.35

Table 5. 21 - Maximum displacement of the wall considering  $\alpha=0.25$  and an elastic soil

The results of stresses acting on the body are shown in the following picture, where positive values mean tension stresses.

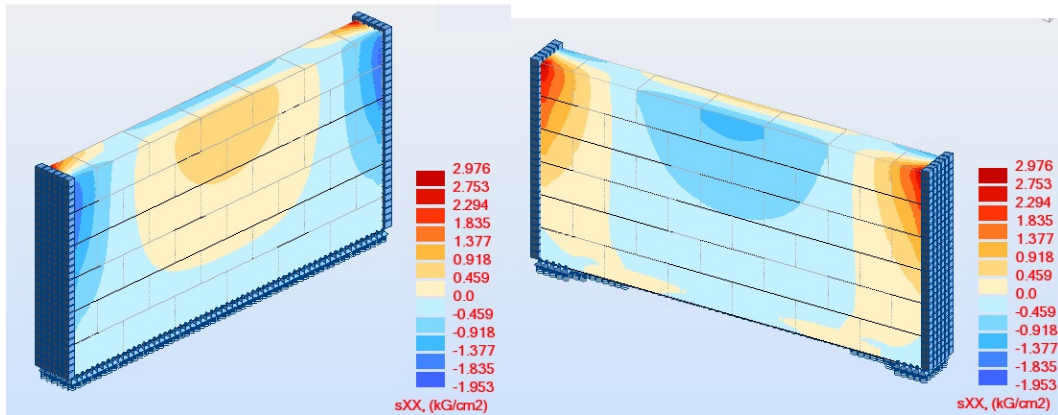


Fig. 5. 54- Map of stresses of the complete wall considering  $\alpha=0.25$  and an elastic soil

Moreover, it has been performed the FEM analysis in order to find the load multiplier that will generate that will generate the maximum prescribed displacement that has been selected as 50cm; this condition was satisfied with a load multiplier  $\alpha=0.35$  and the results are show below.

The reaction at the supports are shown in the following table.

height from 1.5 to 2		height from 2 to 2.5		height from 2.5 to 3	
Max	-1.973	Max	-6.331	Max	-5.079
Min	-39.993	Min	-56.203	Min	-66.248
Mean (Kg)	-15.7312	Mean (Kg)	-24.4326	Mean (Kg)	-29.6656
$T_{mean}$ (kg/cm2)	-0.15731	$T_{mean}$ (kg/cm2)	-0.24433	$T_{mean}$ (kg/cm2)	-0.29666

Table 5. 22- Reaction values at supports of the wall, considering  $\alpha=0.35$  and an elastic soil

The maximum displacement of the wall has been reported below:

L=6m and alpha=0.35g		
Springs at base (only compression) - fix edges		
Maximum in-plane displacement (cm)	Maximum out-of-plane displacement (cm)	Maximum Vertical displacement (cm)
6.00	50.25	-8.47

Table 5. 23 - Maximum displacement of the wall considering  $\alpha=0.35$  and an elastic soil

The results of stresses acting on the body are shown in the following picture, where positive values mean tension stresses.

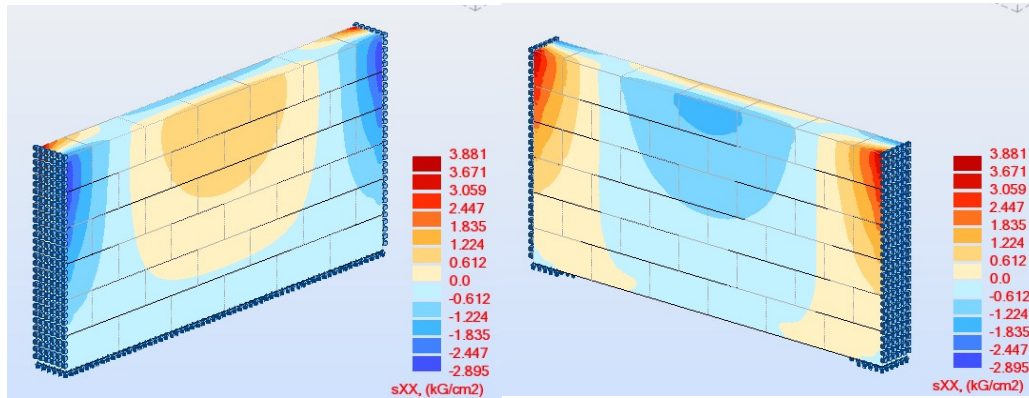


Fig. 5. 55 - Map of stresses of the complete wall considering  $\alpha=0.35$  and an elastic soil

Additionally, it has been compute the number of wires needed per meter in order to be able to resist the tension stress obtained from the FEM results for both cases, the calculations are shown below.

Length of wall = 6m							
distribution of wires at corners							
load multiplier $\alpha$ (g)	S (Kg/cm <sup>2</sup> )	L (cm)	$\phi$ (mm)	n	Spacing (cm)	Safety factor (SF)	Spacing with SF (cm)
0.35	3.88	50	3	40	2.50	2	1.20
	1.84	50	3	19	7.80	2	3.90
	0.6	100	3	13	19.20	2	9.60
0.25	2.98	50	3	31	3.20	2	1.60
	1.38	50	3	15	10.00	2	5.00
	0.46	100	3	10	25.00	2	12.50

Table 5. 24 – Wire reinforcement at corner of a gabion wall with a length of 6m

Length of wall = 6m							
distribution of wires at center of the wall							
load multiplier $\alpha$ (g)	S (Kg/cm <sup>2</sup> )	L (cm)	$\phi$ (mm)	n	Spacing (cm)	Safety factor (SF)	Spacing with SF (cm)
0.35	1.84	400	3	151	6.60	2	3.30
	0.60	400	3	50	20.00	2	10.00
0.25	1.38	400	3	113	8.80	2	4.40
	0.46	400	3	38	26.30	2	13.10

Table 5. 25 – Wire reinforcement at the center of a gabion wall with a length of 6m

### 5.6 Wall of 5m length over elastic soil – FEM model

It has been reduced the length of the wall in order to verified if it's possible to reach a load multiplier of 0.5g without affecting the stability of the structure, and it has been performed the same analysis than before. It has been considered for this case, a new length of the gabion wall equal to 5.0m.

First of all, considering the new length, it has been carried out the FEM analysis in order to find the load multiplier that will generate reaction forces equal or less than the cohesion values at the lateral supports; this condition was satisfied with a load multiplier  $\alpha=0.30$  and the results are show below.

The reaction at the supports are shown in the following table.

height from 1.5 to 2		height from 2 to 2.5		height from 2.5 to 3	
Max	-1.055	Max	-4.395	Max	-3.793
Min	-27.471	Min	-39.666	Min	-49.087
Mean (Kg)	-10.6068	Mean (Kg)	-16.8997	Mean (Kg)	-21.775
T <sub>mean</sub> (kg/cm <sup>2</sup> )	-0.10607	T <sub>mean</sub> (kg/cm <sup>2</sup> )	-0.169	T <sub>mean</sub> (kg/cm <sup>2</sup> )	-0.21775

Table 5. 26 - Reaction values at supports of the 5m wall, considering  $\alpha=0.30$  and an elastic soil

The maximum displacement of the wall has been reported below:

L=5m and alpha=0.3g		
Springs at base (only compression) - fix edges		
Maximum in-plane displacement (cm)	Maximum out-of-plane displacement (cm)	Maximum Vertical displacement (cm)
3.79	25.53	-5.88

Table 5. 27 - Maximum displacement of the 5m wall, considering  $\alpha=0.30$  and an elastic soil



The results of stresses acting on the body are shown in the following picture, where positive values mean tension stresses.

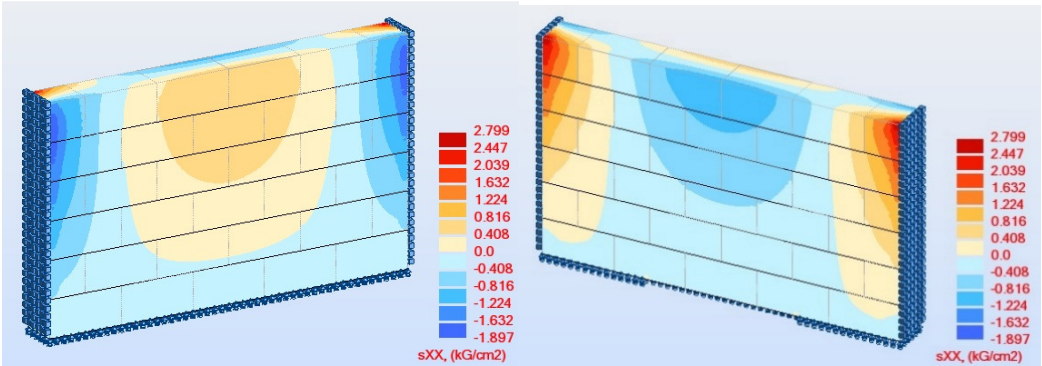


Fig. 5. 56 - Map of stresses of the complete wall of 5m, considering  $\alpha=0.30$  and an elastic soil.

Moreover, it has been performed the FEM analysis in order to find the load multiplier that will generate that will generate the maximum prescribed displacement that has been selected as 50cm; this condition was satisfied with a load multiplier  $\alpha=0.5$  and the results are show below.

The reaction at the supports are shown in the following table.

height from 1.5 to 2		height from 2 to 2.5		height from 2.5 to 3	
Max	-1.055	Max	-4.395	Max	-8.524
Min	-27.471	Min	-39.666	Min	-75.222
Mean (Kg)	-10.6068	Mean (Kg)	-16.8997	Mean (Kg)	-36.4358
T <sub>mean</sub> (kg/cm <sup>2</sup> )	-0.10607	T <sub>mean</sub> (kg/cm <sup>2</sup> )	-0.169	T <sub>mean</sub> (kg/cm <sup>2</sup> )	-0.36436

Table 5. 28 - Reaction values at supports of the 5m wall, considering  $\alpha=0.5$  and an elastic soil

The maximum displacement of the wall has been reported below:

L=5m and alpha=0.5g		
Springs at base (only compression) - fix edges		
Maximum in-plane displacement (cm)	Maximum out-of-plane displacement (cm)	Maximum Vertical displacement (cm)
5.86	42.45	-7.45

Table 5. 29 - Maximum displacement of the 5m wall, considering  $\alpha=0.5$  and an elastic soil

The results of stresses acting on the body are shown in the following picture, where positive values mean tension stresses.

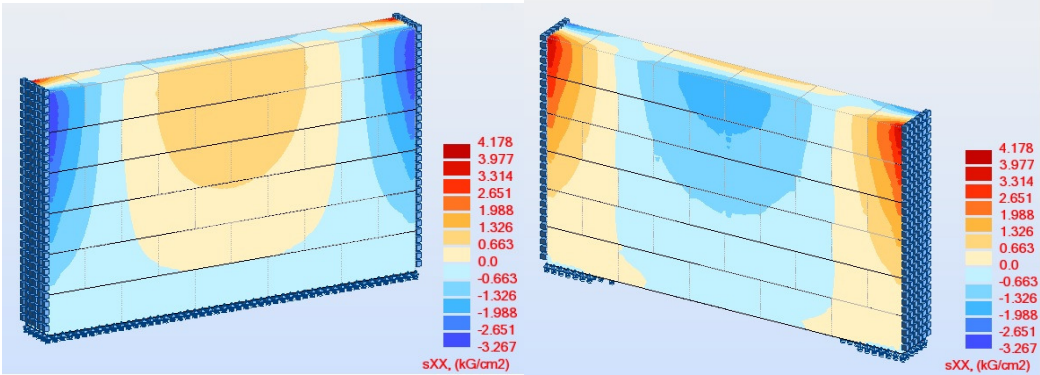


Fig. 5. 57 - Map of stresses of the complete wall of 5m, considering  $\alpha=0.50$  and an elastic soil.

Additionally, it has been compute the number of wires needed per meter in order to be able to resist the tension stress obtained from the FEM results for both cases, the calculations are shown below.

Length of wall = 5m							
distribution of wires at corners							
load multiplier $\alpha$ (g)	S (Kg/cm <sup>2</sup> )	L (cm)	$\phi$ (mm)	n	Spacing (cm)	Safety factor (SF)	Spacing with SF (cm)
0.5	4.18	50	3	43	2.30	2	1.10
	1.99	50	3	21	7.10	2	3.50
	0.66	100	3	14	17.80	2	8.90
0.3	2.8	50	3	29	3.40	2	1.70
	1.22	50	3	13	11.50	2	5.70
	0.41	100	3	9	27.70	2	13.80

Table 5. 30 – Wire reinforcement at corner of a gabion wall with a length of 5m

Length of wall = 5m							
distribution of wires at center of the wall							
load multiplier $\alpha$ (g)	S (Kg/cm <sup>2</sup> )	L (cm)	$\phi$ (mm)	n	Spacing (cm)	Safety factor (SF)	Spacing with SF (cm)
0.5	1.99	300	3	122	6.10	2	3.00
	0.66	300	3	41	18.20	2	9.10
0.3	1.22	300	3	75	10.00	2	5.00
	0.41	300	3	26	28.80	2	14.40

Table 5. 31 – Wire reinforcement at the center of a gabion wall with a length of 5m

## 5.7 Out-of-plane behavior of complete gabion boxes wall – DEM model

The Finite Element Modeling (FEM) is a common computational tool used by structural engineers, giving good solutions for problems of elasticity and strength, but has limitations with the stability of the structure. On the other hand, as DeJong, M. J. (2009) highlighted, “the Discrete Element Modeling (DEM) is able to capture the discontinuous nature of masonry and allows for fully dynamic analysis with large displacements”. Thus, the DEM has the capacity to provide with a good accuracy the collapse of gabion box structures due to instability.

In this document, gabion box structures were modeled with the discrete element method using the commercial program 3DEC (2012 Itasca consulting group, Inc.). The DEM allows finite displacements and rotations of discrete bodies, including complete detachment of the rigid blocks.

In order to perform a DEM analysis, some joint properties have to be defined, these are shear stiffness, normal stiffness, friction angle and tensile strength.

The joint stiffness,  $k_n$  (normal stiffness) and  $k_s$  (shear stiffness), are defined using the material properties of the blocks:

$$k_n = \frac{E * A}{L}$$
$$k_s = \frac{G * A}{L}$$

Where  $E$  is the modulus of elasticity of the masonry blocks,  $G$  is the shear modulus,  $A$  is the area of contact between the blocks, and  $L$  is the length of rigid material represented in the direction perpendicular to the joint.

Some damping must be specified in order to limit extremely high frequency vibrations which are typically damped out in real materials and can cause a realistic bouncing in numerical simulation. In 3DEC, damping is applied in the form of Rayleigh damping:

$$\mathbf{C} = \alpha_R \mathbf{M} + \beta_R \mathbf{K}$$

Where  $\mathbf{C}$ ,  $\mathbf{M}$ , and  $\mathbf{K}$  are the damping, mass, and stiffness matrices, respectively,  $\alpha_R$  is the mass-proportional damping constant, and  $\beta_R$  is the stiffness-proportional damping constant. Rayleigh damping results in a critical damping ratio ( $\xi$ ) which is dependent on frequency ( $\omega$ ):

$$\xi(\omega) = \frac{1}{2} \left( \frac{\alpha_R}{\omega} + \beta_R \omega \right)$$

The mass proportional damping would give damping due to rigid body motion. The mass proportional damping is therefore normally neglected for compliant structures undergoing large rigid body motion.

The natural frequencies for a rigid block of the impact are straightforward:

$$\text{Corner impact: } \omega_c = \sqrt{\frac{k_z}{m_B}}$$

$$\text{Edge impact: } \omega_e = \sqrt{\frac{2k_z}{m_B}}$$

So we can find the fundamental frequencies,  $f = \omega_{\min} / 2 * \pi$ .

It has been performed 2 different models:

- 1) A wall with length of 6m without connection with perpendicular walls
- 2) A wall with length of 5m with interlocking in the connection with the orthogonal walls.

The following pictures represent the out-of-plane displacement of the gabion wall.

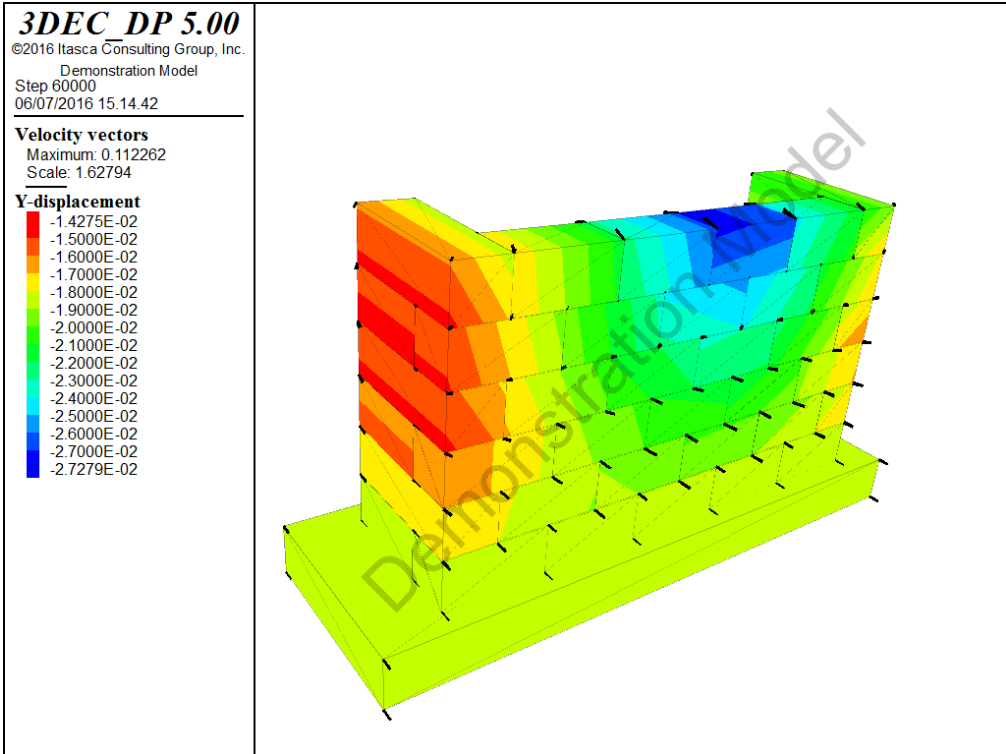


Fig. 5. 58 - DEM model of the gabion wall

In these models have been performed a dynamic analysis with increasing the applied acceleration at the base.

The wall of 6m length collapse with PGA=0.16g, instead the wall of 5m length with the interlocking at the connections resists until a PGA around 0.4g.

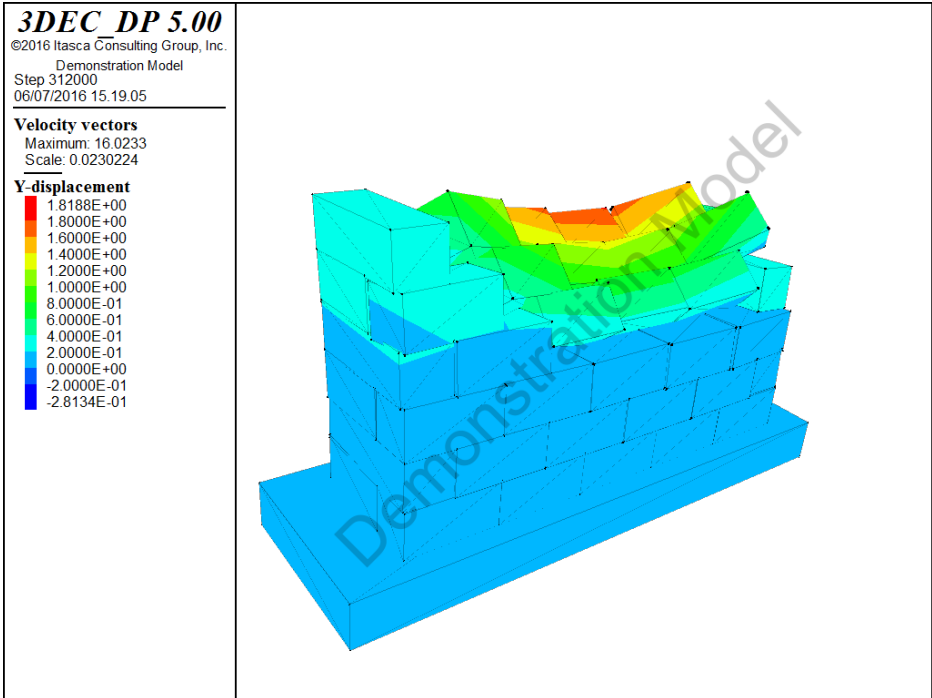


Fig. 5. 59 - Collapse of a gabion wall of 5m with a PGA around 0.4g

**CHAPTER 6 PRACTICAL RULES OF THUMB FOR CONSTRUCTION OF GABION BOXES STRUCTURES**

**6.1 Rules of thumb**

After performing all the analysis, it has been created some rules of thumb, that have to be satisfy in order to ensure a good behavior of the structure under a seismic action, this rules are very simple and understandable for everybody, thus, to formulate simple instructions for the correct construction of the gabion walls in a seismic area for non-technical or qualified personnel.

Thus, the rules of thumb derivate after performing all the analysis are listed below:

- Dimensions of the gabion box= 1m x 0.5 m x 0.5 m (L x H x W)
- Maximum height of the gabion wall = 3.0 m
- Maximum length of the gabion wall
  - ✓ 6m for a PGA=0.15 g without steel wire connectors.
  - ✓ 6m for a PGA=0.35 g, with  $\phi 3$  steel wires distributed as show below.

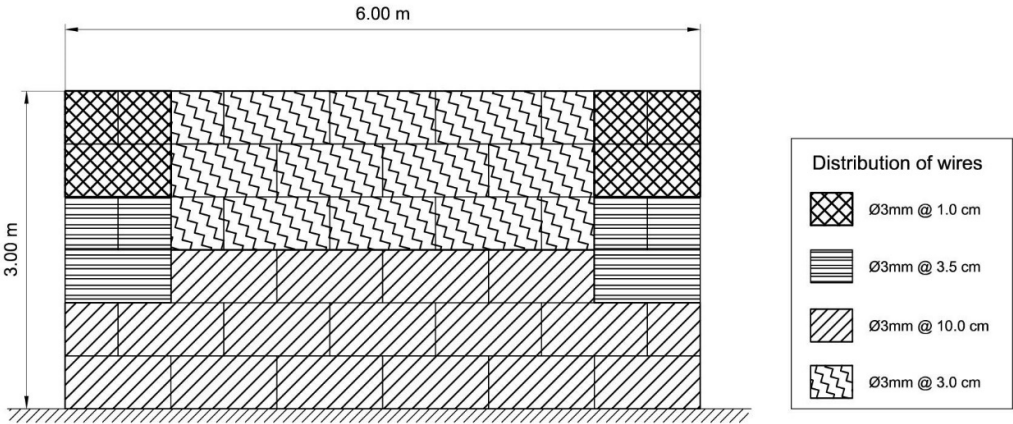


Fig. 6. 1 - Distribution of wires for a length of 6m and PGA=0.35

- ✓ 5m for a PGA=0.20 g without steel wire connectors.
- ✓ 5m for a PGA=0.50 g, with  $\phi 3$  steel wires distributed as show below.

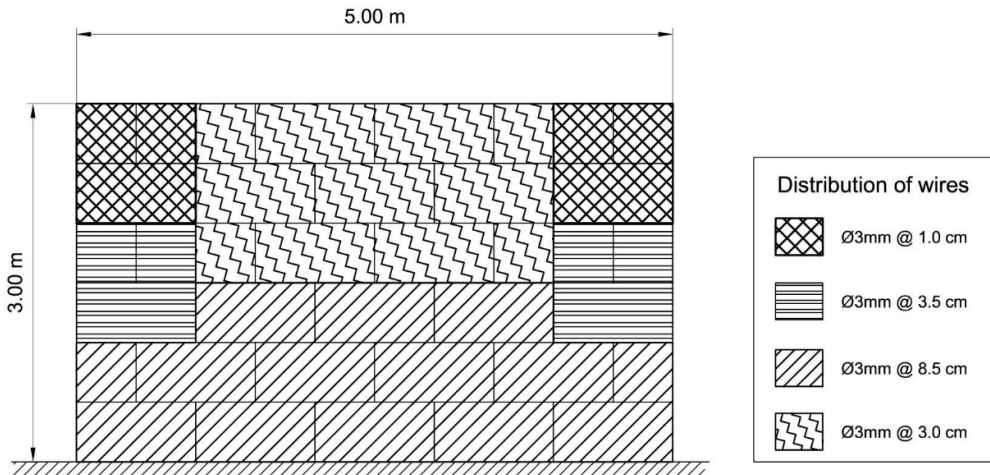


Fig. 6. 2 - Distribution of wires for a length of 6m and PGA=0.50 g.

- The dimensions for the openings of the doors are 1m x 2m (Width x Height).
- The dimensions for the openings of the windows are 1m x 1m (Width x Height).
- The minimum distance of the opening to the external border of the wall is 1m.
- The maximum length of an opening is 1m.
- Above each opening, must be two lines of gabions
- The lintel timber beam must be at least: 2 wooden tables, one next to the other with a section of 24cm x 6cm (B x Thickness) and 3 meters long.

## CHAPTER 7 CONCLUSIONS AND RECOMMENDATIONS

### 7.1 Conclusions

After performing hand calculations for the study of the in-plane seismic behavior, it has been observed that the gabion walls have a large shear strength when dealing with forces oriented with the length of the wall, happens the same while evaluating the sliding resistance of two consecutive layers. Thereby, there will not be any issue regarding sliding or shear failure of the gabion box wall.

While evaluating the in-plane response in the presence of openings, it has been observed a reduction of the load multiplier that will cause the collapse of the system, but even with this decrease, the lateral force that can sustain is larger than 0.85g that is a value larger than the maximum expected acceleration that is around 0.5g.

In the other hand, the results obtained from the out-of-plane seismic behavior are the most unfavorable, particularly when the effect of the perpendicular walls were neglected; but the maximum load that can be achieve can be improved with a good connection with the perpendicular walls, creating an interlocking connection on the corners that can be compared with a “Lego” system, helping to prevent the rotation of the wall in the out of plane; this kind of connection must be tested and a further research is needed in order to validate the results obtained in this document.

As it can be notice in all the previous results that have been performed, the displacement that occurs when it has been found the maximum load multipliers is around 50-60 cm, thereby it has been considered the maximum prescribed displacement equal to 50cm for the gabion box wall that have been considered in this document.

The results of the DEM are correlated with the result performed by hand and with the FEM model, hence the results obtained in this document are validated by each method of analysis that was performed, on the other hand, it is recommended further experimental test in order to validate them.



## **BIBLIOGRAPHY**

- [1] Agostini, R., Cesario, L., & Conte, A. (1987). Flexible gabion structures in earth retaining works.
- [2] Lin, D. G., Lin, Y. H., & Yu, F. C. (2010). Deformation analyses of gabion structures. INTERPRAEVENT 2010, 512-526.
- [3] Jiang, Y., & Wang, X. (2011). Stress-Strain Behavior of Gabion in Compression Test and Direct Shear Test. In Third International Conference on Transportation Engineering (ICTE).
- [4] Von Mises, R. (1913). Mechanik der festen Körper im plastisch deformablen Zustand. Göttin. Nachr. Math. Phys., vol. 1, pp. 582–592
- [5] Statics of Historic Masonry Constructions. M. Como, Springer, 2013.
- [6] Como, M. (2015). Statics of Historic Masonry Constructions: An Essay. In Masonry Structures. Springer International Publishing.
- [7] DeJong, M. J. (2009). Seismic assessment strategies for masonry structures (Doctoral dissertation, Massachusetts Institute of Technology).